https://ntrs.nasa.gov/search.jsp?R=19930092685 2020-06-17T01:23:38+00:00Z

FILE COPY
NO. 1-W

CASE FILE
COPY

MR May 1944
MR July 1944

NATIONAL ADVISORY COMMITTEE FOR AERONAUTICS

WARTIME REPORT

ORIGINALLY ISSUED
May and July 1944 as
Memorandum Reports

WIND-TUNNEL INVESTIGATION OF A 1/20-SCALE POWERED MODEL OF A FOUR-ENGINE TRANSPORT AIRPLANE

By Victor I. Stevens, William M. Douglass
and Jules B. Dods, Jr.

Ames Aeronautical Laboratory
Moffett Field, California

FILE COPY
To be returned to
the files of the National
Advisory Committee
for Aeronautics
Washington, D. C.

WASHINGTON

NACA WARTIME REPORTS are reprints of papers originally issued to provide rapid distribution of advance research results to an authorized group requiring them for the war effort. They were previously held under a security status but are now unclassified. Some of these reports were not technically edited. All have been reproduced without change in order to expedite general distribution.

NATIONAL ADVISORY COMMITTEE FOR AERONAUTICS

MEMORANDUM REPORT

WIND-TUNNEL INVESTIGATION OF A 1/20-SCALE POWERED MODEL OF A FOUR-ENGINE TRANSPORT AIRPLANE

By Victor I. Stevens, William M. Douglass, and Jules B. Dods, Jr.

SUMMARY

Tests have been made on a 1/20-scale model of a four-engine transport airplane to determine the stability characteristics, empennage control-surface effectiveness, the effect of propeller rotation on longitudinal stability, and a method for carrying spare wing panels under the fuselage. The effect of two modes of model power operation on the characteristics of the model was studied. The effect of landing gear, open cowl flaps, and center-section split flaps was also investigated.

The results indicate that the model possesses satisfactory stick-fixed longitudinal stability for all normal flight conditions except for high power with flaps extended. The stick-free longitudinal stability is unsatisfactory in a rated-power climb, although it may be remedied through the use of a spring in the elevator system counteracted by nose-up tab. Stick-free stability is also lacking for any power condition with flaps fully extended, owing to under-surface tail stall.

The elevator power in landing is marginal. Control forces are high for landing and accelerated flight for the design control linkage; however, a change in the control linkage should bring the forces within the desired limits.

A change in direction of propeller rotation produces little change in longitudinal stability of this model, primarily because the horizontal tail completely spans the slipstreams of the inboard propellers.

Directional characteristics of the model are satisfactory. The rudder power is sufficient to maintain zero

side slip upon failure of any one engine, and the control forces required are satisfactorily low.

Application of take-off power in the landing configuration completely neutralizes the normal dihedral effect, requiring use of the ailerons rather than the rudder to keep the wings level.

From an aerodynamic viewpoint, wing panels carried under the fuselage should be placed lengthwise of the fuselage with the inboard ends butted together.

Practically no difference is indicated between the results for the two modes of model power operation, provided the horizontal tail is not stalled.

In general, the landing gear increases the static longitudinal stability, power off. However, with power at a flap deflection of 25°, stability is decreased. The effect at a flap deflection of 50° is obscured by the stalling of the tail.

INTRODUCTION

An investigation of the characteristics of a four-engine transport airplane through tests of a 1/20-scale powered model was conducted at the request of the Materiel Command, U.S. Army Air Forces. Results are presented which show the empennage control-surface effectiveness and the effect of propeller rotation on longitudinal stability. Data are presented to show flap effectiveness, effect of landing gear, effect of cowl flaps, and an optimum method for carrying spare wing panels under the fuselage. A comparison is also presented of the longitudinal characteristics obtained by two methods of model power operation (i.e., the advance ratio V/nD was varied by changing either the propeller rotational speed or the dynamic pressure).

The tests were conducted in the Ames 7- by 10-foot tunnel.

MODEL AND APPARATUS

The 1/20-scale model of a four-engine transport airplane is characterized by a high-aspect-ratio wing set back and low

on the fuselage with generous fillets at the wing-fuselage juncture. Three outstanding features of the wing are (1) full-span vaned flaps, (2) a spoiler-flap-aileron combination (commonly called a flip-flap-flop) for lateral control, and (3) an airfoil section which at the design lift coefficient has pressure gradients favorable to laminar flow on the lower surface only. A combination of direct control and servo-control is utilized on the airplane to reduce control forces. The linkage in the system is partially adjustable, providing a means for obtaining the most suitable ratio of direct-to-servo control.

A three-view drawing of the model is shown in figure 1, and a sketch showing the location of thrust lines and center of gravity is presented in figure 2. Section details of the vaned flap and the spoiler-flap-aileron combination are given in figure 3. Figures 4 and 5 give detailed dimensions for the horizontal and vertical tail, respectively. The model elevators were equipped with both trim and control tabs; however, the trim tab was neutral for all tests. A tabulation of the important model dimensions and a list of configuration symbols used in the report are presented in appendixes A and B.

The model was powered with four variable-speed motors driving three-blade propellers. A propeller-blade setting of 22° at the 0.75 radius was maintained throughout the tests. A unit composed of a motor and torsion strain gage was installed in the tail cone, permitting the operator to deflect either the rudder or elevator and read the resulting hinge moments while the tunnel was operating. Two wooden wing panels, simulating the right and left outboard panels of the model, were provided to be mounted under the fuselage in various positions.

The model was mounted on three struts, as shown in figure 6. All power and control leads were carried through the rear support strut, allowing the use of small-tip struts on the wing.

TESTS AND RESULTS

The tests were conducted in two series. The results of the first series have been segregated into four groups: (1) longitudinal stability and control, (2) the effect of

propeller rotation on longitudinal stability, (3) lateral-directional characteristics, and (4) tests showing flap effects and effects of externally transported wing panels. For tests in which full-scale power was to be simulated, the relationships of thrust coefficient T_c to lift coefficient C_L, shown in figure 7, were used. The propeller characteristics (T_c as a function of V/nD) determined experimentally are given in figure 8.

A second series of tests was later conducted to obtain a comparison of the results obtained using two different methods of power operation, to determine the effect of the landing gear and cowl flaps, and to determine the effectiveness of the center-section split flap.

The test results are presented in the form of standard NACA coefficients. Except where noted, the coefficients are referred to the stability axes passing through a point above the 25 percent mean aerodynamic chord (fig. 2) and are corrected for support tares and jet-boundary effects as given in the appendix.

Longitudinal Stability and Control

The longitudinal characteristics of the model were determined as a function of angle of attack for various combinations of flap and power settings and are presented as the variation of angle of attack and of drag, pitching moment, and hinge-moment coefficients with lift coefficient. The characteristics of the model with various power conditions are compared in figure 9 for flaps undeflected, in figure 10 for flaps deflected 25°, and in figure 11 for flaps deflected 50°.

Elevator and elevator-control-tab-effectiveness data were obtained for the model with propellers removed and flaps undeflected by varying elevator deflection for several model attitudes and control-tab settings. The results for control tab neutral are presented in figure 12 as the variation of lift, drag, pitching-moment, and elevator hinge-moment coefficients with elevator deflection. For nominal control-tab deflections of −10°, 10°, 15°, and 20°, pitching-moment and elevator hinge-moment coefficients are given in figures 13 to 16. Figures 12 to 16 have been cross-plotted to determine tab effectiveness and the results are presented in figures 17 and 18.

A limited series of tests was also made to measure elevator and elevator-tab effectiveness with propellers operating. Results of these tests, for which rated power at 5000 feet was simulated, are presented in figure 19.

To determine sufficiency of elevator power for landing, the model in the landing configuration was tested with elevator deflected 0°, -20°, and -25° for control-tab deflections of 0°, 10°, and 20°. The results are shown in figure 20.

Effect of Propeller Rotation on Longitudinal Stability

Tests of twin-engine airplanes have shown loss in longitudinal stability with application of power to be a function of propeller rotation: The optimum rotation is such that the inboard blades are traveling up, giving a larger part of the tail benefit of upwash due to slipstream rotation. With these results in mind, tests were made on this model with engines 1 and 2 rotating counterclockwise and engines 3 and 4 clockwise. The variation of angle of attack, pitching-moment coefficient, and elevator hinge-moment coefficient with lift coefficient for this rotation is compared with the conventional rotation (all clockwise) in figure 21 for flaps undeflected, in figure 22 for flaps deflected 25°, and in figure 23 for flaps deflected 50°.

Lateral-Directional Characteristics

The aerodynamic characteristics of the model in yaw were evaluated for the cruising attitude ($C_L \cong 0.5$), climb attitude ($C_L \cong 1.0$), and the landing-approach attitude ($C_L \cong 2.0$ with flaps extended 50°). Characteristics of the model in the cruise attitude are presented in [1]figure 24 for the propellers-removed and cruising-power conditions. Similarly, [1]figure 25

---

[1]In the original data obtained for the conditions shown in figures 24, 25, and 35, there occurred discontinuities in the cross-force and yawing-moment coefficients. However, in a later investigation it was found that a separation flow over the thick airfoil section of the third strut was the cause of the observed discontinuities. By placing spoilers on the strut it was possible to eliminate these discontinuities.

presents the characteristics for the climb attitude with rated power simulated and with propellers removed, and figure 26 presents the characteristics for the landing-approach attitude with 50-percent-rated and 100-percent take-off power simulated and propellers removed. In figure 27 are shown tuft photographs of flow over the vertical tail for the model in the cruise attitude.

Rudder-and rudder-tab-effectiveness tests with propellers removed were made at the cruise attitude by varying rudder angle for several angles of yaw and control-tab settings. The results are presented in figures 28 to 31 as the variation of yawing-moment and rudder hinge-moment coefficients with rudder angle. These data have been cross-plotted to give control-tab effectiveness in figures 32 to 34.

To ascertain the rudder effectiveness with propellers operating, rated power at the climb attitude was simulated for tab neutral only. These data are included in [2]figure 35.

To test adequacy of directional control in the event of single-engine failure during take-off, the model in the take-off configuration (flaps deflected 25°, landing gear extended) was yawed for each of several rudder deflections while maintaining take-off power in engines 2, 3, and 4, and allowing engine 1 to windmill. Figure 36 shows the results of these tests.

Effects of Flaps and External Wing Panels

For convenience of comparison the lift curves for the model with propellers removed are summarized in figure 37 for flaps deflected 0°, 25°, and 50°. In figure 38 are shown the combined effects of Reynolds number and Mach number on the lift characteristics for flaps deflected.

It was suspected that the outboard flap had passed its peak effectiveness at a full 50° deflection. Such a condition would be particularly undesirable since the aileron is on this portion of the flap. To check this condition, tests were made with the inboard flap deflected 50° and the outboard flap at 0°, 12½°, 25°, 37½°, and 50°. The results are

[2]See footnote, p. 5.

presented in figure 40.

Since one of the functions of this airplane will be the transportation of wing panels too large to be carried in the fuselage, tests were made with outboard panels mounted under the fuselage to determine the optimum arrangement. Two of the three arrangements tested are shown in figure 40. The test results for the three arrangements are presented in figures 41, 42, and 43.

Effect of Method of Power Operation

The first series of tests indicated a translation in the pitching moments with change in dynamic pressure for a 50° flap deflection with the tail removed. Since in that series the power tests were made with a variable dynamic pressure, it was considered possible that errors were introduced into the pitching moments. Therefore, it was proposed to make a comparable series of power tests in which the variable dynamic pressure was eliminated. To do this, the thrust coefficient was varied by changing the propeller rotational speed rather than the dynamic pressure. The comparison of the longitudinal characteristics obtained by both methods are presented in figures 44 to 47 for the model with flaps undeflected, deflected 25°, 37½°, and 50°. Because tests were not previously obtained for a flap deflection of 37½°, all the required tests were made during this phase of the investigation. A summary plot showing power-on results for all flap deflections made by the constant-dynamic-pressure method is given in figure 48. The load carried by the tail is shown in figure 49 for a 50° flap deflection with take-off power.

Effect of Landing Gear and Center-Section Flap

For most of the tests made with flaps deflected, the landing gear was retracted, the effect of the landing gear was determined separately with and without power. Results obtained by the constant-propeller rotational-speed power method are presented in figure 50 for flap deflections of 25° and 50°. Results obtained by the constant-dynamic-pressure method for flap deflections of 0°, 25°, and 50° are presented in figures 51 to 53 for tail removed and in figures 54 to 56 for tail on.

The effect of the cowl flaps on the longitudinal-stability characteristics is presented in figure 57 with the tail on and in figure 58 with the tail removed. Both the power-off and power-on conditions are included.

Results of tests made to determine the effectiveness of the center-section split flap are presented in figures 59 and 60 for flap deflections of 25° and 50°.

DISCUSSION

Longitudinal Stability and Control

Power off.- The power-off stability with flaps undeflected as shown by dC_m/dC_L indicates a static margin of about 19 percent M.A.C. up to a C_L of 0.9 (fig. 9). Beyond this point dC_m/dC_L increases sharply due to a premature loss in wing effectiveness ($dC_L/d\alpha$). It should be noted that this effect is typical for scale models of airplanes having low-drag wing sections, but at the full-scale Reynolds number it is believed that the effect will be considerably reduced. The average static margin for the model with flaps deflected 25° and 50° is again equal to 19 percent M.A.C., but there is no loss in wing effectiveness with the corresponding increase in dC_m/dC_L at high lift coefficients (figs. 10 and 11).

The computed variation of elevator deflection and stick force (without servo and $\frac{d\ (\text{stick force})}{d\ (\text{elevator hinge moment})} = 0.647$ lb/ft lb) with speed, in figure 61, again shows the sharp increase in stability at an indicated airspeed of 140 miles per hour ($C_L = 0.9$) for the propellers-removed and flaps-retracted position. (Throughout this discussion, the analysis of control-force variation is simplified to the extent that forces are given neglecting benefit of servo action; however, the ability of the servo tab to reduce these forces satisfactorily is indicated.) The high stick forces are due to the size of the surface rather than to large hinge-moment coefficients. The normal range of flight speeds can be covered using only 5° of servo tab (figs. 12 to 16).

The characteristics of the airplane in accelerated flight with propellers removed for an airspeed of 220 miles per hour (sea level) have also been estimated (fig. 62). The variations of elevator angle and stick force with acceleration are stable

and nearly linear, as desired. Although the control tab is capable of enforcing the required elevator deflection, it is estimated that for the design linkage the stick forces required will exceed the 50-pound-per-g limit. This could be remedied by adjusting the linkage to give a greater mechanical advantage between control column and tab.

Characteristics of the airplane in the landing condition have been estimated and are given in figure 63. The calculations involved are based on a gross weight of 125,000 pounds with the center of gravity located at 17 percent of the M.A.C. and with the airplane trimmed away from the ground at 120 miles per hour. Ground effects have been added, using the methods and charts given in references 1 and 2. Since tab hinge moments could not be measured, they were estimated from results of tests on a geometrically similar tail. The minimum landing speed indicated for full elevator and control-tab deflections ($\delta_e = -25^\circ$, $\delta_{c_T} = 20^\circ$) is 95 miles per hour ($C_L \cong 2.13$). However, for the design control linkage of $\left(\frac{\text{stick force}}{\text{elevator hinge moment}}\right)_{\delta_{c_T}} = 0.647$ pound per foot-pound and of $\left(\frac{\text{stick force}}{\text{tab hinge moment}}\right)_{\delta_e} = 2.20$ pounds per foot-pound, an elevator deflection of slightly less than -20°, owing to the large elevator hinge moment, will be obtained when control tab is fully deflected. For this condition the landing speed would be greater than 100 miles per hour and control forces would be excessive. In consideration of these results and the fact that the control-tab effectiveness is still linear at 20°, it is recommended that the maximum tab angle be increased to 25°. Such a change should make it possible to reach elevator deflections in excess of 20° and also keep stick forces satisfactorily low. It should be noted that at the test Reynolds number the elevator is relatively ineffective at angles greater than 20° but that at full-scale Reynolds number the elevator may maintain effectiveness to slightly greater deflections. Also, the above estimations neglect the ground effect on wing characteristics, which results in a loss of maximum lift and a decrease in wing diving moment (reference 3). At present there are insufficient data to estimate accurately this effect, although it is believed that the latter effect would permit the airplane to be trimmed to higher lift coefficients which would reduce the minimum landing speed by about 5 miles per hour. In any case, the

sufficiency of elevator power for landing is marginal, since the minimum landing speed indicated above (including ground effect on wing pitching moment) is 90 miles per hour compared to the desired speed of 85 miles per hour.

Power on.- From the experimental results, it was found that the addition of rated power reduced the longitudinal stability, placing the neutral point at the 33 percent M.A.C. for the climb attitude (fig. 9). (Power-off neutral point is at 44 percent M.A.C. for the range of lift coefficient for which wing effectiveness is normal.) Since 32 percent of the M.A.C. is the estimated aft center-of-gravity position, stick-fixed stability in a rated-power climb will be marginal for the aft center of gravity but should be satisfactory for the design center of gravity (25 percent M.A.C.). To ascertain the relative importance of the different power effects on model characteristics, the pitching-moment increments produced by simulating rated power have been broken down into the various components and are shown in figure 64. At an angle of attack of 6° ($V_i \cong 135$ mph for gross weight = 125,000 lb), the calculated propeller thrust and normal forces produced ΔC_{m_1} and $\Delta C_{m_2} = 0.05$. The slipstream effects upon wing and nacelles were negligible. This was established by comparing the moments produced by calculated propeller forces and the moments produced by power for the tail-removed condition. The greatest effect of power was the change in downwash at the tail, resulting in a $\Delta C_{m_3} = 0.062$ determined from $\Delta C_{m_3} = (dC_m/di_t)_{\text{power off}}(\alpha_{T_{\text{power on}}} - \alpha_{T_{\text{power off}}})$ where α_T was deduced from tail pitching moment and dC_m/di_t. The effect of slipstream velocity over the tail was stabilizing, producing a $\Delta C_{m_4} = -0.021$. The value of ΔC_{m_4} was obtained from the equation $\Delta C_{m_4} = (q/q_o - 1)$(tail pitching-moment coefficient assuming $q/q_o = 1.0$) where q/q_o was obtained from the variation of elevator effectiveness with power.

The variations of elevator angle and stick force (without servo) with speed are given in figure 65 for rated power at 5000 feet. Static longitudinal stability, as indicated by $d\delta_e/dV$, is present throughout the speed range. High stick-fixed stability is exhibited at low speeds because of the decrease in $dC_L/d\alpha$ and the resultant increase in dC_m/dC_L (also noted for the propeller-removed condition). Stick-free stability is exhibited for speeds below 150 miles per hour; above this speed, stability is lacking, owing to the reduction

in stick-fixed stability. Stick-free stability could be improved by the introduction of a spring in the elevator control such that nose-up tab is required for trim.

With flaps deflected, power effects on the moment characteristics are similar to those existing with flaps undeflected except for the following:

1. The slipstream velocity over the flaps produces sufficient negative pitching moment to more than overcome the moment produced by direct propeller forces.

2. The flaps accentuate the downwash produced by the propeller.

3. The tail load is negative, making any effect of slipstream velocity over the tail destabilizing. With take-off power the static longitudinal stability, as indicated by dC_m/dC_L, becomes neutral at $C_L = 2.0$ for flaps deflected 25°, and at $C_L = 1.1$ for flaps deflected 50°. At lift coefficients below 1.2 for the model with flaps deflected 50°, there is an under-surface tail stall which is particularly noticeable with 50-percent rated power (simulated approach condition). For higher lift coefficients, dC_m/dC_L indicates adequate stability. A tendency for under-surface stall at low lift coefficients is indicated by dC_{h_e}/dC_L for all tests made with flaps deflected. The magnitude increases with flap deflection and power and is sufficient to produce severe stick-free instability. However, previous tests made on similar models have indicated that the under-surface stall observed at low Reynolds number tends to disappear at high Reynolds number.

Effect of Propeller Rotation on Longitudinal Stability

Changing propeller rotation on engines 1 and 2 from clockwise to counterclockwise moved the stick-fixed neutral point 1 percent of the M.A.C. aft for the rated-power climb but failed to change the stick-fixed stability when flaps were extended (figs. 21, 22, and 23). Stick-free characteristics are changed little, if any, although there appears to be a tendency toward greater stick-free stability in rated-power climb (dC_{h_e}/dC_L less negative) with change in rotation.

The magnitude of the change in stability was less than expected. The improvement in stability for rated-power climb was the difference between the beneficial effect of the upturning blades operating on the relatively large chord section of the stabilizer and the detrimental effect of the downturning blades operating on the small chord section of the stabilizer. If the tip of the horizontal tail extended only to the center of the inboard slipstream, as is approximately true on twin-engine airplanes, the effect would have been greater.

Lateral-Directional Characteristics

Power off.- The directional stability in the cruise attitude as measured by $dC_n/d\psi$ is -0.0028 and the corresponding $dC_n/d\delta_r$ is -0.0019. Using the methods of reference 4, the estimated values of $dC_{n_t}/d\psi$ and $dC_{n_t}/d\delta_r$ are less than the measured values, indicating that the vertical tail is operating efficiently near zero yaw. However, in figures 24, 25, and 26, the variation of C_n with ψ shows a loss in tail effectiveness at $\psi \cong 18^\circ$, as indicated by a loss in the restoring moment. Also, the rudder hinge moments show a marked increase. The tuft photographs of the model in the cruise attitude (fig. 27) indicate increasing roughness at about the midspan of the rudder for a yaw-angle range of 6° to 14°. Between 14° and 16° of yaw, the roughness progresses to a stall which extends to the rudder tip. Since the hinge moments were affected more than the yawing moments, the cause was probably separation at the rudder trailing edge, which changed the pressure distribution over the vertical surface.

The variation of rudder angle to trim and pedal force with the angle of sideslip is given in figure 66. A design control linkage of $\left(\frac{d\ (\text{pedal force})}{d\ (\text{rudder hinge moment})}\right)_{\delta_{r_t}} = 1.51$ with servo tab locked was used for the computation of rudder pedal forces. These results indicate that 16° of sideslip can be enforced with a full rudder deflection of 25°. The rudder hinge moment resulting can be neutralized with less than half (about 9°) of the available servo-tab deflection.

Power on.- The application of power in both the cruise and climb conditions decreases $dC_n/d\psi$ by 11 percent. For

both conditions, the power-on $dC_n/d\psi = -0.0025$.

The variation of the pedal forces and rudder deflection to trim with angle of sideslip is nearly linear for the airplane in the climb condition (V_i = 140 mph, rated power) as shown in figure 67. With a rudder deflection of 20°, the airplane will trim at 12.8° angle of sideslip. At larger deflections the rudder stalls, thereby greatly increasing the pedal forces. It is expected that, at full-scale Reynolds number, the effectiveness will be extended and a larger angle of sideslip will result.

It is emphasized that the large pedal forces indicated in the range between 0° and 20° rudder deflection are due to the size of the surface, not high hinge-moment coefficients, and that 17° of servo tab should be sufficient to neutralize the rudder hinge moments. The resulting change in the trim angle of sideslip caused by this tab deflection would be small.

With flaps extended, addition of power causes a marked decrease in $dC_l/d\psi$, which neutralizes the dihedral effect for 50 percent rated power and 100 percent take-off power. Such a reduction in dihedral effect is caused by a movement of the center of wing lift produced by the slipstream toward the trailing wing tip as the model is yawed, making the reduction a function of section lift coefficient, thrust coefficient, and distance from propeller disk to lifting line. Since the dihedral effect is not appreciably negative, the pilot should be able to maintain satisfactory control by using the ailerons.

Upon failure of the left outboard engine during take-off, about 11° of right rudder are required to maintain zero sideslip (fig. 36). For this deflection the servo tab is capable of reducing pedal forces considerably below the 180-pound limit. Since this is the most critical condition for single-engine failure, the rudder is capable of handling the unbalanced yawing moments produced by failure of any one engine.

Flap Effectiveness

The change in flap characteristics with dynamic pressure shown in figure 38 is influenced by Mach number as well as Reynolds number. As Reynolds number increases, the maximum lift should increase, which is verified by the lift curves

for q = 20 and 40 pounds per square foot. For higher dynamic pressures, the effect of Mach number cancels the beneficial effect of Reynolds number and there is negligible change in maximum lift coefficient with dynamic pressure. The Mach number reached in normal flight with flaps extended will not exceed the Mach number at a dynamic pressure of 40 pounds per square foot; therefore, the full-scale airplane should not suffer the detrimental Mach number effect on maximum lift coefficient.

The effectiveness of the outboard flap (fig. 39) remains nearly constant to a deflection of 30°. Beyond this point effectiveness decreases, reaching neutral effectiveness at about 45°. Based upon these results, it would appear that the deflection of the outboard flap should be limited to 35° or 40° to improve effectiveness of the aileron. As the outboard flap is retracted, the reduction of effective aspect ratio of the wing is clearly illustrated by the marked increase in C_D at a given C_L.

Effect of Wing Panels Carried Under Fuselage

The test results in figures 42 and 43 indicate that the wing panels mounted as shown in figure 40 cause little if any change in either the lift or the longitudinal- and directional-stability characteristics. They did cause a slight change in longitudinal trim and an appreciable increase in drag. The drag increments are summarized in the following table for the flap-undeflected condition:

Wing-panel configuration	Diagram of attachment	ΔC_D at $C_L = 0.5$	ΔC_D at $C_L = 1.0$
W_1	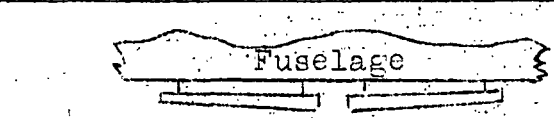	0.0035	0.0010
W_2	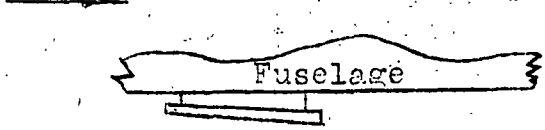	.0063	.0045
W_3	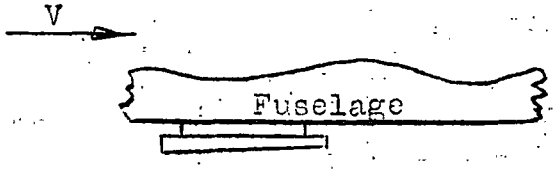	.0033	.0032

The foregoing results indicate that from an aerodynamic viewpoint configuration W_1 provides the most satisfactory method for carrying wing panels under the fuselage. It should be noted that use of this method required that the center-section flap remain undeflected. The accompanying mechanical complications and the loss of the center flap as a lifting device might not be justified by the low drag for this configuration.

Comparison of Method of Power Operation

The results indicate an agreement between the methods of power operation for the model with flaps undeflected, deflected 25°, and 37-1/2°. The pitching moments with the flaps deflected 50° are erratic, however, and there is a lack of agreement between the two methods. The reason for the erratic nature of the pitching-moment curves is shown in an examination of figure 49. The tail-removed pitching-moment curve has practically a constant slope. With the tail on, however, the variation of the pitching-moment curves is irregular, leading to the conclusion that the tail is stalled. Such a tail stall has been observed on several airplanes in which the tail is required to supply a large download because of large flap deflections and high power conditions. Thus, a closer agreement at this flap deflection would not be expected.

Effect of the Landing Gear and Cowl Flaps

Aside from the anticipated increase in drag, there are changes in pitching moment caused by the extension of the tricycle landing gear. It is evident that the effect of the landing gear on the power-off tail-removed characteristics is a positive incremental pitching moment. This characteristic, although unexpected, often occurs due to the interference between the landing gear and the wing; however, the change in the downwash at the tail caused by the landing gear produces a nearly equal but opposite shift in pitching moment. The resulting effect of the gear (power off and tail on) is a slight increase in the longitudinal stability. With the addition of power, the landing gear increases the longitudinal stability with flaps undeflected, and decreases the stability with flaps deflected 25°. With the flaps deflected 50°, the effect of the landing gear is obscured because of the unsteady tail stall mentioned previously.

With the wing flaps deflected 25° and with the tail on, there is no change in the longitudinal stability occasioned by opening the cowl flaps; however, a small trim change ($\Delta C_L = 0.07$, power off) is observed.

Effectiveness of the Center-Section Split Flap

The utility of the center-section split flap was questioned because of the tendency of the lift to carry over the unflapped area of the fuselage and because additional weight and mechanical complications would be involved in the flap installation.

It is apparent that the lift contributed by the center-section flap is small (figs. 59 and 60). However, the incremental pitching moment resulting from the increased downwash at the tail is beneficial in reducing the up-elevator required in landing. The latter effect may be the determining factor in retaining the center-section split flap, since it was estimated that the ability of the elevator to maintain the landing attitude in the presence of the ground was marginal. (See fig. 63).

CONCLUSIONS

The foregoing discussion indicates the following:

1. The stick-fixed longitudinal stability of the airplane should be satisfactory since it is positive for all normal flight conditions except for take-off power with flaps deflected where neutral stability is exhibited.

2. The stick-free longitudinal stability is unsatisfactory in a rated-power climb and for any power condition with flaps fully extended. In the case of the rated-power climb, a spring in the elevator system counteracted by nose-up tab should give satisfactory stability. With flaps extended, the instability is due to under-surface stall (which may not exist at full-scale Reynolds number), and the combination of spring and tab would probably be ineffective owing to the loss in tab effectiveness with surface stalled.

3. The elevator power in landing is marginal. Deflection of the center-section split flap, although providing no

additional lift, causes an incremental pitching moment which is beneficial in reducing the up-elevator required. The control forces for landing will be high unless the maximum tab deflection is increased to 25°. Control forces in accelerated flight will also be high for the design control linkage but could be improved by adjustment of the linkage.

4. Change in propeller rotation produced very little increase in the longitudinal stability, primarily because the tail completely spanned the slipstream of the inboard propellers.

5. The directional characteristics of the model which were investigated are satisfactory. The rudder power is sufficient to maintain zero yaw upon failure of any one engine, and the control forces required are not excessive.

6. Lateral characteristics are satisfactory except for 50-percent and 100-percent take-off power in the landing configuration. Use of the ailerons is required to pick up a wing but this should cause no particular difficulty provided the ailerons are effective in this condition. The deflection of the outboard flap should be limited to 35° or 40° to improve the effectiveness of the lateral control unless the outboard flap effectiveness improves with Reynolds number.

7. The results obtained by the two methods of power operation are equivalent provided the horizontal tail is not stalled.

8. In general, the landing gear increases the static longitudinal stability, power off. However, with power at a flap deflection of 25°, stability is decreased. The effect at a flap deflection of 50° is obscured by the stalling of the tail.

APPENDIX A

Model Dimensions

Wing	
Area, square feet	6.275
Span, feet	3.662
Mean aerodynamic chord, feet	0.820
Aspect ratio	11.96
Taper ratio	4.25:1
Dihedral	6°
Sweepback	40-percent chord line straight
Incidence of root chord	3.91°
Geometric twist	1.29° of washout
Tail lengths	
Center of gravity (25 percent M.A.C.) to elevator hinge, feet	2.97
Center of gravity (25 percent M.A.C.) to rudder hinge, feet	2.93
Horizontal tail	
Area, square feet	1.702
Span, feet	2.750
Aspect ratio	4.45

Elevator	
Area, square feet	0.718
[1]Area aft of hinge line, square feet	0.536
[1]M.A.C. of area aft of hinge line, feet	0.244
Vertical tail (excluding dorsal fin)	
Area, square feet	1.163
Span, feet	1.424
Aspect ratio	1.75
Rudder	
Area, square feet	0.466
[1]Area aft of hinge line, square feet	0.357
[1]M.A.C. of area aft of hinge line, feet	0.321
Propeller	
Diameter, feet	0.950
Blades	three

[1]Areas and chords used to obtain elevator and rudder hinge-moment coefficients

APPENDIX B

Configuration Symbols

S	standard configuration which includes wing with full-span flaps, nacelles, pilots' enclosures, horizontal tail, and vertical tail
HV	horizontal and vertical tails including dorsal fin
F^{α}	full-span flaps deflected α degrees
$F_S{}^{\alpha}F_I{}^{\alpha}$	center-section (split) flap and inboard flaps deflected α degrees
$F_O{}^{\alpha}$	outboard flap deflected α degrees
C^{α}	cowl flaps opened to α degrees
G	landing gear (tricycle type) including doors
P_1	left outboard propeller
P_2	left inboard propeller
P_3	right inboard propeller
P_4	right outboard propeller
P	P_1, P_2, P_3, P_4

Superscripts R or L denote clockwise or counterclockwise rotation as observed from tail of airplane

W_1	two outboard wing panels mounted under fuselage with inboard ends butted together
W_2	one outboard wing panel; that is, W_1 with rear panel removed
W_3	one outboard wing panel; that is, W_2 turned so that inboard end of panel is forward
δ_e	deflection of elevators, degrees
δ_{e_T}	deflection of elevator control (servo) tab, degrees
δ_r	deflection of rudder, degrees

δ_{r_T} deflection of rudder control (servo) tab, degrees

α angle of attack of fuselage reference line corrected for upflow and tunnel-wall effects.

Corrections

Except where noted, all results are presented in the form of standard NACA coefficients referred to the stability axes passing through a center of gravity located at the 25 percent M.A.C. (fig. 2). Corrections for support tares and jet-boundary effects have been made. The jet-boundary corrections are as follows:

$$\Delta\alpha_T = \delta_w \frac{S}{C} C_L (57.3)$$

$$\Delta C_{D_T} = \delta_w \frac{S}{C} C_L$$

$$\Delta C_{m_T} = \delta_{a_{c.s.}} \frac{S}{C} C_L (57.3) \frac{dC_m}{di_t}$$

where

δ_w 0.125

$\delta_{a_{c.s.}}$ 0.075

S wing area, 6.27 square feet

C tunnel area, 70 square feet

C_L lift coefficient

$\frac{dC_m}{di_t}$ change in model pitching-moment coefficient per degree change in tail incidence, computed to be -0.052

REFERENCES

1. Katzoff, S., and Sweberg, Harold H.: Ground Effect on Downwash Angles and Wake Location. Rep. No. 738, NACA, 1943.

2. Silverstein, Abe, and Katzoff, S.: Design Charts for Predicting Downwash Angles and Wake Characteristics behind Plain and Flapped Wings. Rep. No. 648, NACA, 1939.

3. Recant, Isidore G.: Wind-Tunnel Investigation of Ground Effect on Wings with Flaps. T.N. No. 705, NACA, May 1939.

4. Pass, H. R.: Analysis of Wind-Tunnel Data on Directional Stability and Control. T.N. No. 775, NACA, Sept. 1940.

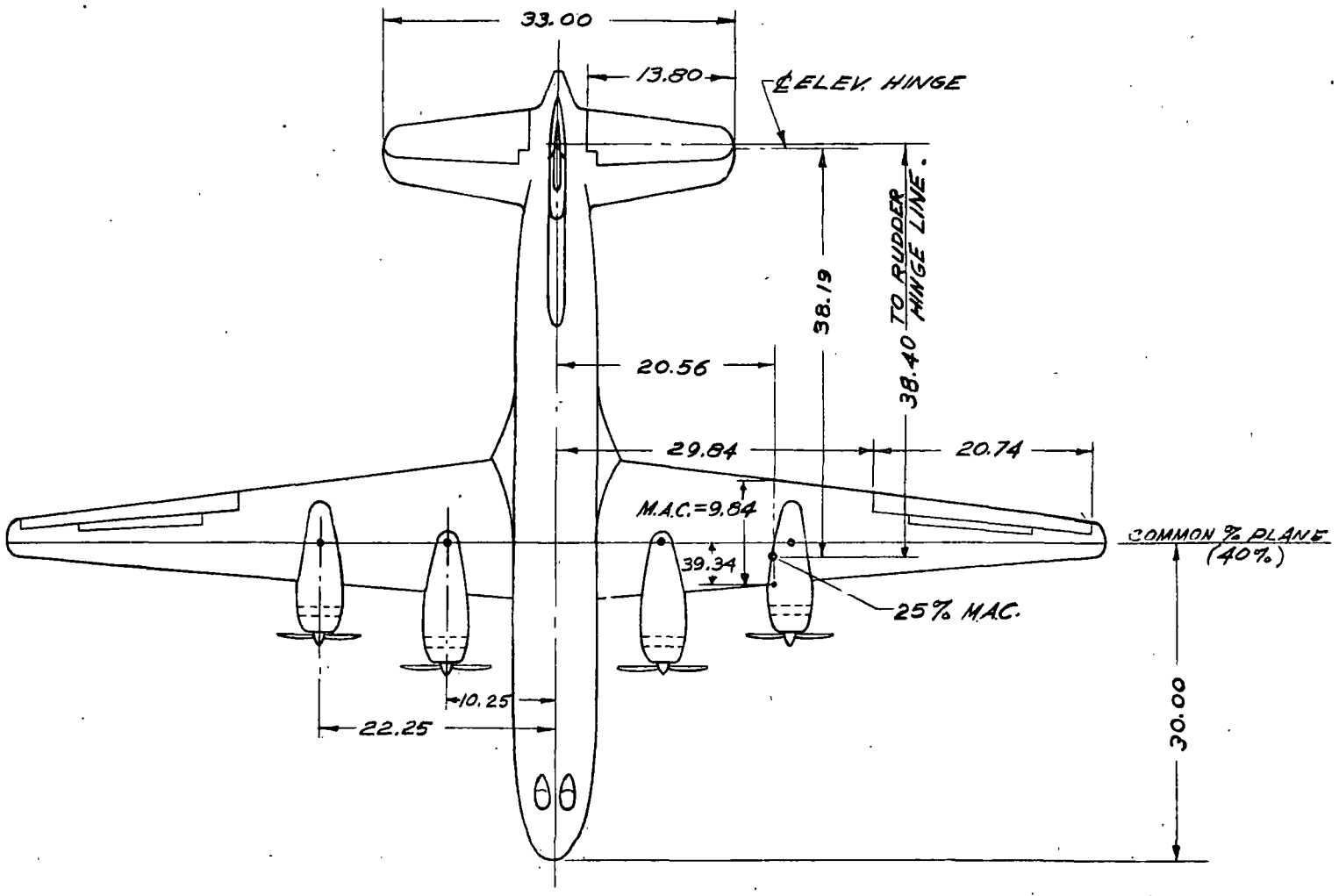

NATIONAL ADVISORY
COMMITTEE FOR AERONAUTICS

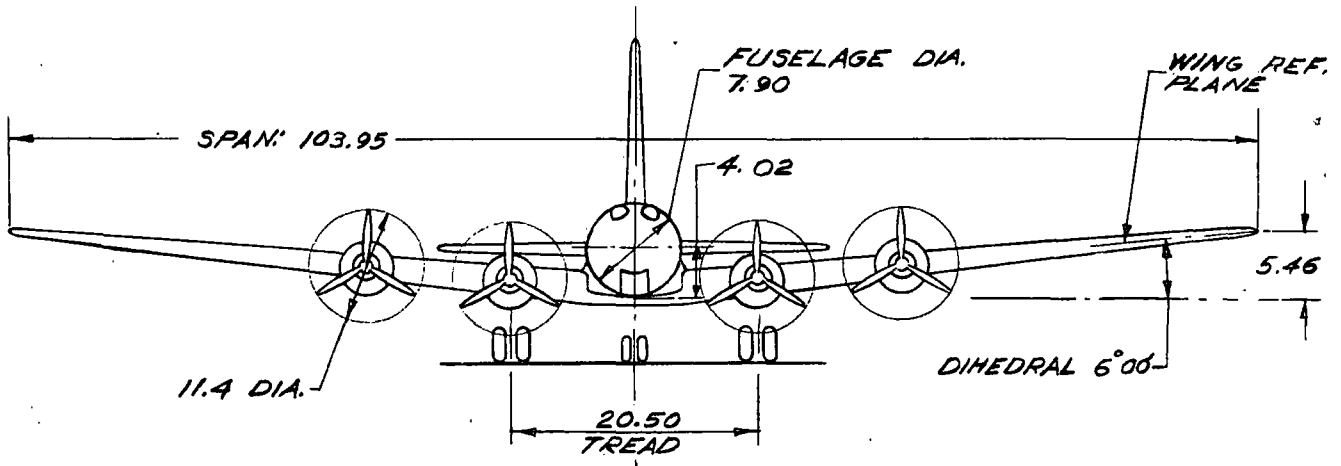

NOTE:
ALL DIMENSIONS
ARE IN INCHES

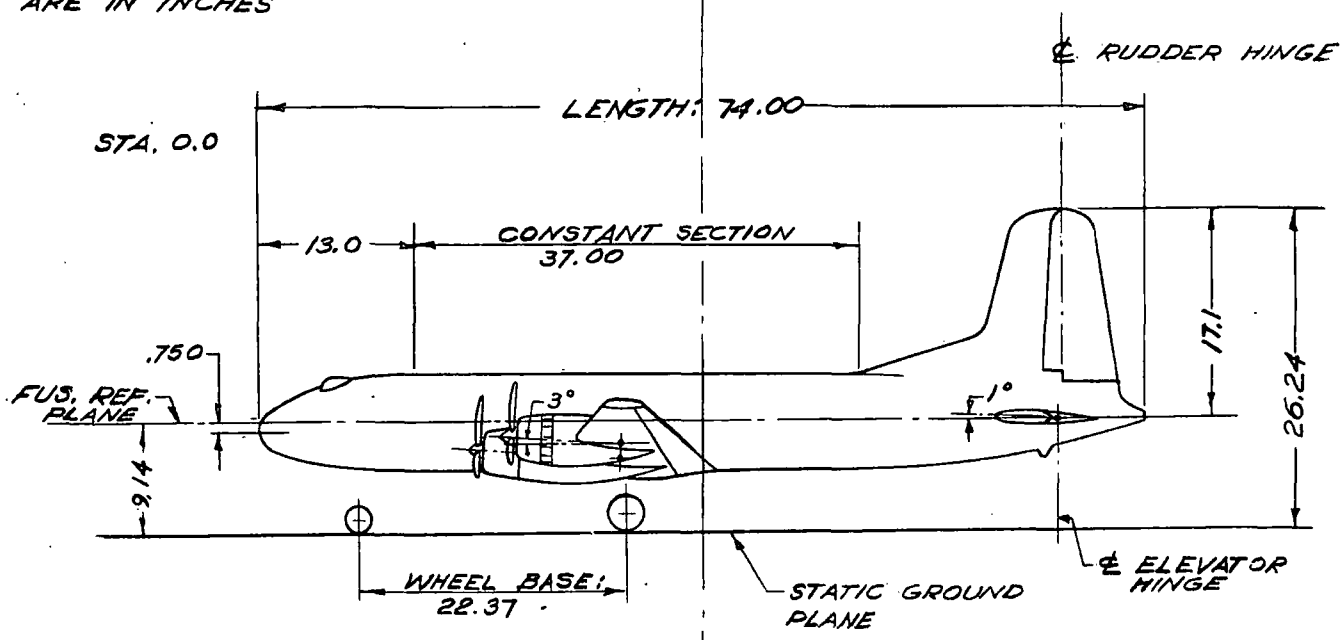

FIGURE 1.- THREE-VIEW DRAWING OF TEST MODEL.

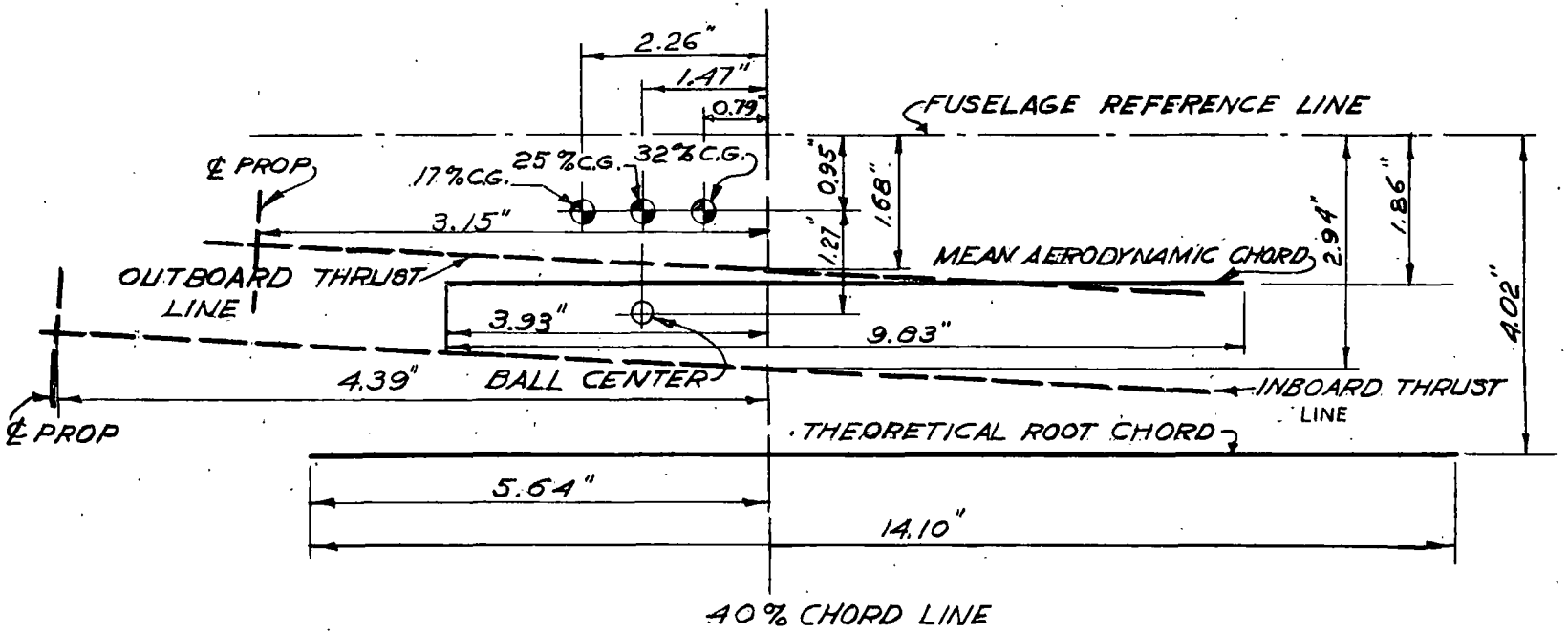

THRUST LINES ARE INCLINED +3° WITH FUSELAGE REFERENCE LINE

SCALE = $\frac{1}{2}$" = 1"

NATIONAL ADVISORY
COMMITTEE FOR AERONAUTICS

FIGURE 2. DIAGRAM OF CENTER-OF-GRAVITY LOCATION.

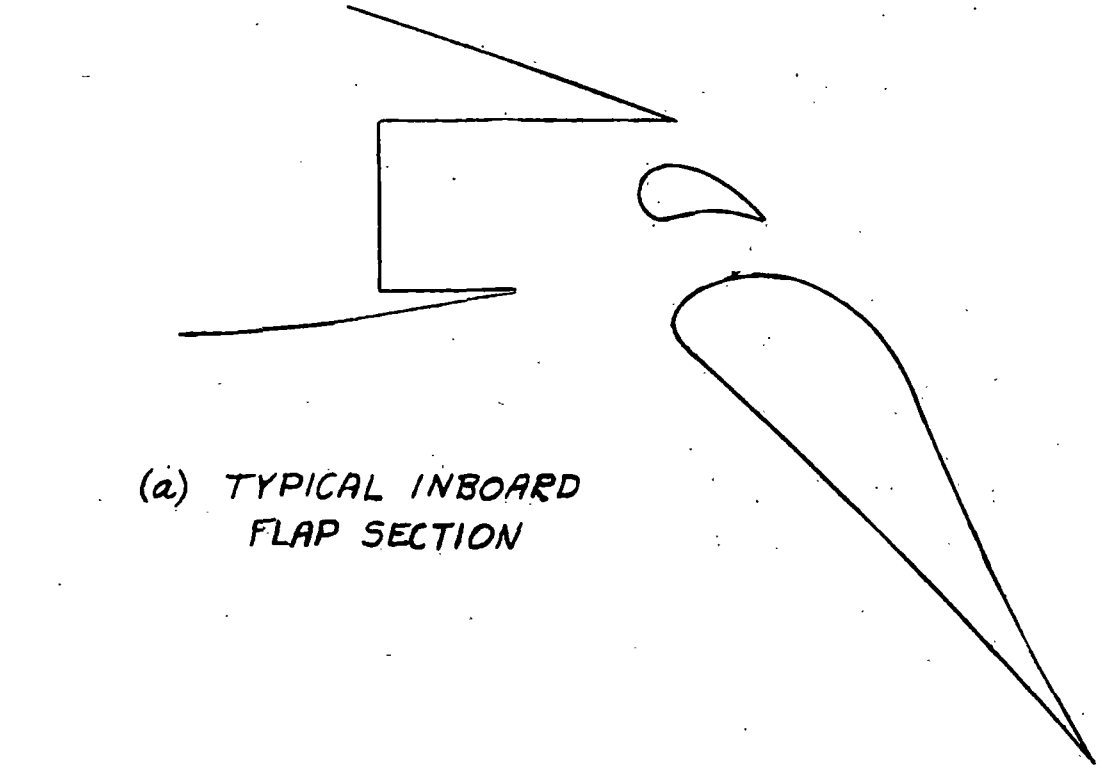

(a) TYPICAL INBOARD FLAP SECTION

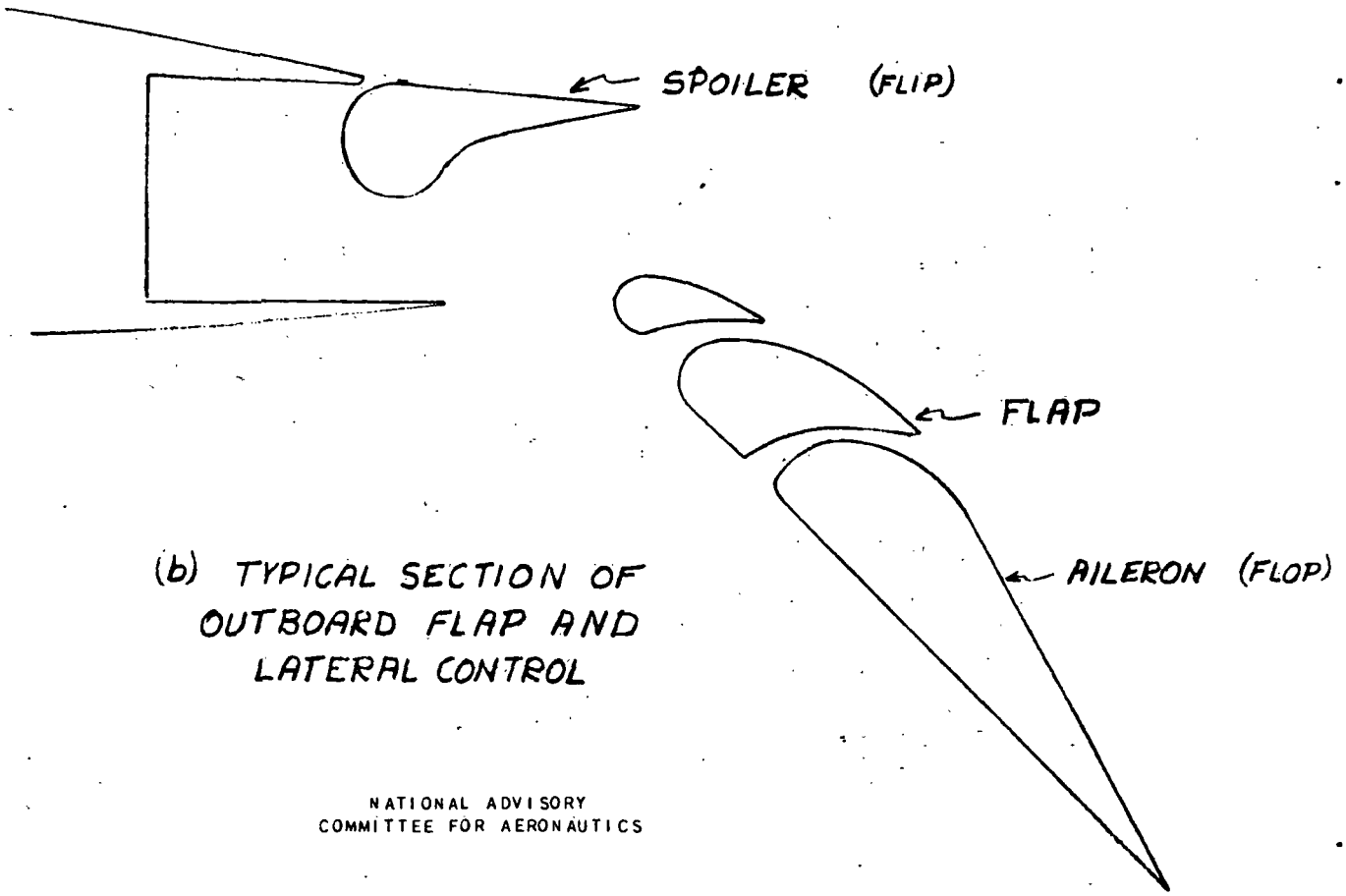

(b) TYPICAL SECTION OF OUTBOARD FLAP AND LATERAL CONTROL

NATIONAL ADVISORY
COMMITTEE FOR AERONAUTICS

FIGURE 3.— SKETCH SHOWING SECTIONS OF VANED FLAP AND SPOILER-FLAP-AILERON COMBINATION TEST MODEL.

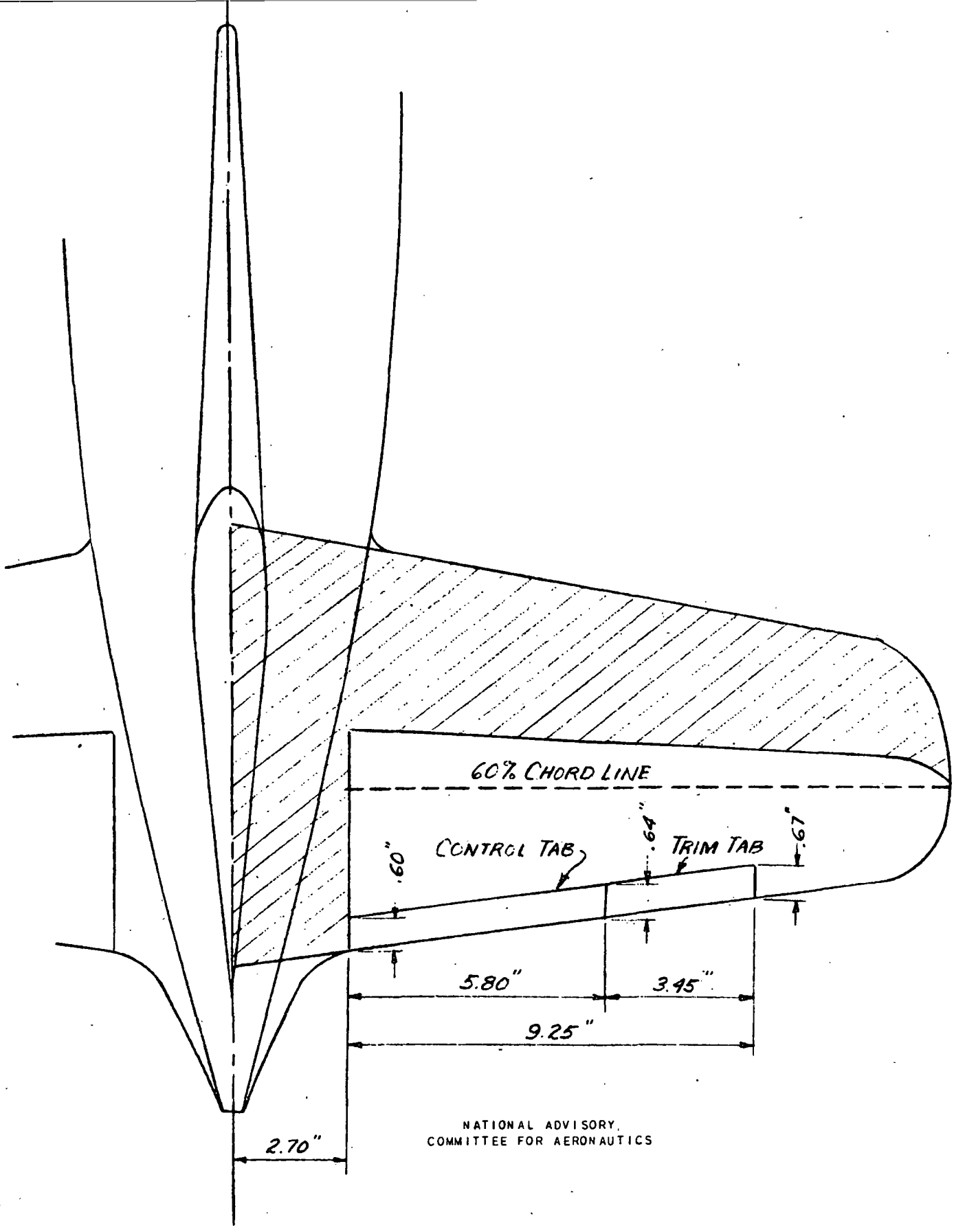

FIGURE 4.- DETAILS OF THE ELEVATOR AND ELEVATOR TAB ON THE TEST MODEL.

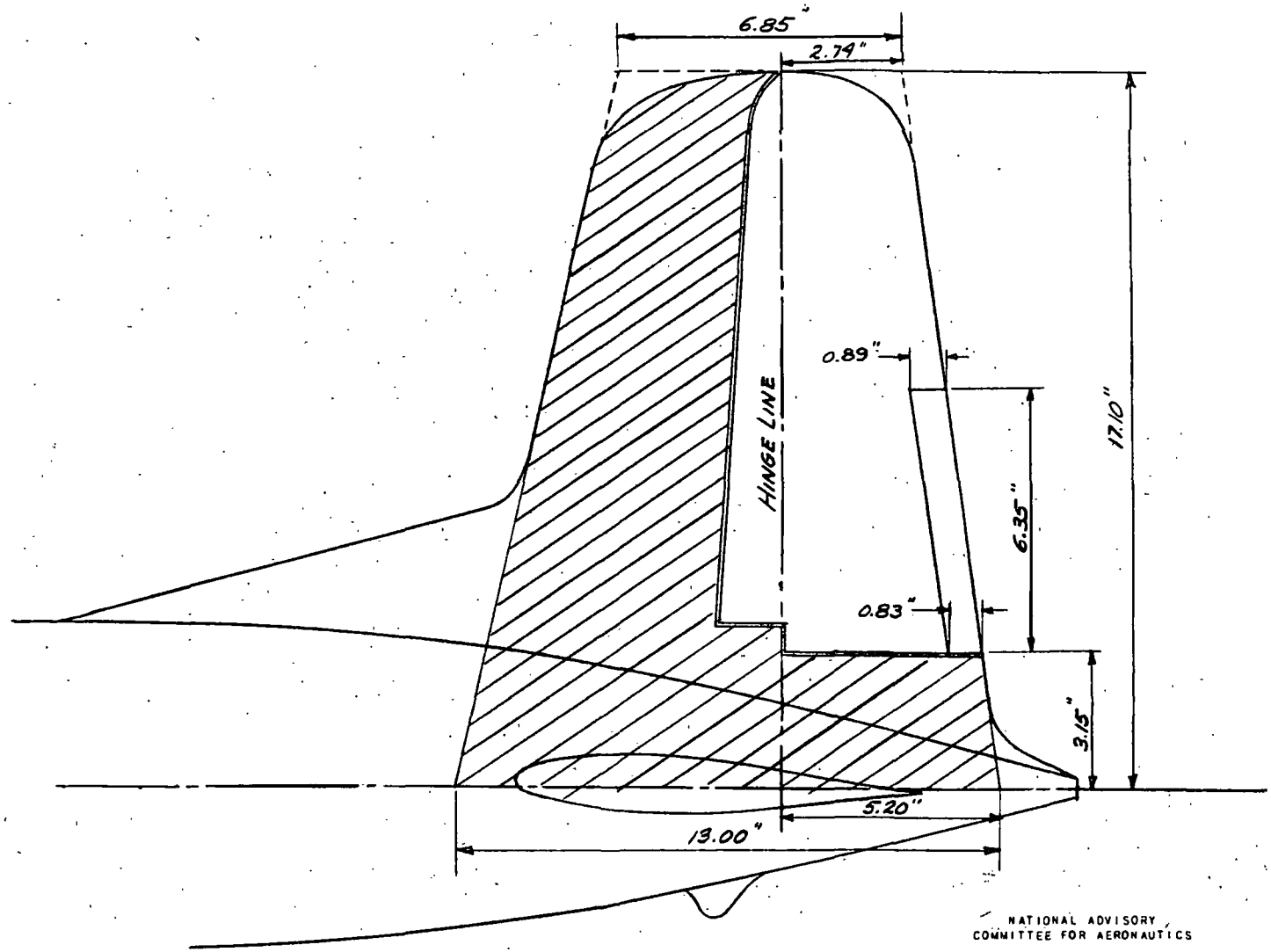

FIGURE 5.-DETAILS OF THE RUDDER AND RUDDER TAB ON THE TEST MODEL.

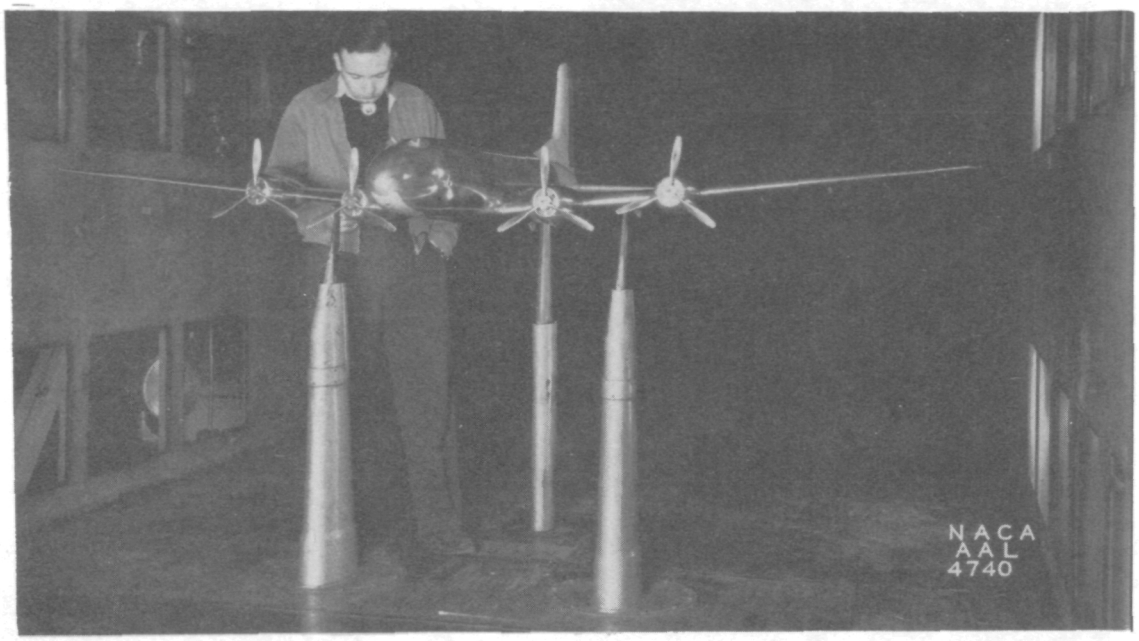

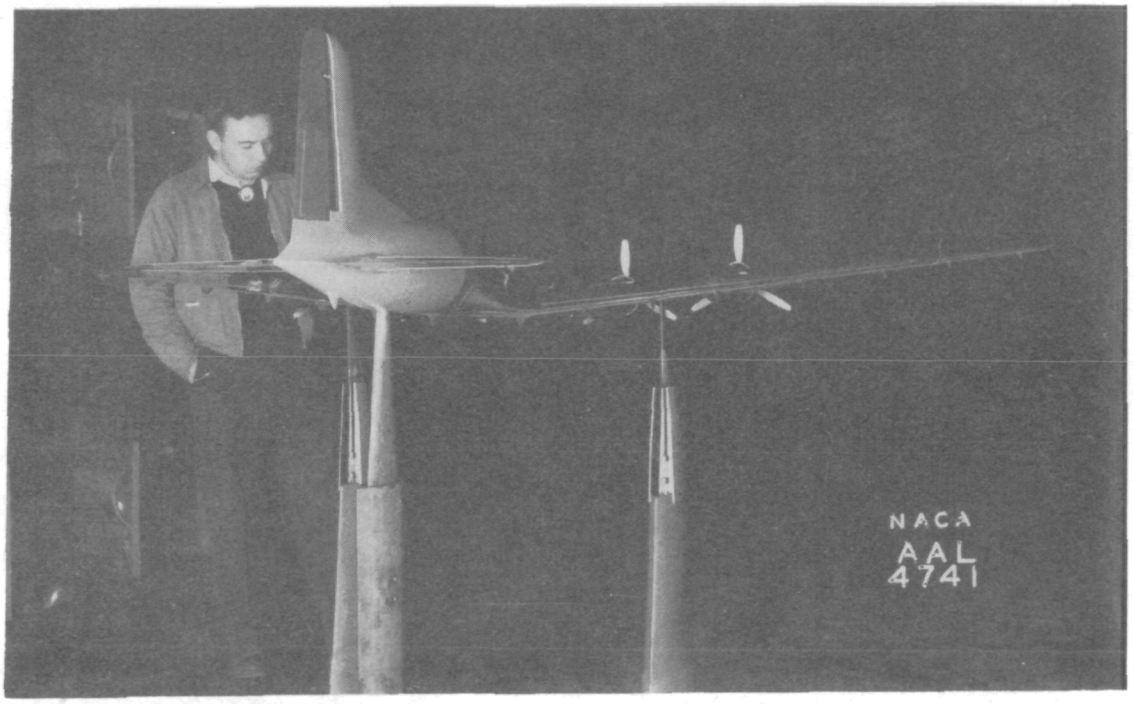

(a) Flaps undeflected and landing gear retracted.

Figure 6. - Photograph of test model mounted in the tunnel.

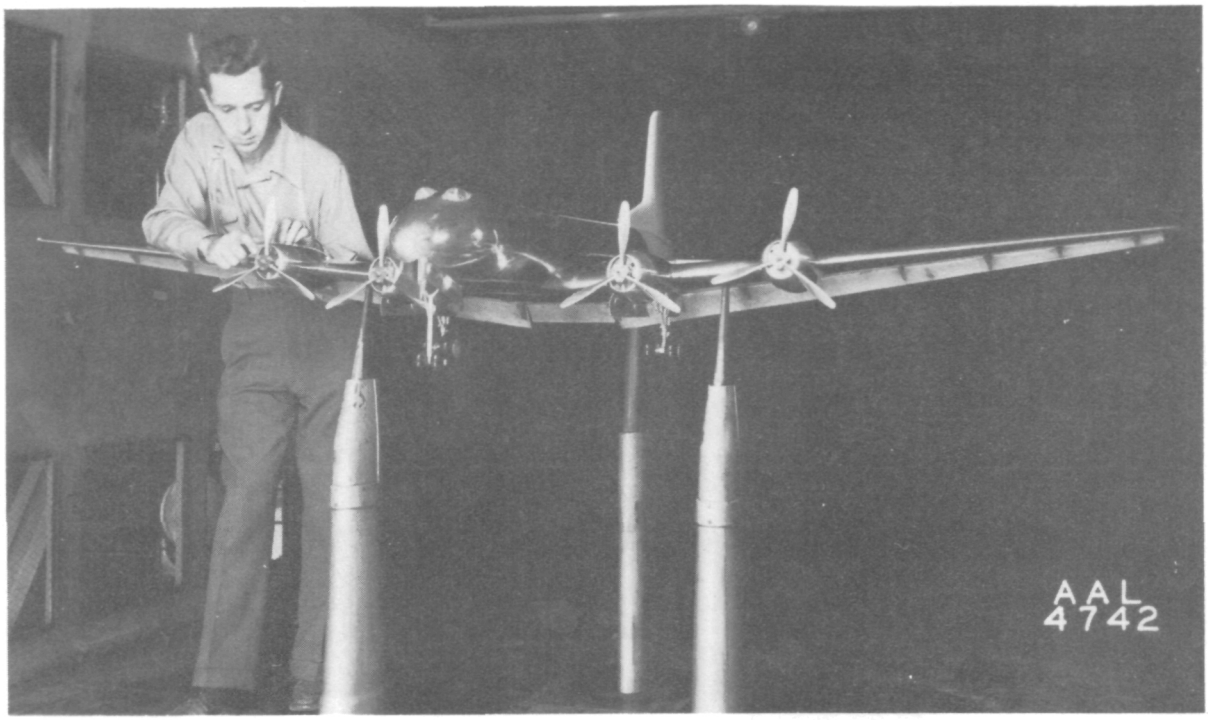

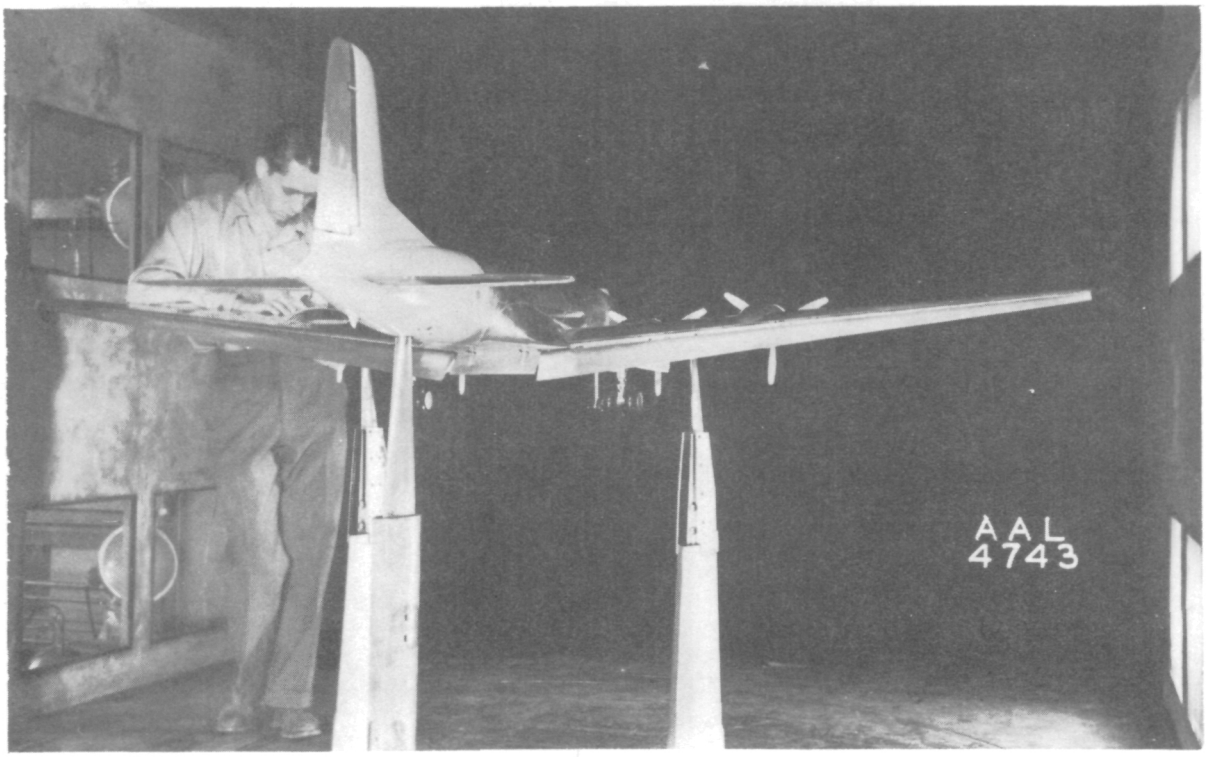

(b) Flaps deflected and landing gear extended.

Figure 6.- Concluded.

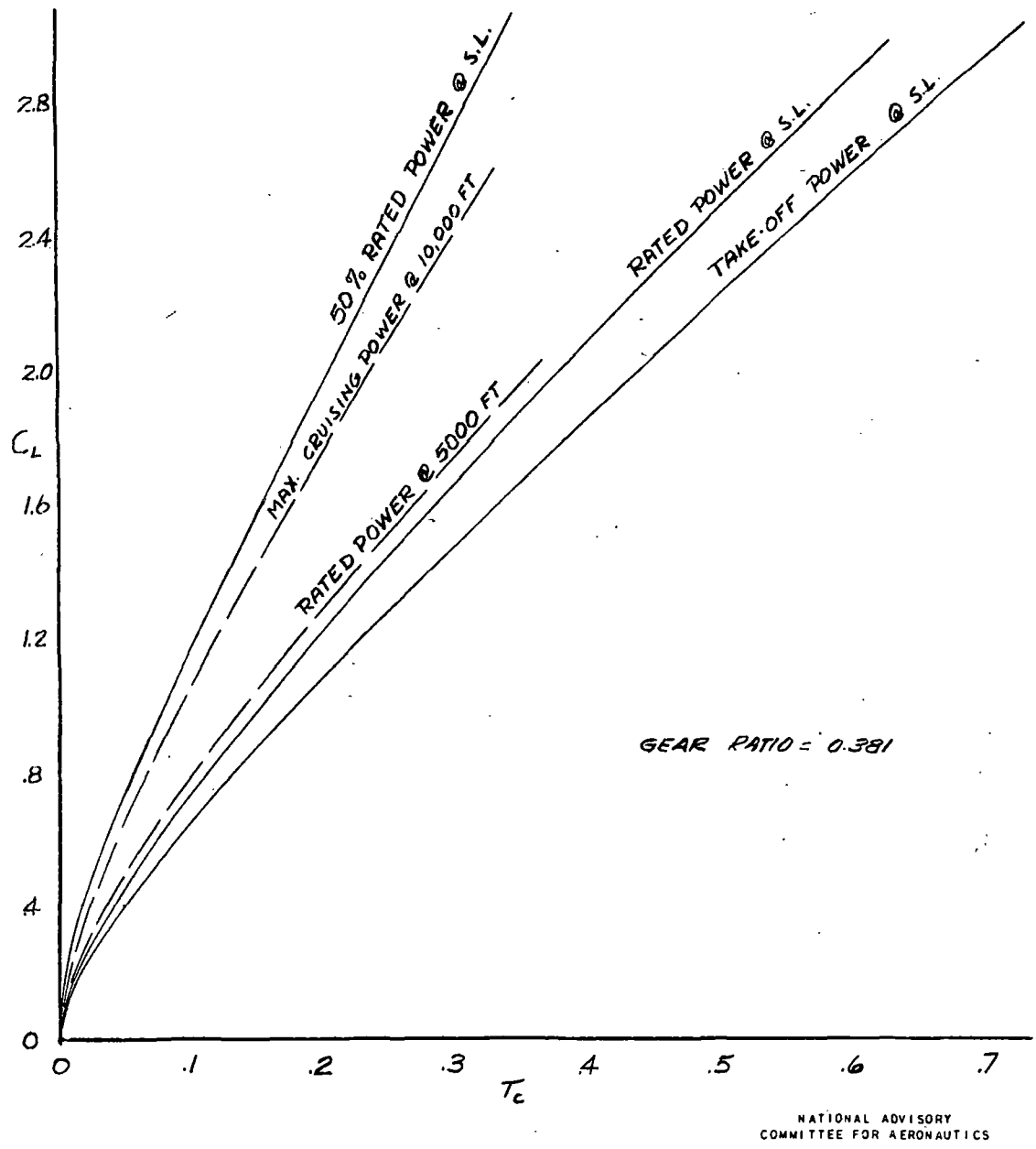

FIGURE 7. – THE VARIATION OF THRUST COEFFICIENT WITH LIFT COEFFICIENT FOR THE TEST AIRPLANE. GROSS WT = 125,000 LBS; PROPELLER DIAMETER = 19.0 FT.

EXPERIMENTALLY DETERMINED VARIATION OF T_c WITH V/nD FOR $\beta = 22°$

$$T_c = \frac{T_e}{\rho V^2 D^2}$$

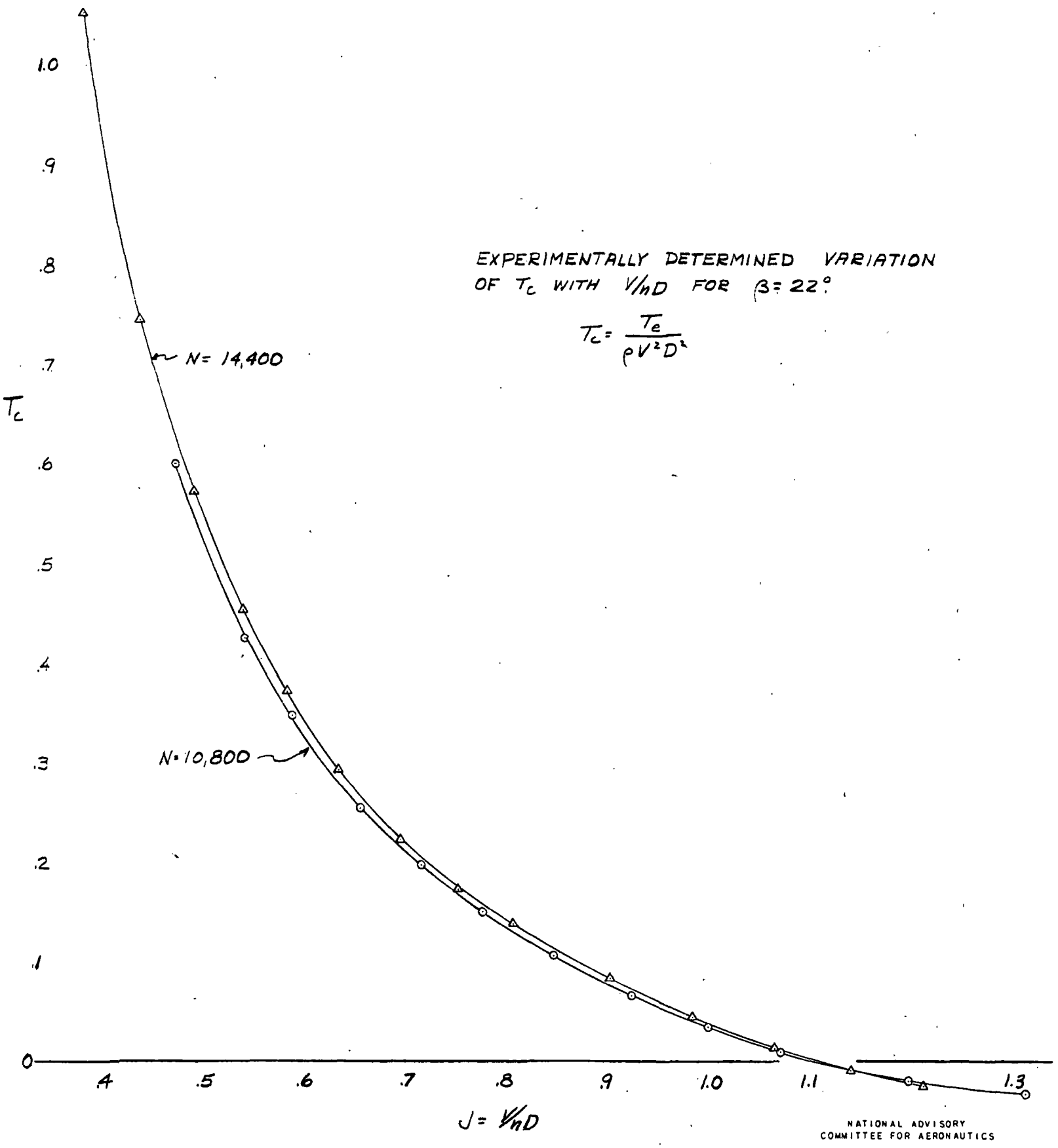

FIGURE 8.- THE VARIATION OF T_c WITH V/nD FOR THE TEST MODEL PROPELLERS. $\beta = 22°$; $\alpha = 0°$.

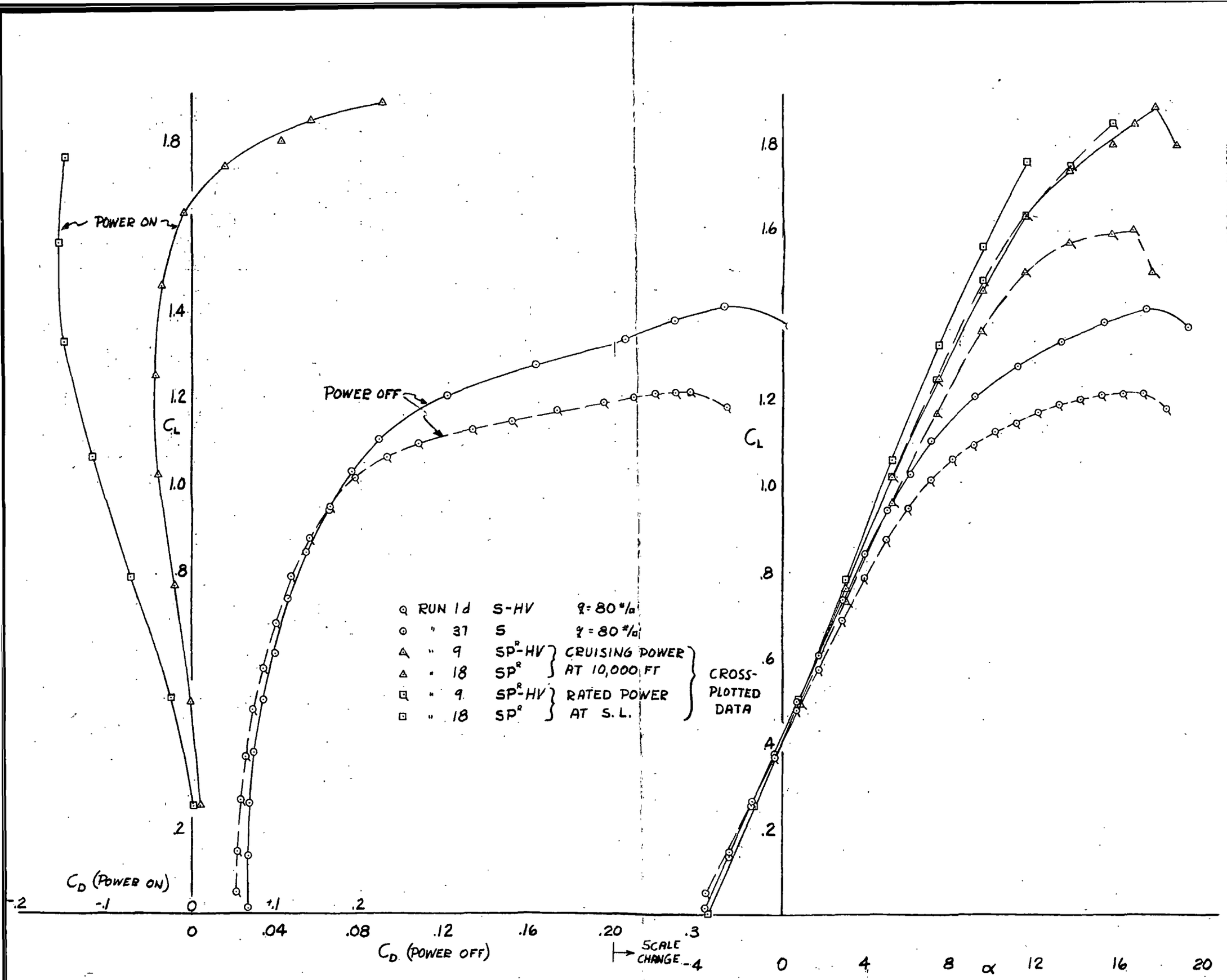

NATIONAL ADVISORY COMMITTEE FOR AERONAUTICS

FIGURE 9.- VARIATION OF AERODYNAMIC CHARACTERISTICS WITH LIFT COEFFICIENT SHOWING THE EFFECT OF POWER ON THE TEST MODEL. TAIL ON AND REMOVED; FLAPS UNDEFLECTED.

(a) C_D & α vs C_L

FIGURE 9.- (CONCLUDED)

(b) C_m & C_{h_e} VS C_L

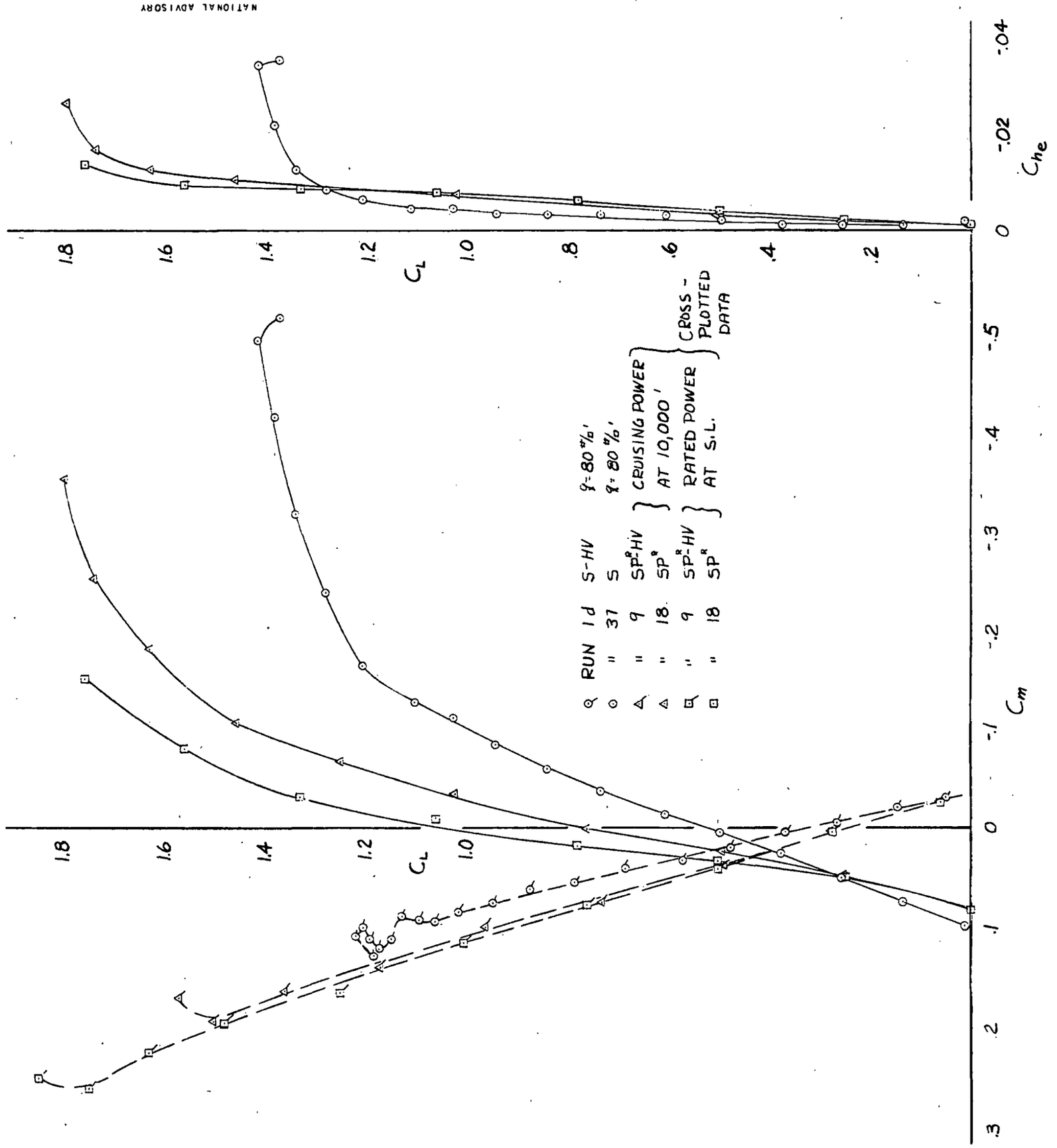

NATIONAL ADVISORY
COMMITTEE FOR AERONAUTICS

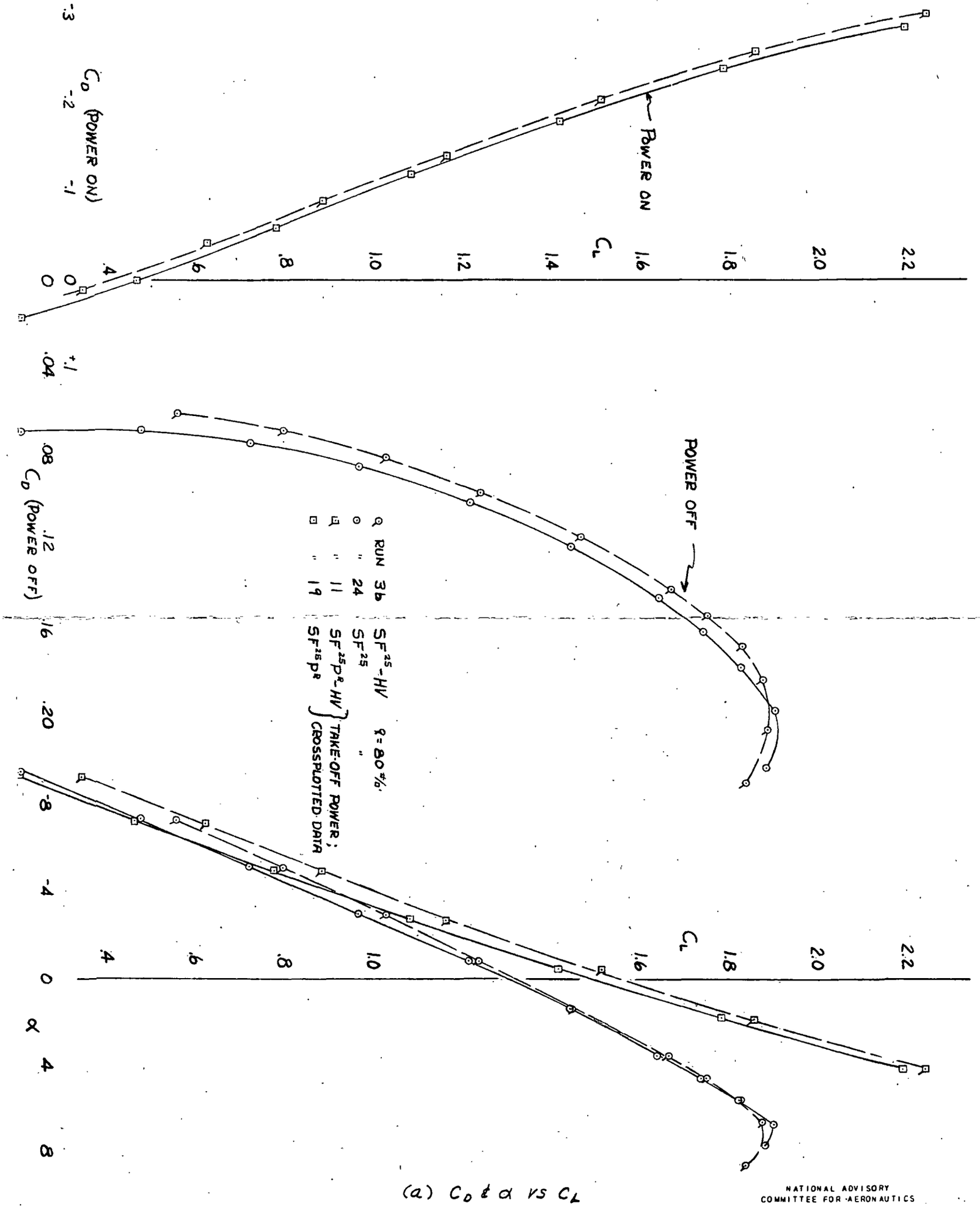

(a) C_D & α vs C_L

FIGURE 10.- VARIATION OF AERODYNAMIC CHARACTERISTICS WITH LIFT COEFFICIENT SHOWING THE EFFECT OF POWER ON THE TEST MODEL. TAIL ON AND REMOVED; FLAPS DEFLECTED 25°.

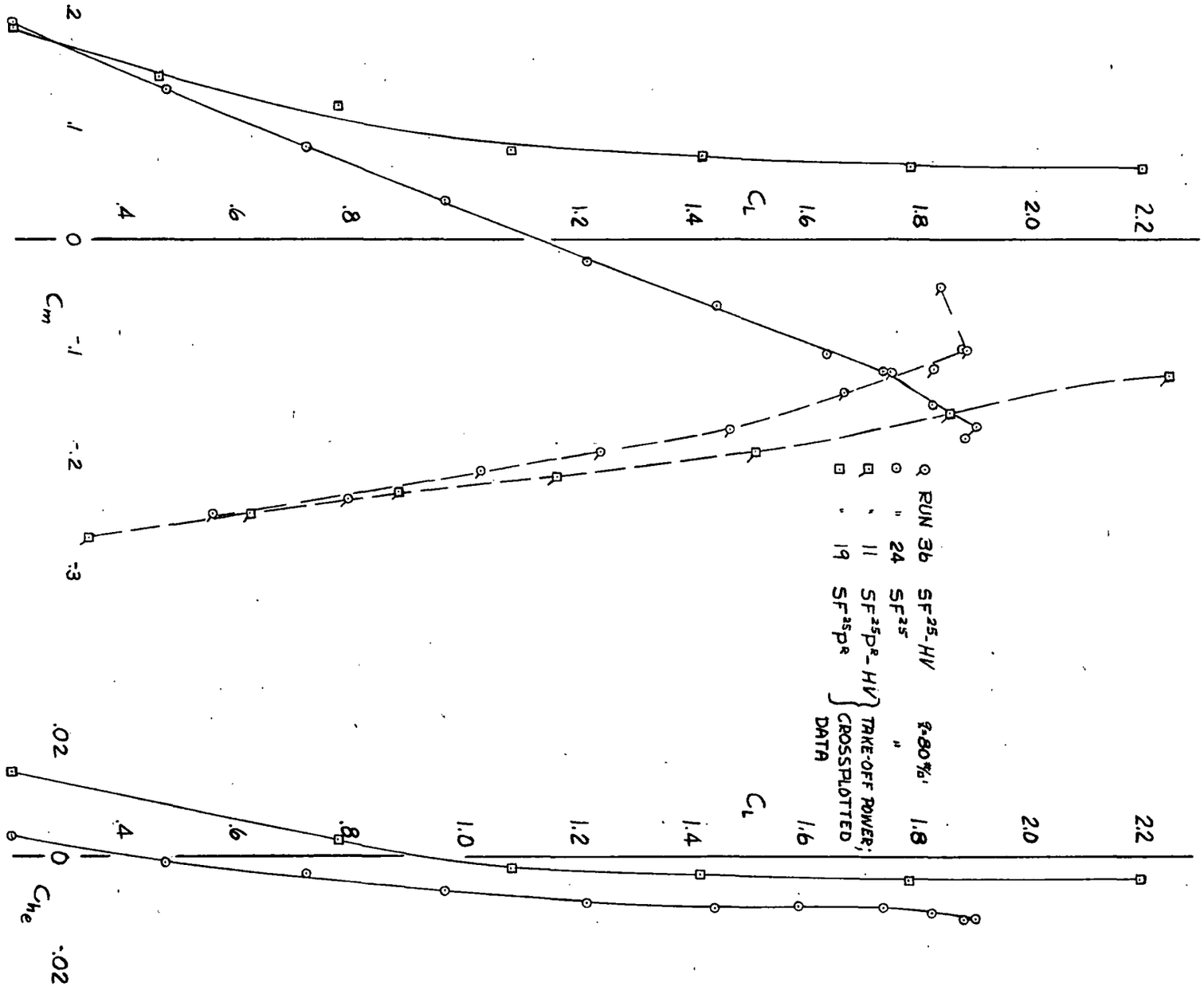

(b) C_m & C_{he} VS C_L

NATIONAL ADVISORY COMMITTEE FOR AERONAUTICS

FIGURE 10.- (CONCLUDED)

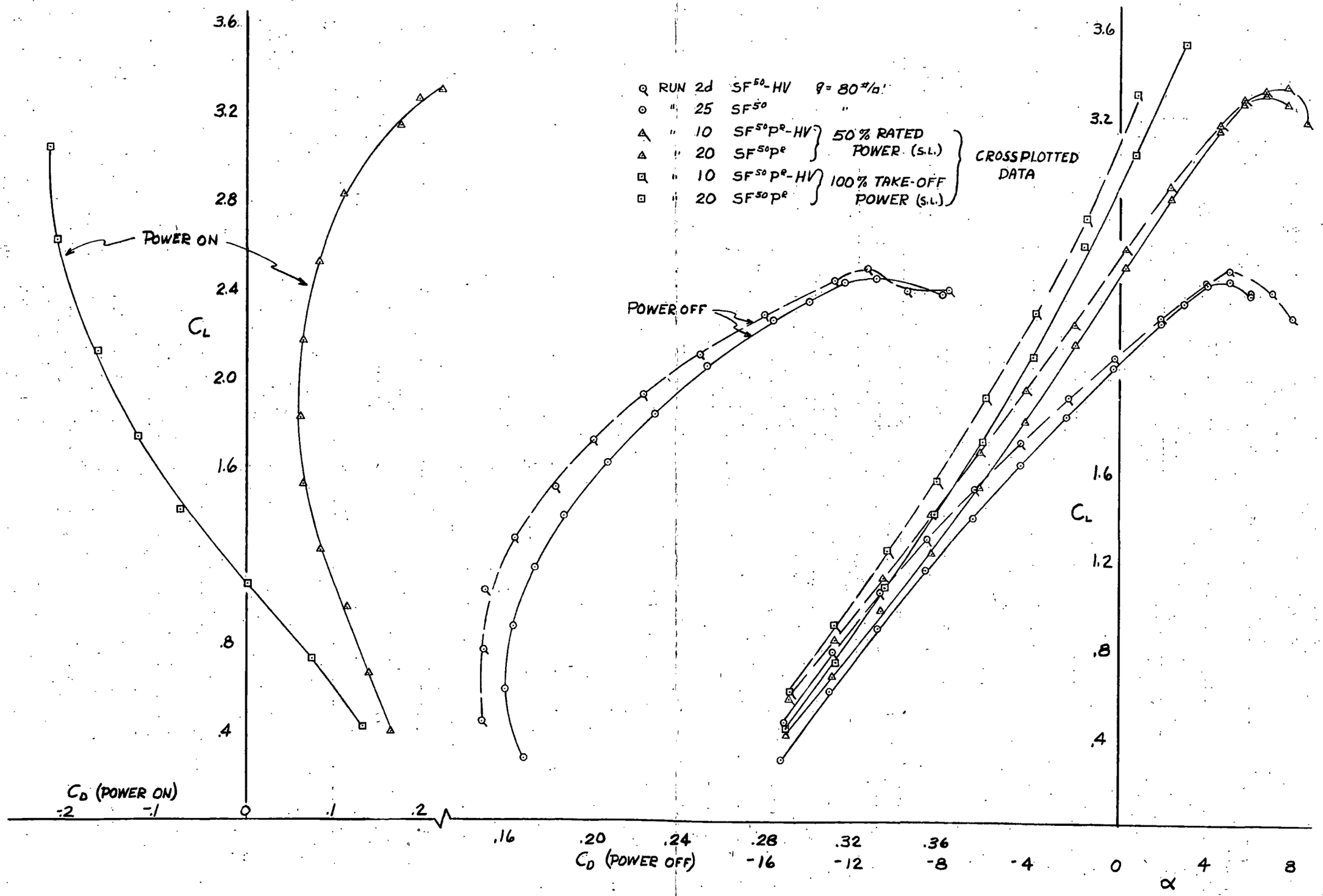

NATIONAL ADVISORY COMMITTEE FOR AERONAUTICS

FIGURE 11.- VARIATION OF AERODYNAMIC CHARACTERISTICS WITH LIFT COEFFICIENT SHOWING THE EFFECTS OF POWER ON THE TEST MODEL. TAIL ON AND REMOVED; FLAPS DEFLECTED 50°.

(a) C_D & α vs C_L

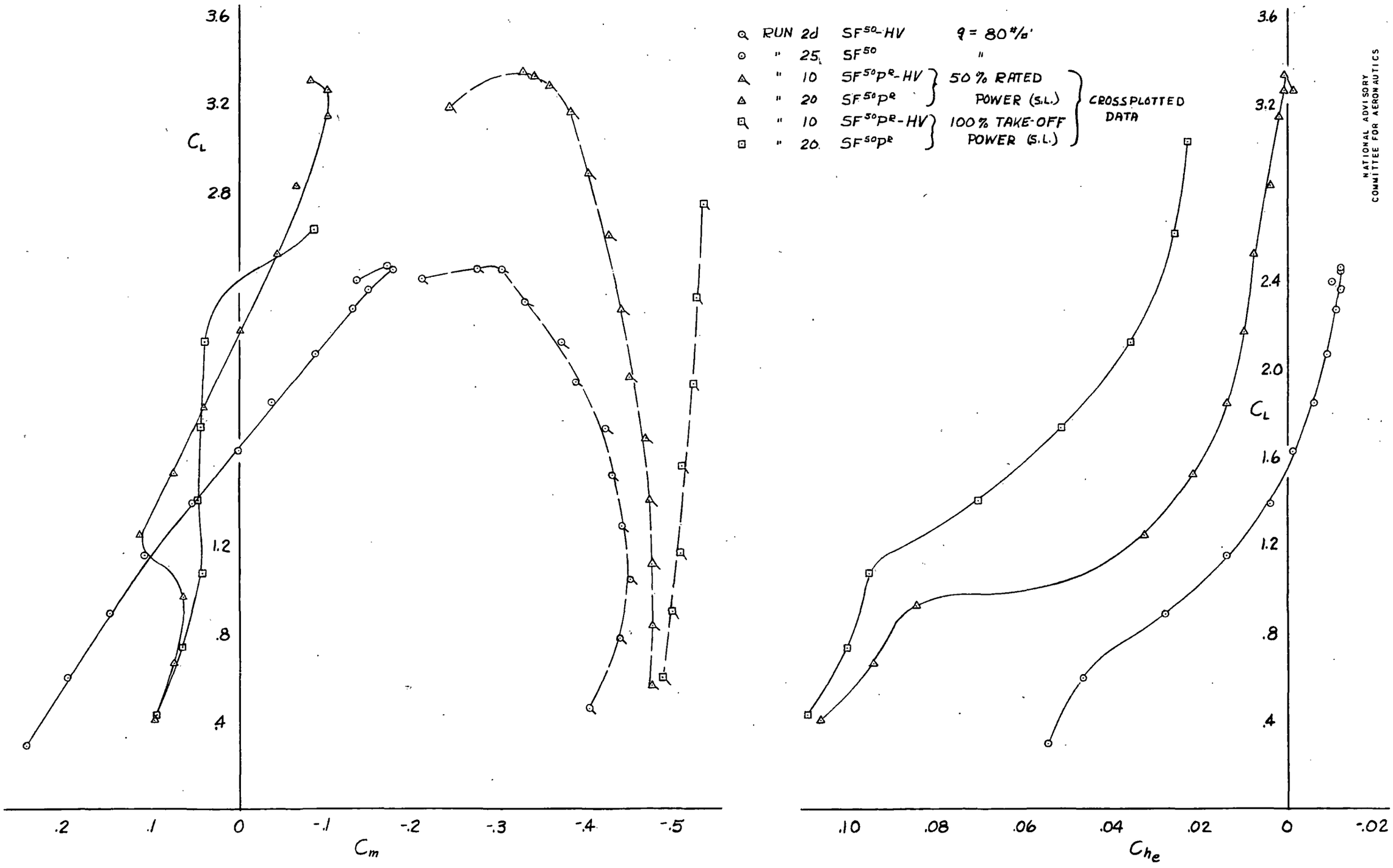

(6) C_m & C_L VS C_L

FIGURE 11.- (CONCLUDED)

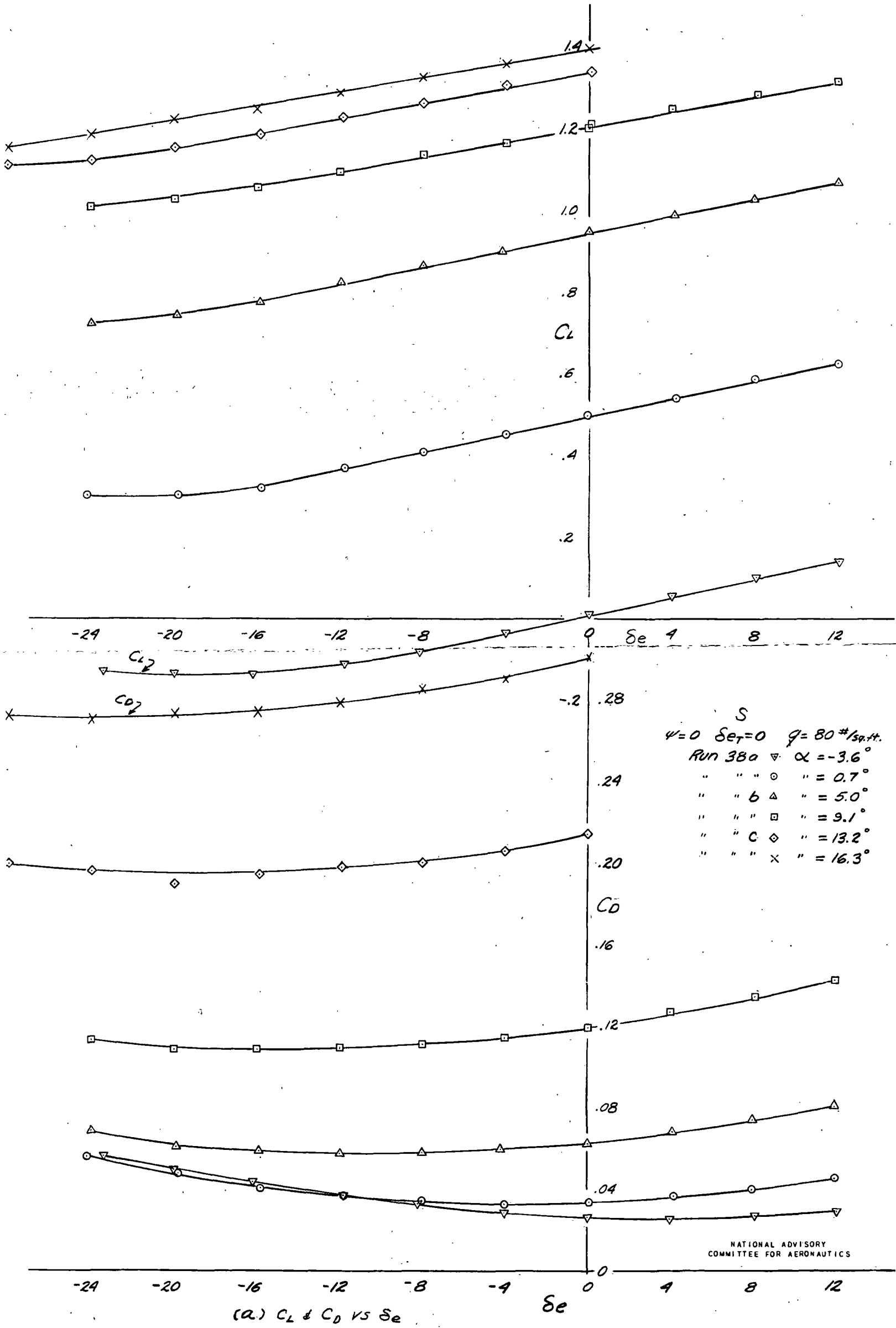

(a) C_L & C_D vs δ_e

FIGURE 12. - VARIATION OF AERODYNAMIC CHARACTERISTICS WITH ELEVATOR ANGLE FOR THE TEST MODEL; FLAPS AND GEAR RETRACTED; ELEVATOR TAB UNDEFLECTED; PROPELLERS REMOVED.

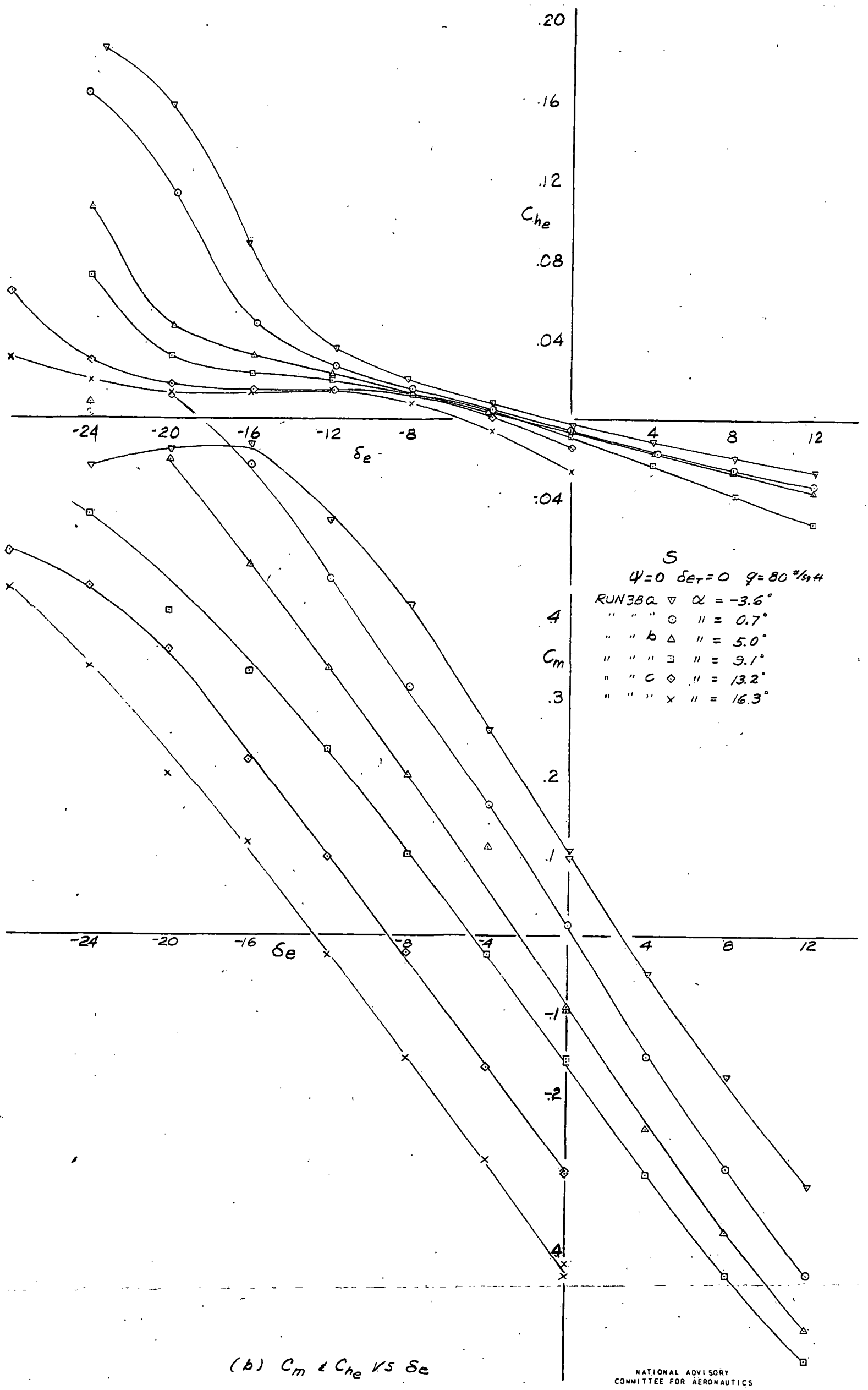

(b) C_m & C_{he} VS δe

FIGURE 12.-(CONCLUDED)

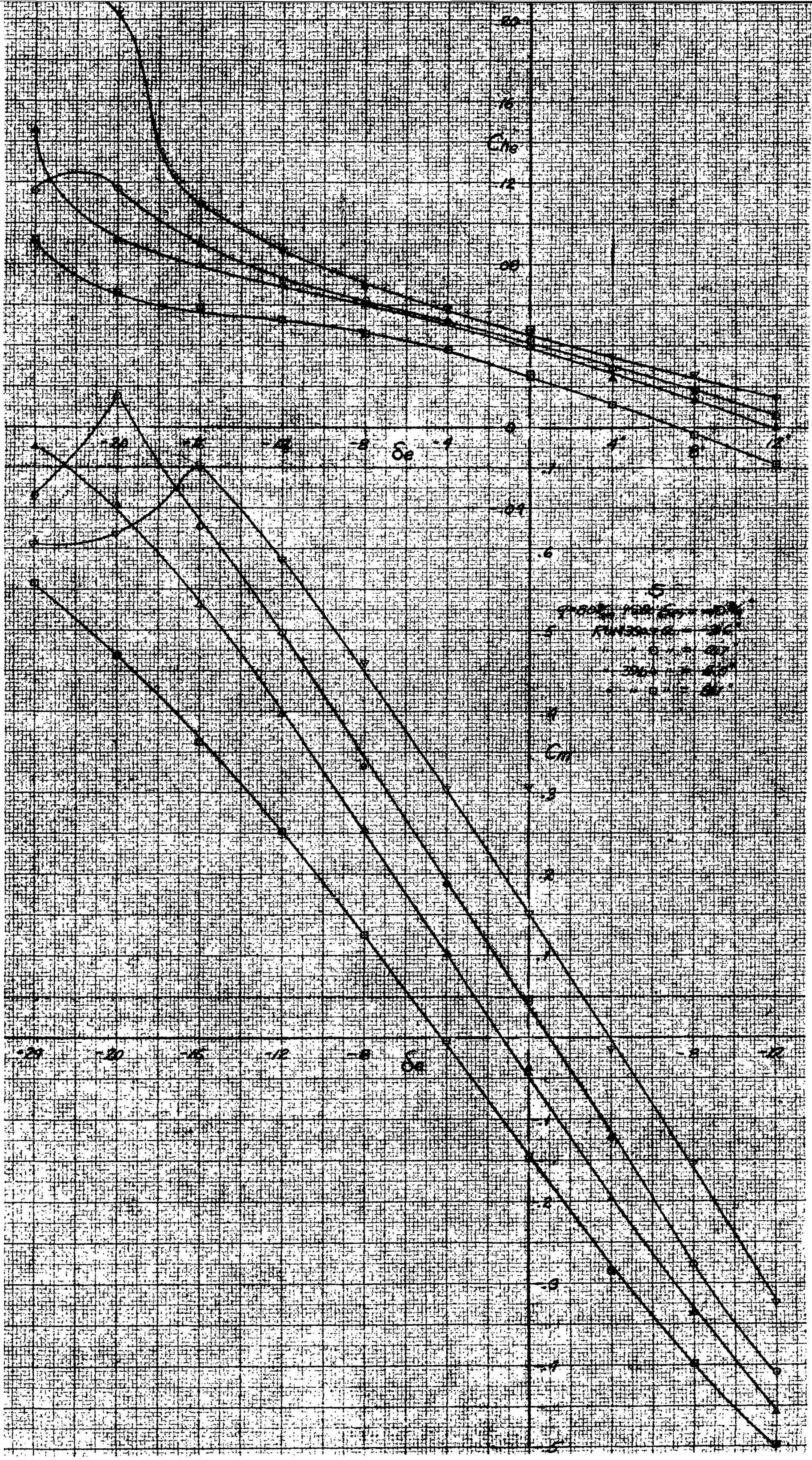

FIGURE 13.- VARIATION OF ELEVATOR HINGE-MOMENT AND PITCHING-MOMENT COEFFICIENTS WITH ELEVATOR ANGLE FOR THE TEST MODEL; FLAPS AND GEAR RETRACTED; ELEVATOR TAB DEFLECTED UP 10 3/4°, PROPELLERS REMOVED.

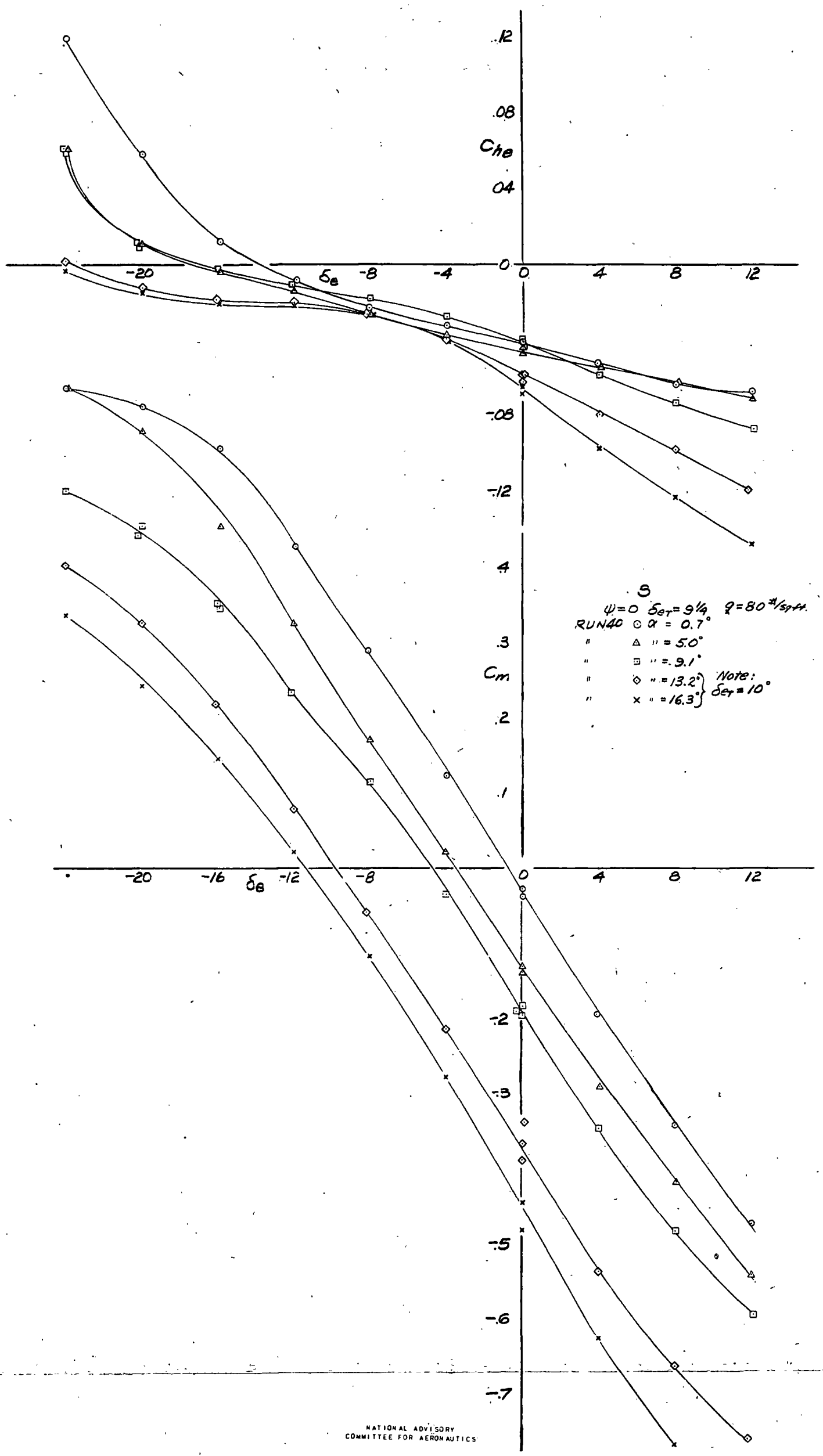

FIGURE 14.- VARIATION OF ELEVATOR HINGE-MOMENT AND PITCHING-MOMENT COEFFICIENTS WITH ELEVATOR ANGLE FOR THE TEST MODEL; FLAPS AND GEAR RETRACTED, ELEVATOR TAB DEFLECTED DOWN 9¼°, PROPELLERS REMOVED

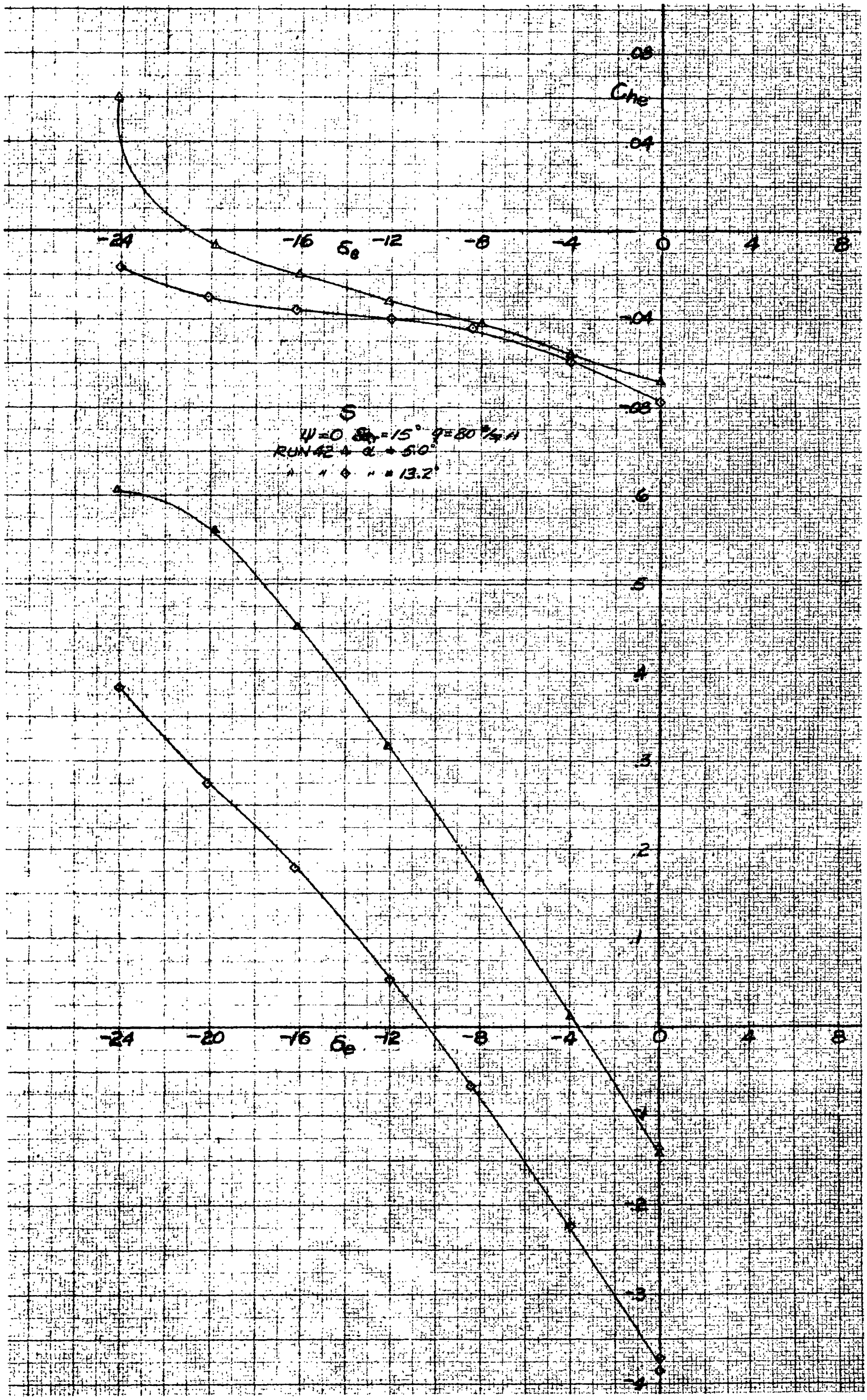

FIGURE 15.- VARIATION OF ELEVATOR HINGE-MOMENT AND PITCHING-MOMENT COEFFICIENTS WITH ELEVATOR ANGLE FOR THE TEST MODEL; FLAPS AND GEAR RETRACTED, ELEVATOR TAB DEFLECTED DOWN 15°, PROPELLERS REMOVED.

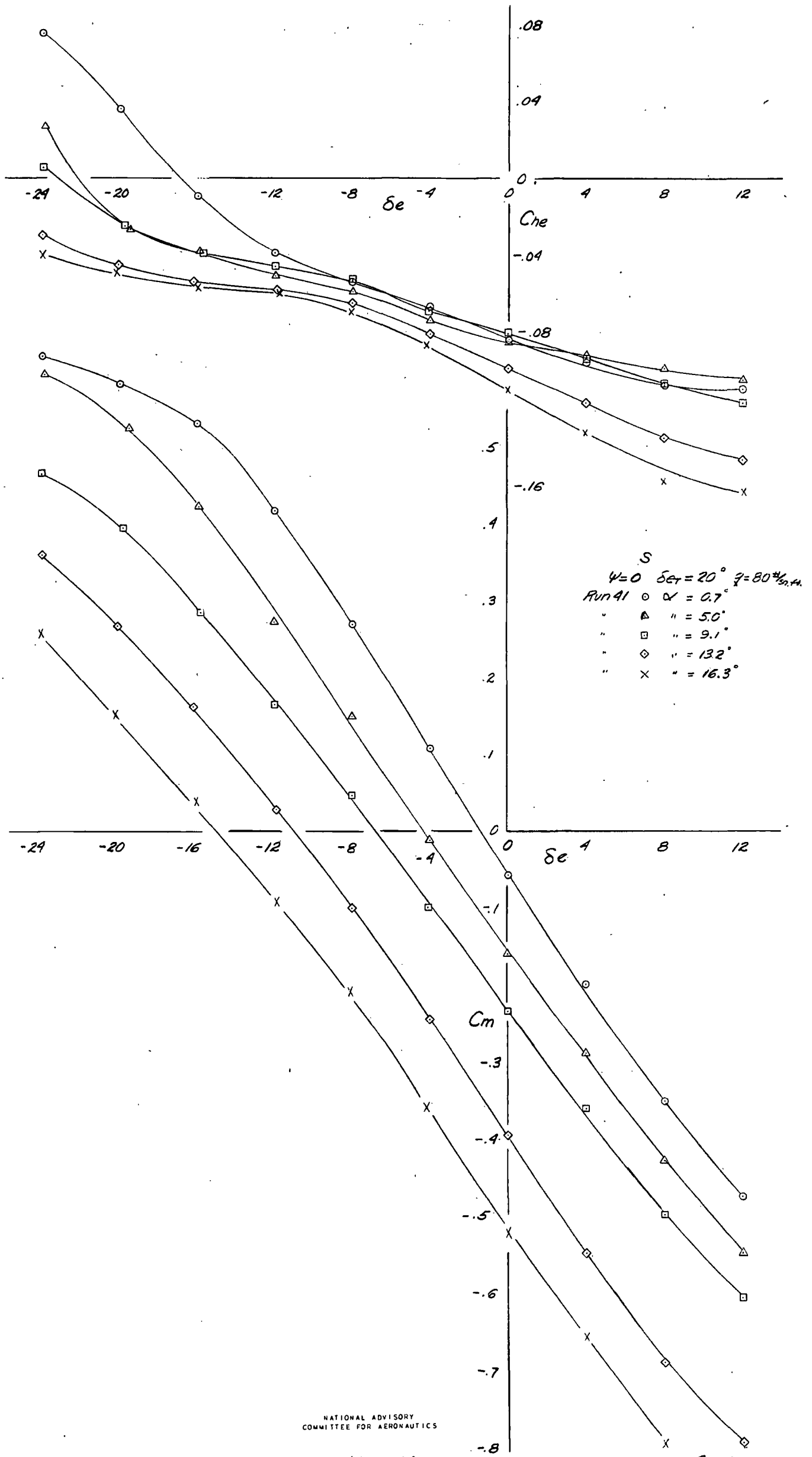

FIGURE 16. - VARIATION OF ELEVATOR HINGE-MOMENT AND PITCHING-MOMENT COEFFICIENTS WITH ELEVATOR ANGLE FOR THE TEST MODEL; FLAPS AND GEAR RETRACTED, ELEVATOR TAB DEFLECTED DOWN 20°; PROPELLERS REMOVED.

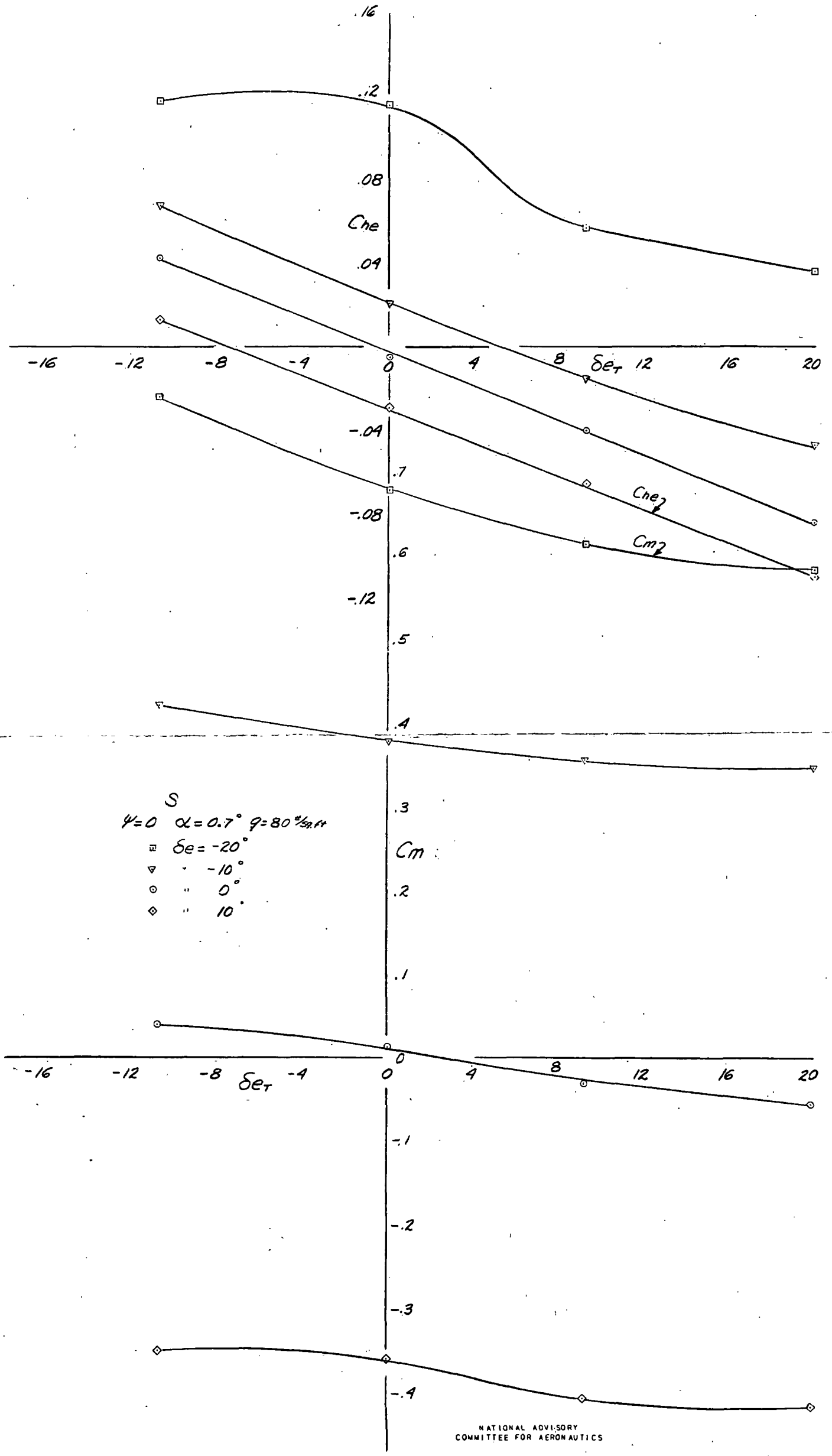

FIGURE 17. - VARIATION OF ELEVATOR HINGE-MOMENT AND PITCHING-MOMENT COEFFICIENTS WITH ELEVATOR TAB ANGLE FOR THE TEST MODEL; FLAPS AND GEAR RETRACTED, FOR 0° ANGLE OF ATTACK, PROPELLERS REMOVED.

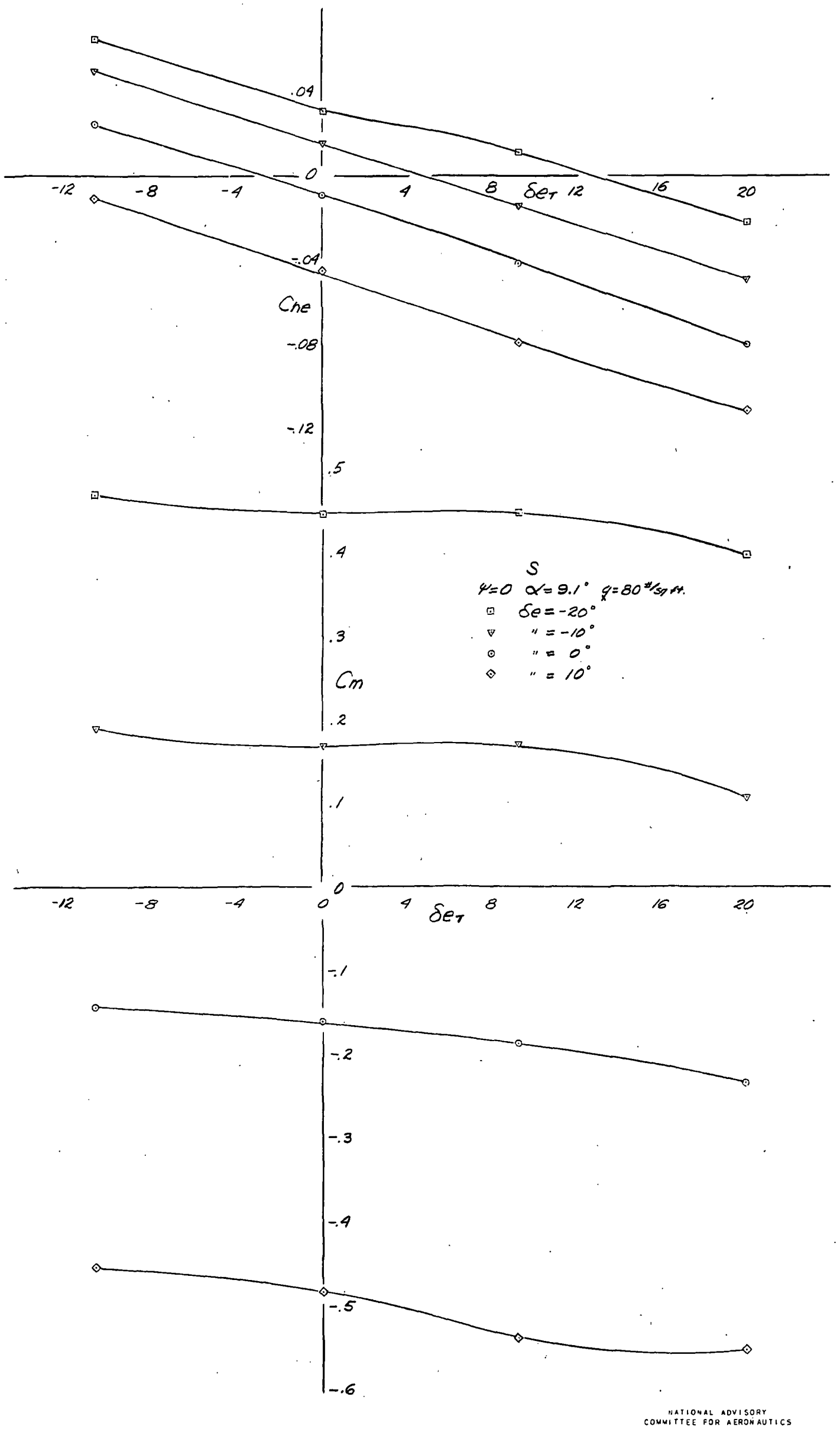

FIGURE 18. - VARIATION OF ELEVATOR HINGE-MOMENT AND PITCHING-MOMENT COEFFICIENTS WITH ELEVATOR TAB ANGLE FOR THE TEST MODEL; FLAPS AND GEAR RETRACTED, FOR 8° ANGLE OF ATTACK. PROPELLERS REMOVED.

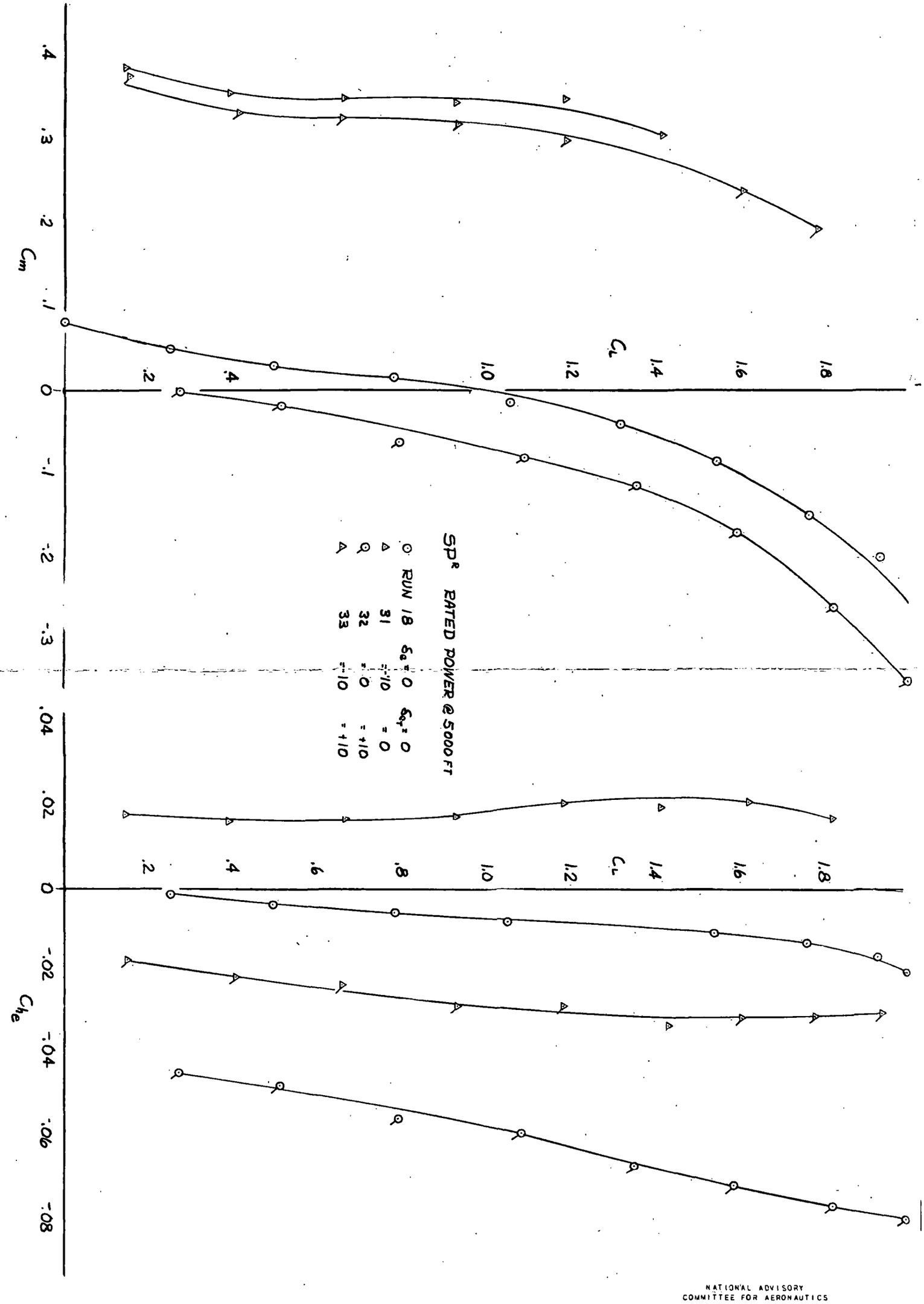

FIGURE 19.- VARIATION OF PITCHING-MOMENT AND ELEVATOR HINGE-MOMENT COEFFICIENTS WITH LIFT COEFFICIENT FOR THE TEST MODEL. RATED POWER AT 5000 FT SIMULATED.

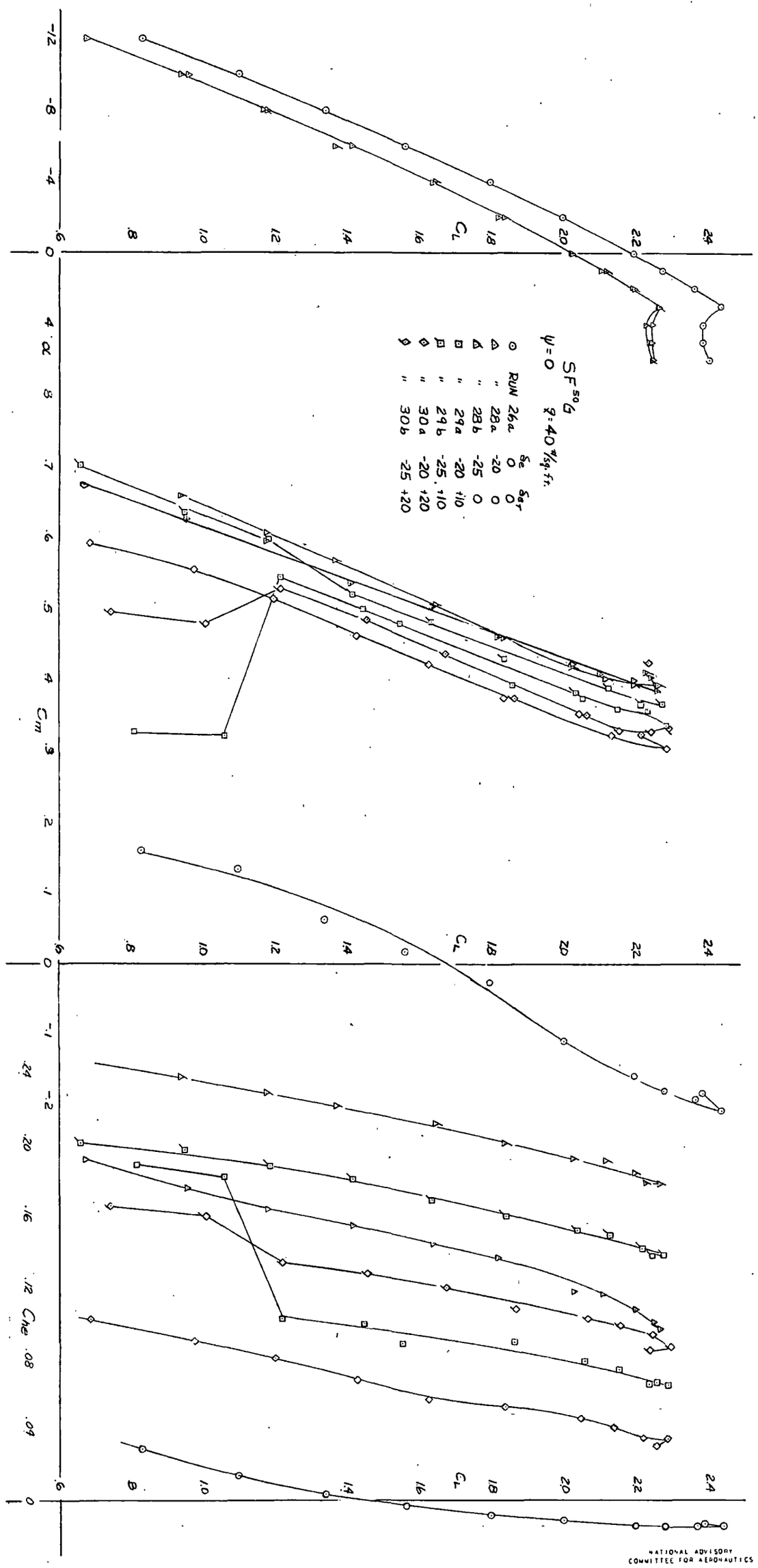

FIGURE 20.- THE LONGITUDINAL CHARACTERISTICS OF THE TEST MODEL FOR SEVERAL ELEVATOR AND TAB DEFLECTIONS; FLAPS EXTENDED 50° AND GEAR EXTENDED, PROPELLERS REMOVED.

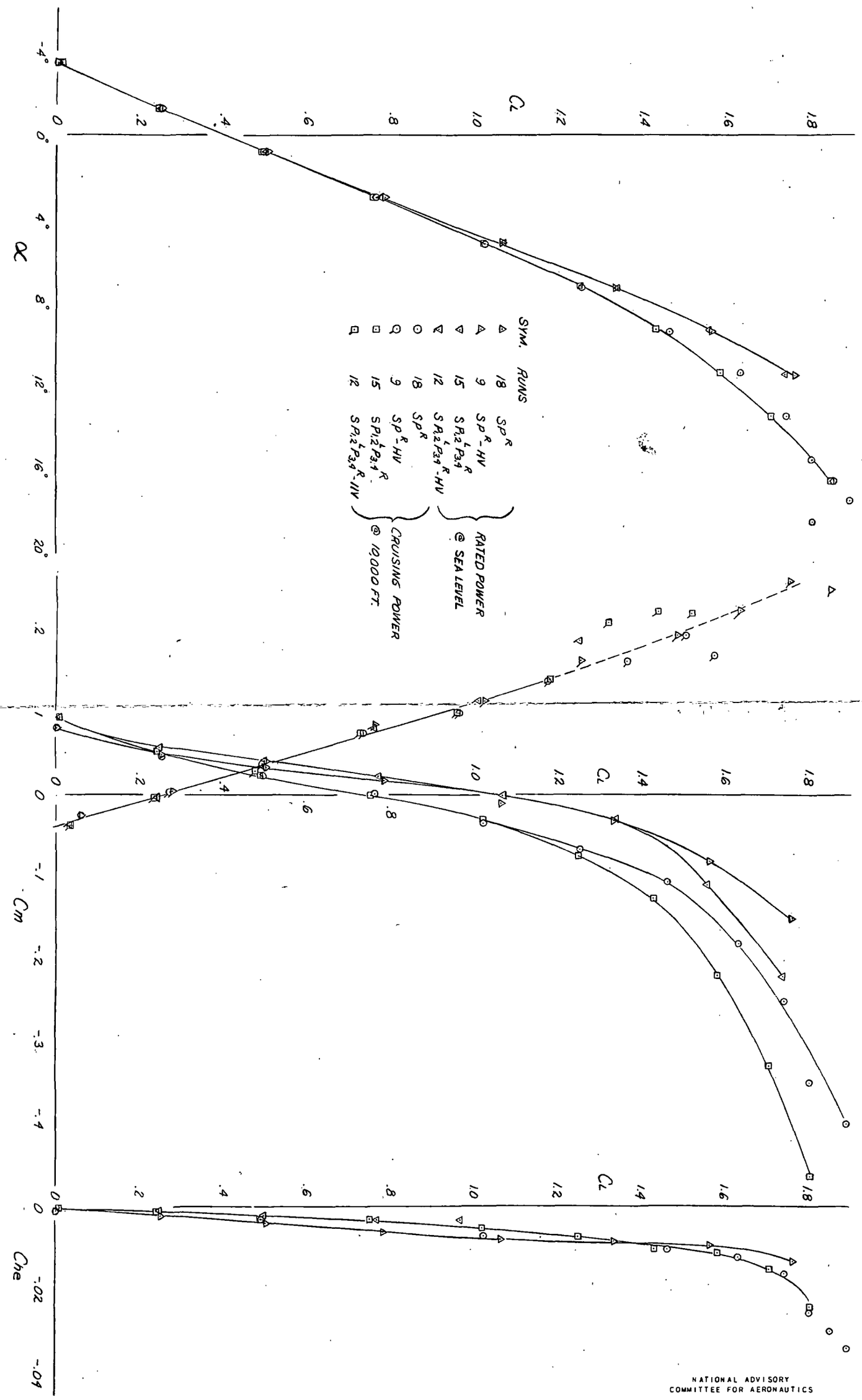

FIGURE 21.— THE EFFECT OF DIRECTION OF PROPELLER ROTATION ON THE AERODYNAMIC CHARACTERISTICS OF THE TEST MODEL. TAIL ON AND REMOVED; FLAPS UNDEFLECTED.

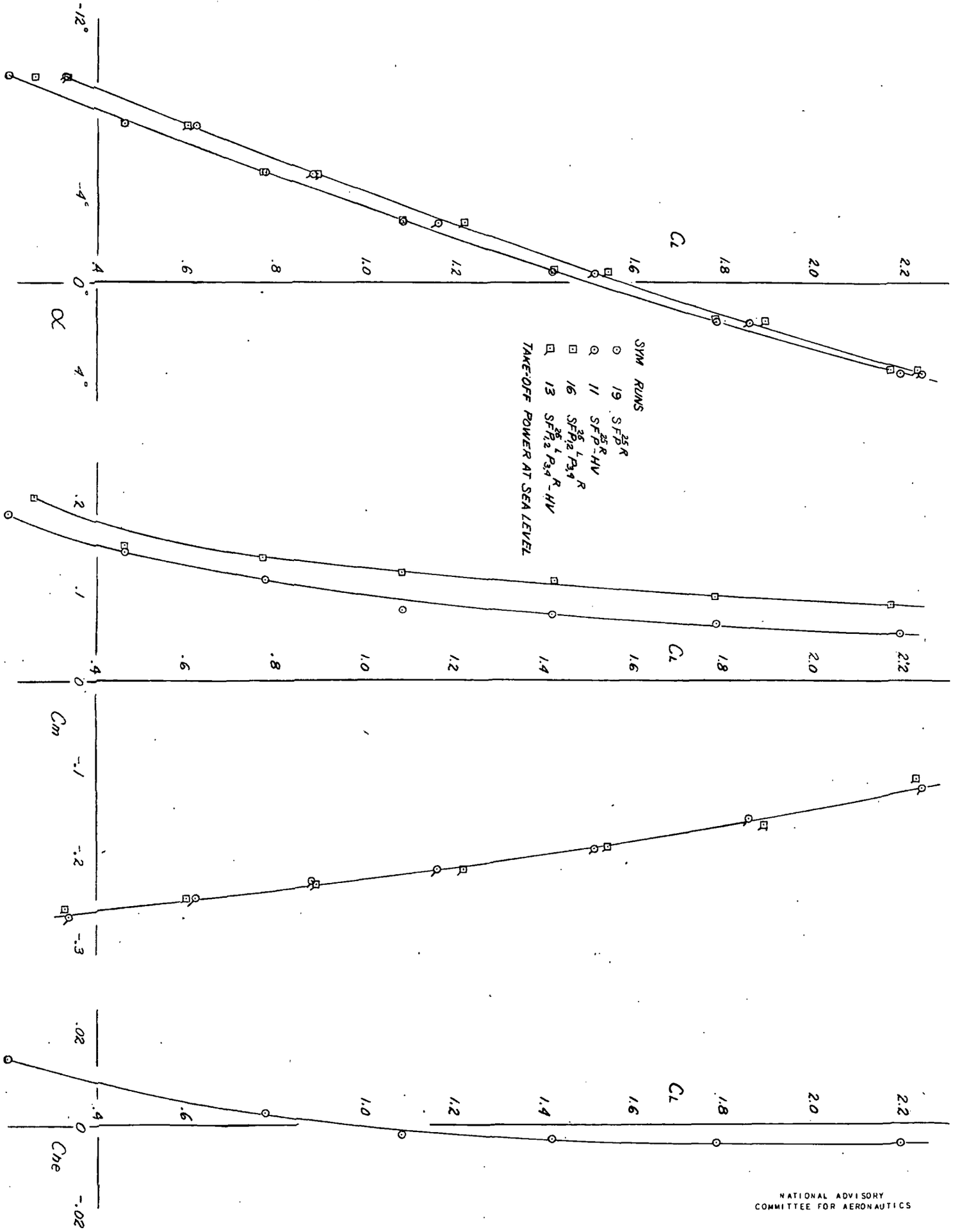

FIGURE 22.— THE EFFECT OF DIRECTION OF PROPELLER ROTATION ON THE AERODYNAMIC CHARACTERISTICS OF THE TEST MODEL. TAIL ON AND REMOVED; FLAPS DEFLECTED 25°; TAKE-OFF POWER.

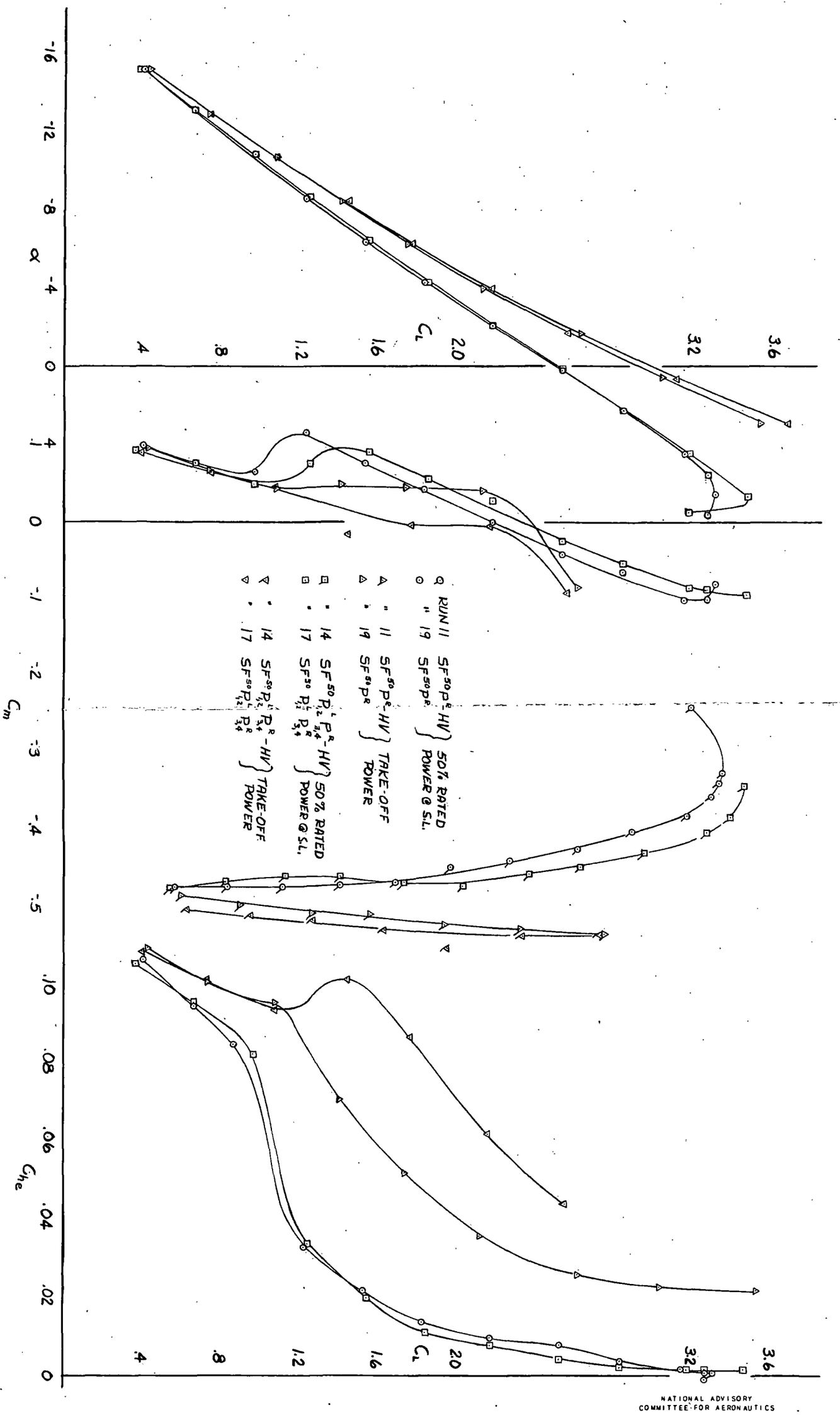

FIGURE 23. - THE EFFECT OF DIRECTION OF PROPELLER ROTATION ON THE AERODYNAMIC CHARACTERISTICS OF THE TEST MODEL. TAIL ON AND REMOVED; FLAPS DEFLECTED 50°.

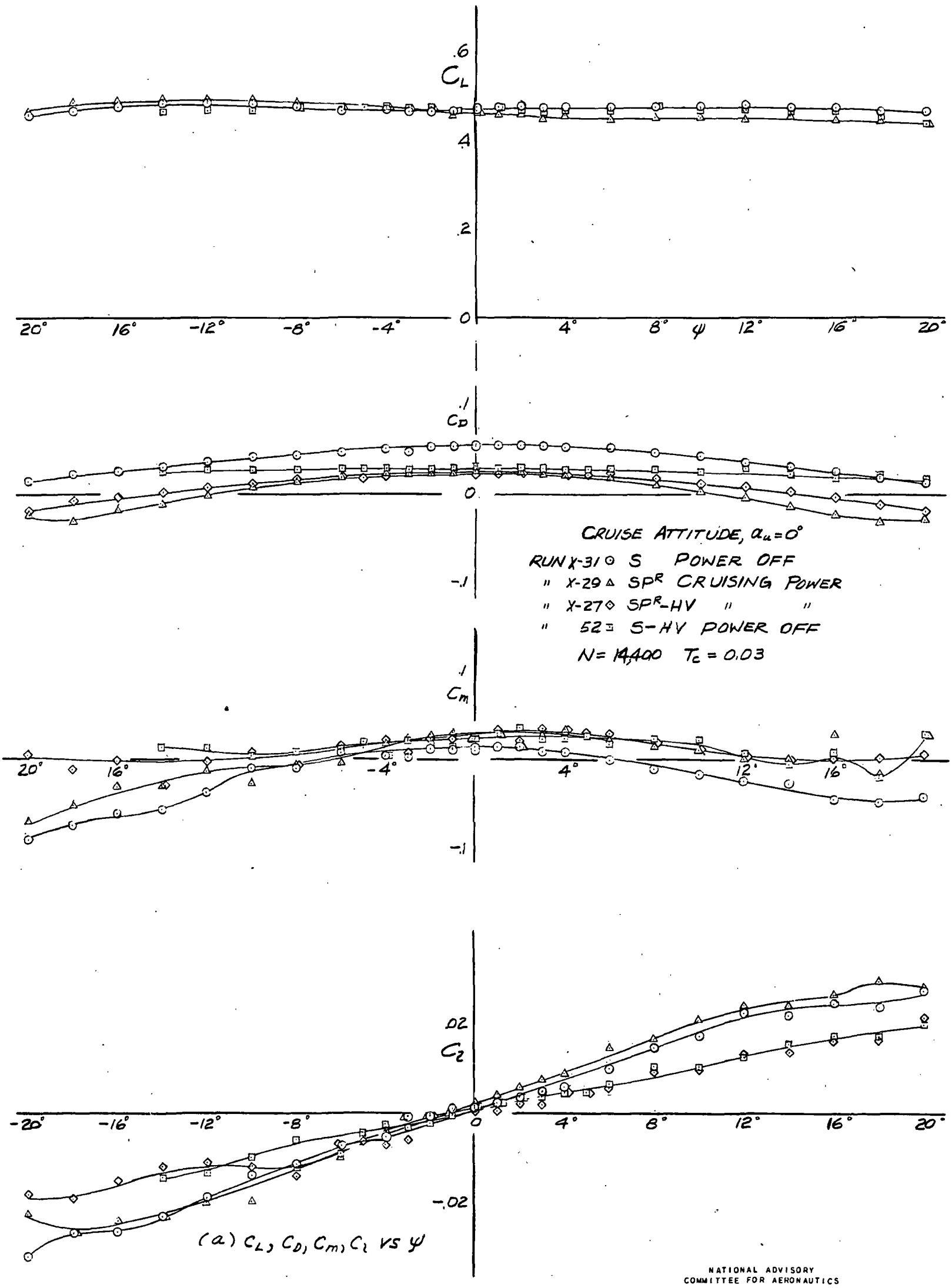

FIGURE 24.- VARIATION OF AERODYNAMIC CHARACTERISTICS WITH ANGLE OF YAW FOR THE TEST MODEL. TAIL ON AND REMOVED; PROPELLERS REMOVED AND CRUISING POWER; CRUISING ATTITUDE.

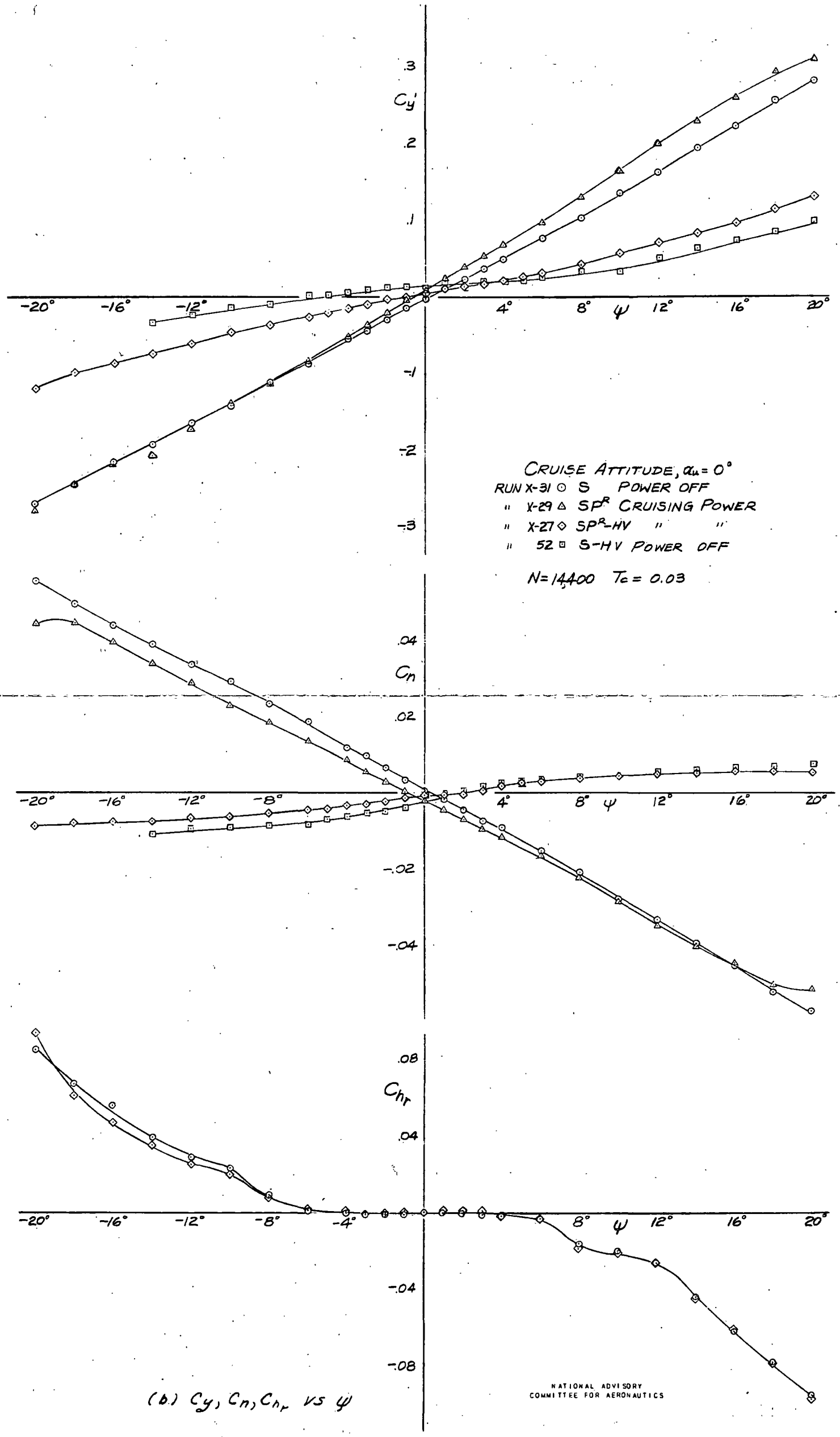

(b.) C_y, C_n, C_{h_r} vs ψ

FIGURE 24 .— (CONCLUDED).

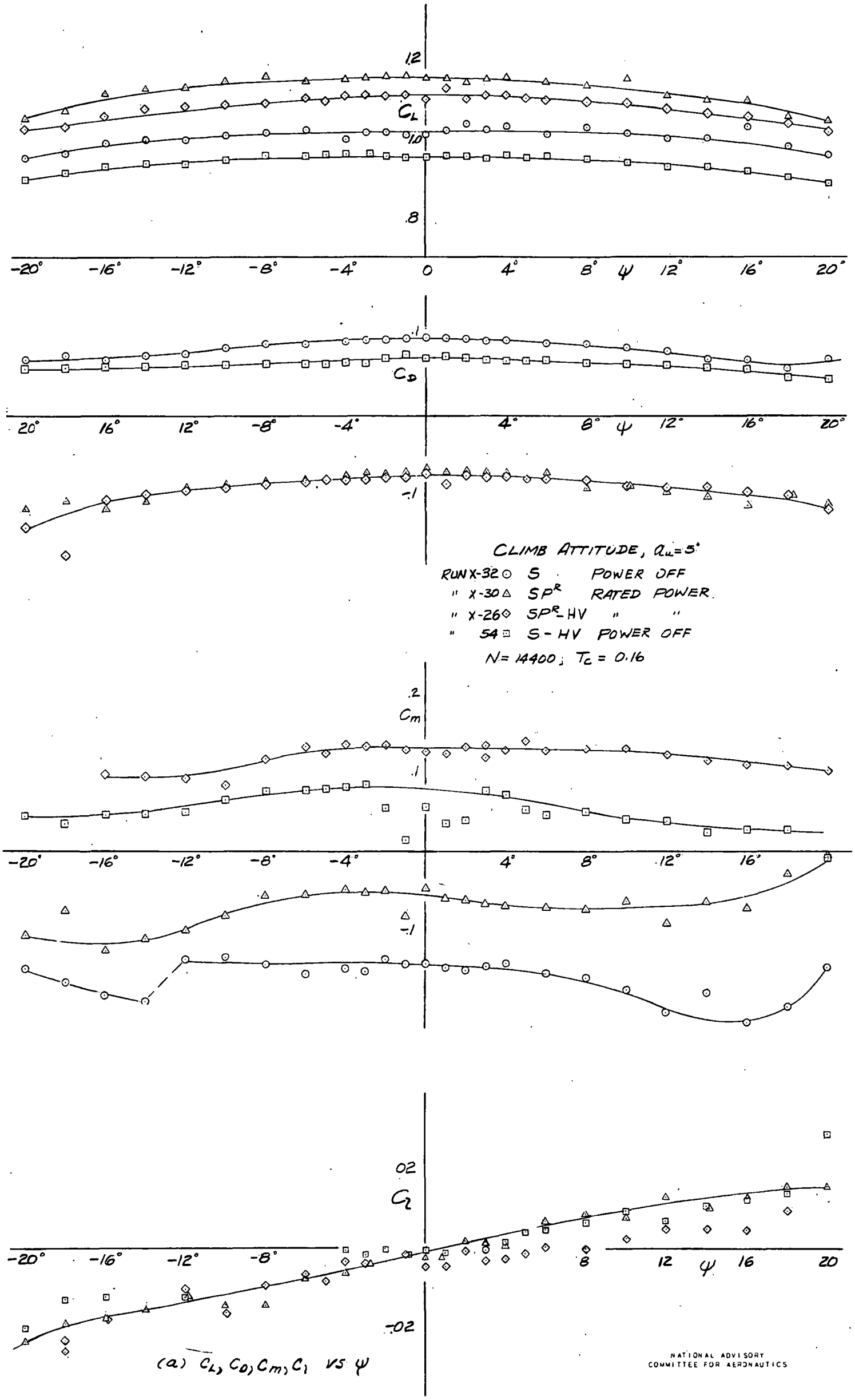

FIGURE 25 .-VARIATION OF AERODYNAMIC CHARACTERISTICS WITH ANGLE OF YAW FOR THE TEST MODEL; TAIL ON AND REMOVED; PROPELLERS REMOVED AND RATED POWER; CLIMBING ATTITUDE.

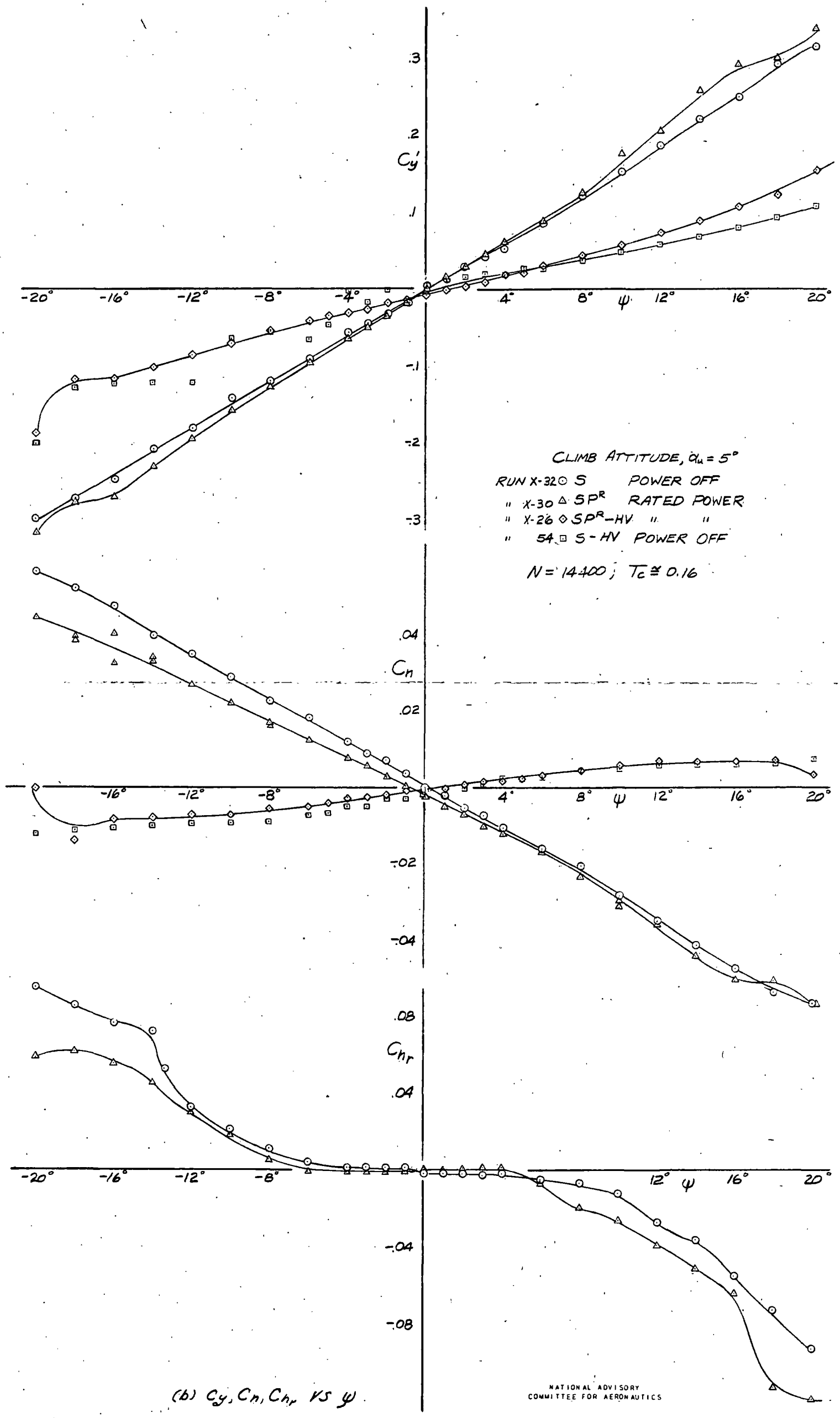

(b) C_y, C_n, C_{h_r} VS ψ.

FIGURE 25.— (CONCLUDED).

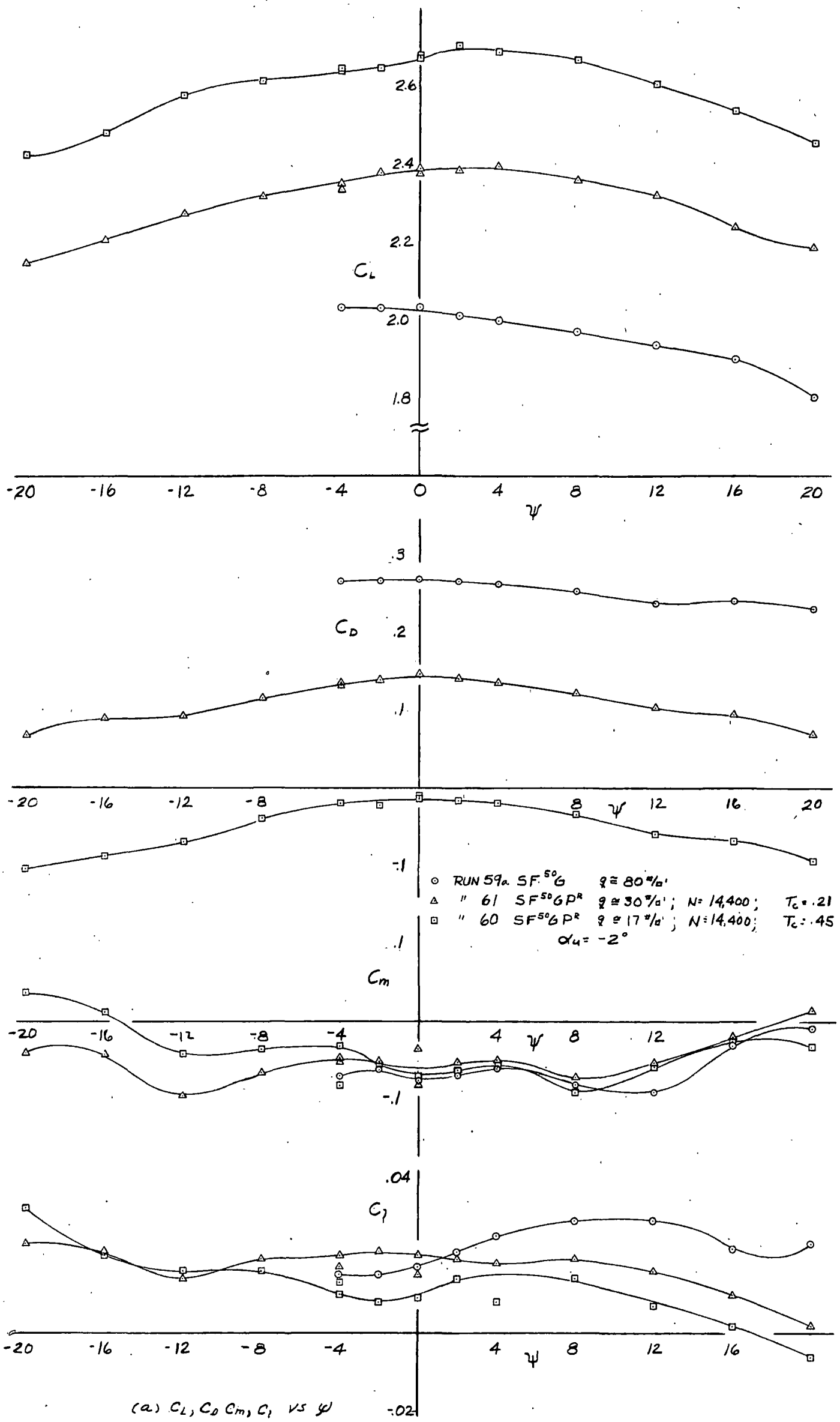

(a) C_L, C_D C_m, C_l vs ψ

NATIONAL ADVISORY COMMITTEE FOR AERONAUTICS

FIGURE 26.- VARIATION OF AERODYNAMIC CHARACTERISTICS WITH ANGLE OF YAW FOR THE TEST MODEL. TAIL ON ; FLAPS DEFLECTED 50°; LANDING GEAR EXTENDED; PROPELLERS REMOVED, 50% RATED POWER AND TAKE-OFF POWER.

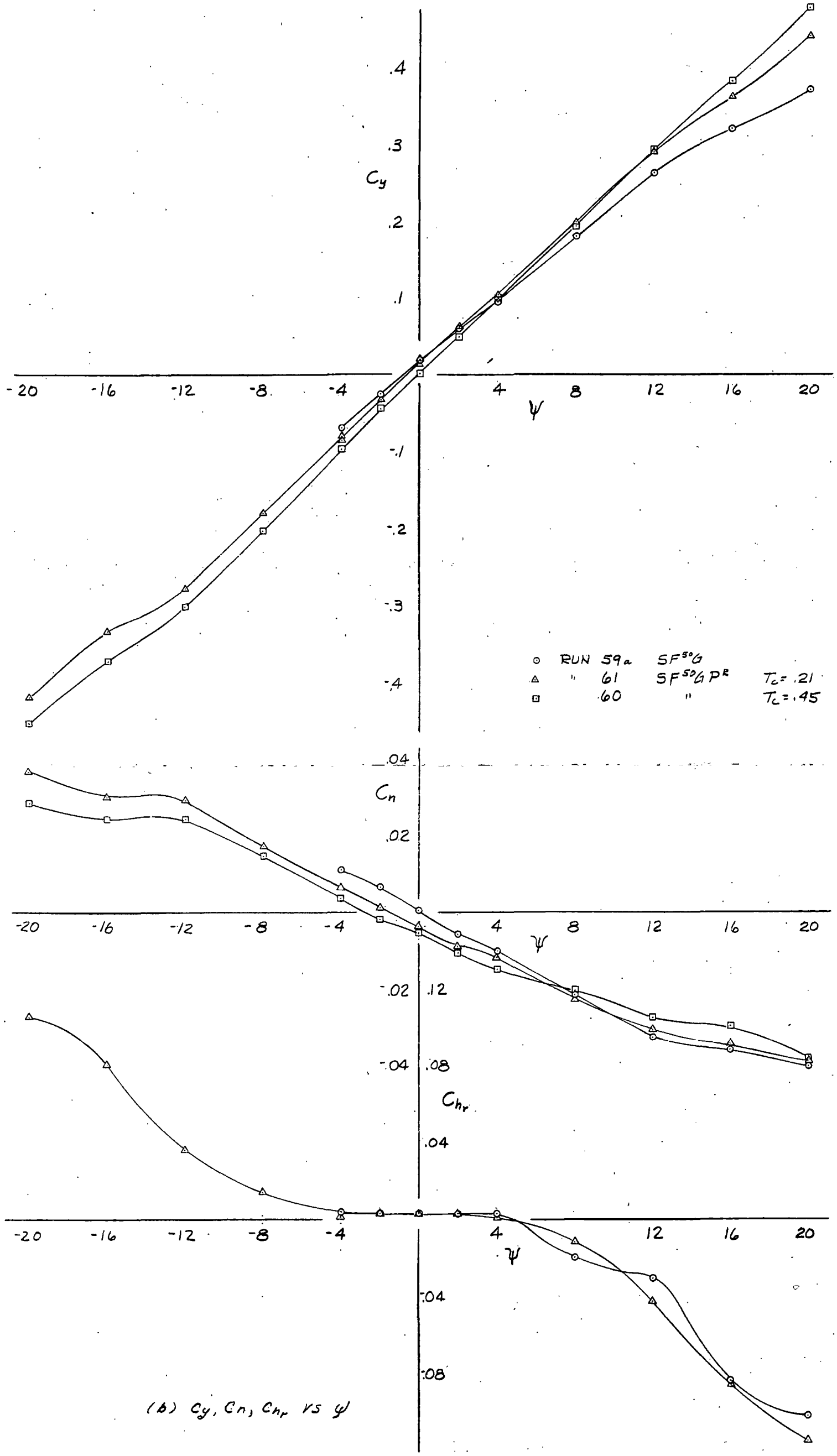

(b) C_y, C_n, C_{h_r} vs ψ

FIGURE 26.-(CONCLUDED)

NATIONAL ADVISORY
COMMITTEE FOR AERONAUTICS

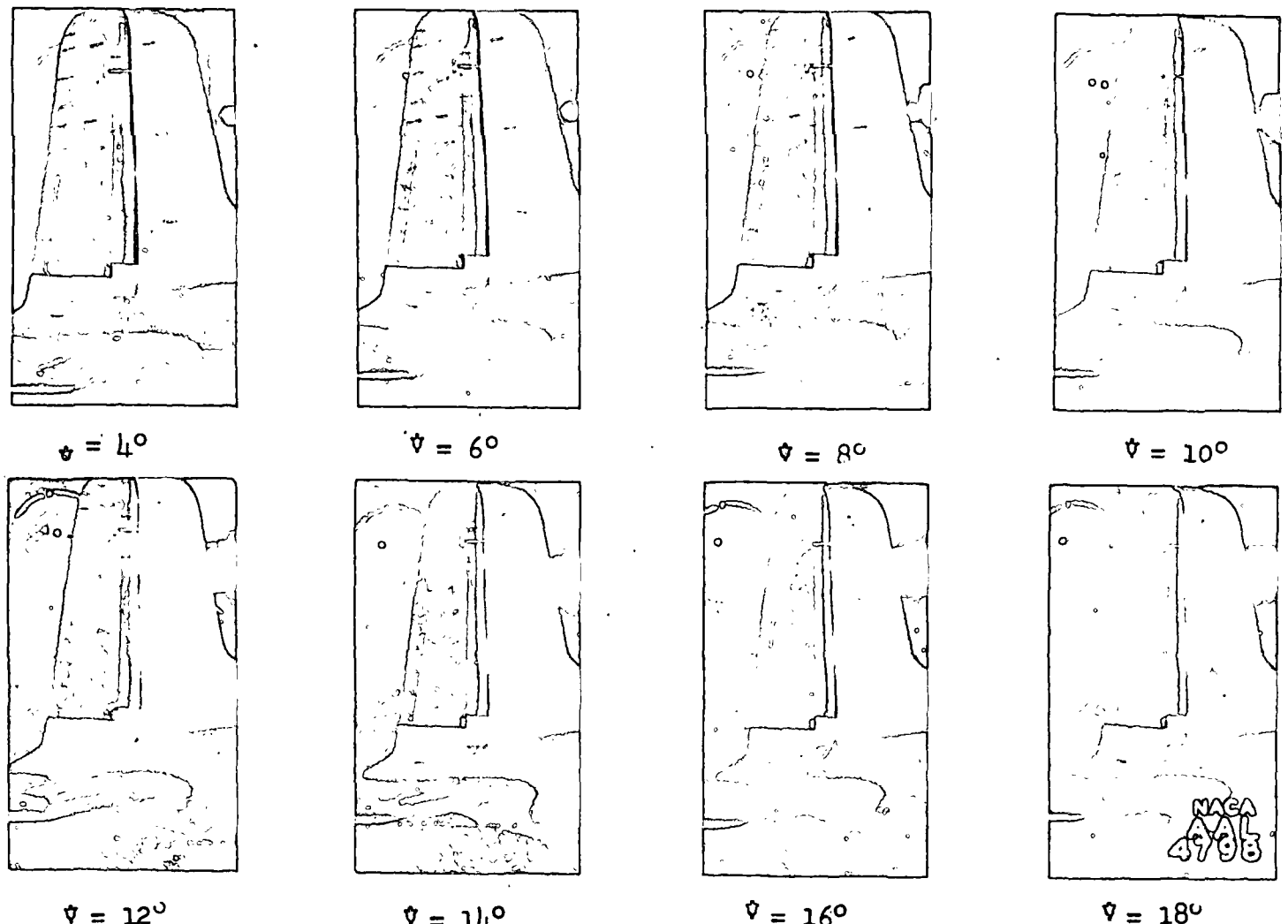

Figure 27. - Tuft photographs of stall on vertical surface of test model; cruising attitude.

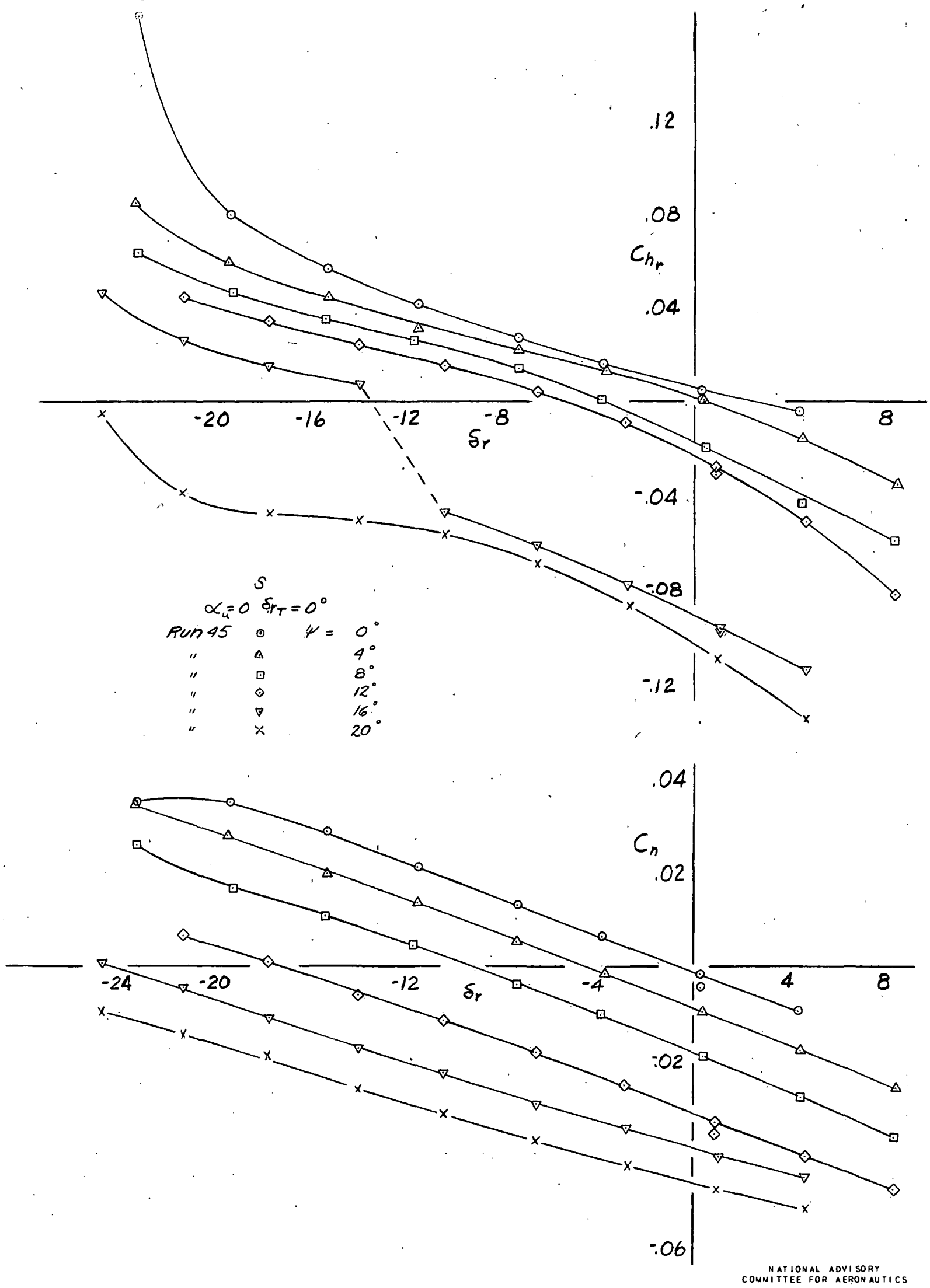

FIGURE 28. - VARIATION OF RUDDER HINGE-MOMENT AND YAWING-MOMENT COEFFICIENTS WITH RUDDER ANGLE FOR THE TEST MODEL; FLAPS AND GEAR RETRACTED, RUDDER TAB UNDEFLECTED, PROPELLERS REMOVED.

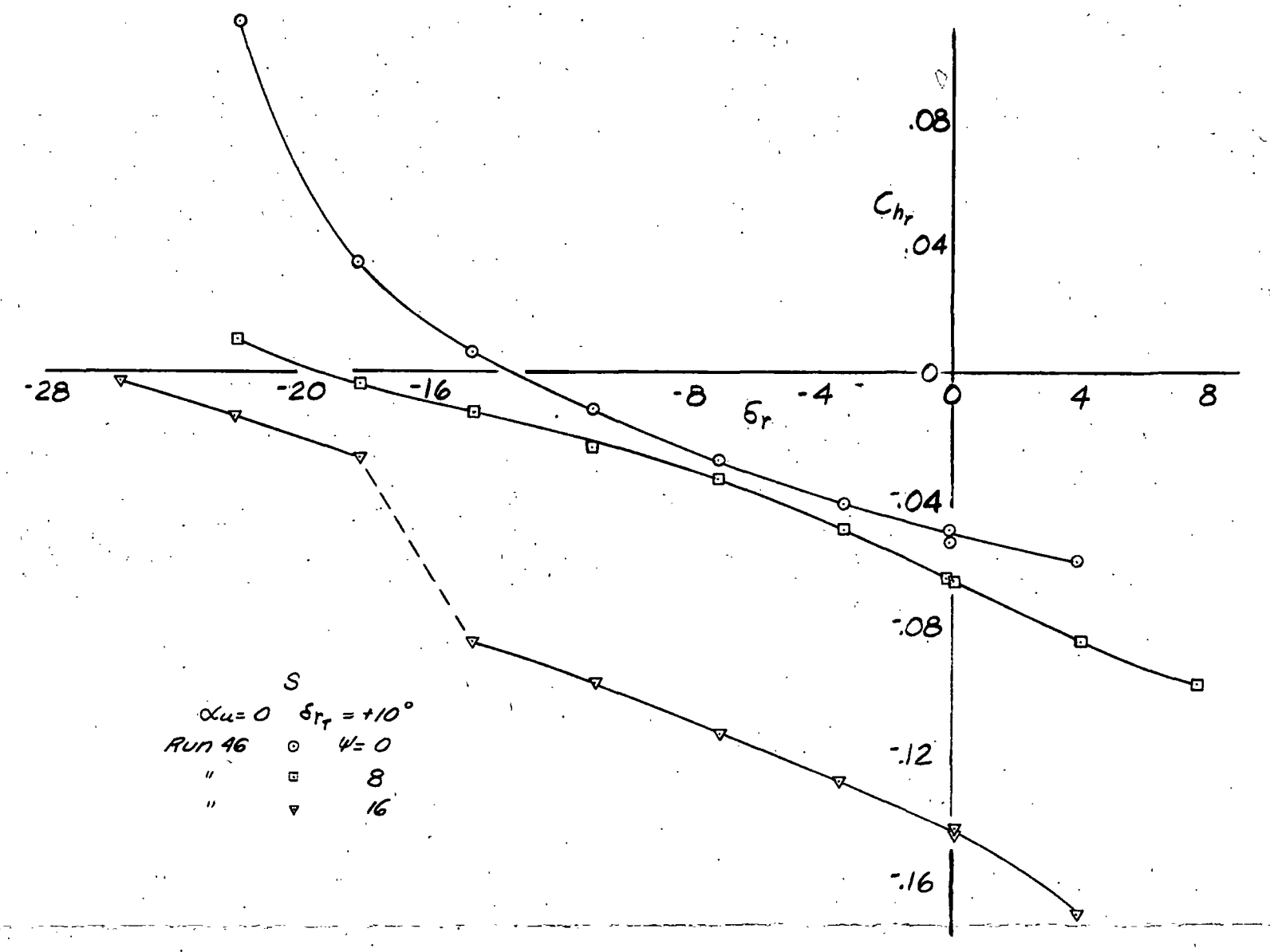

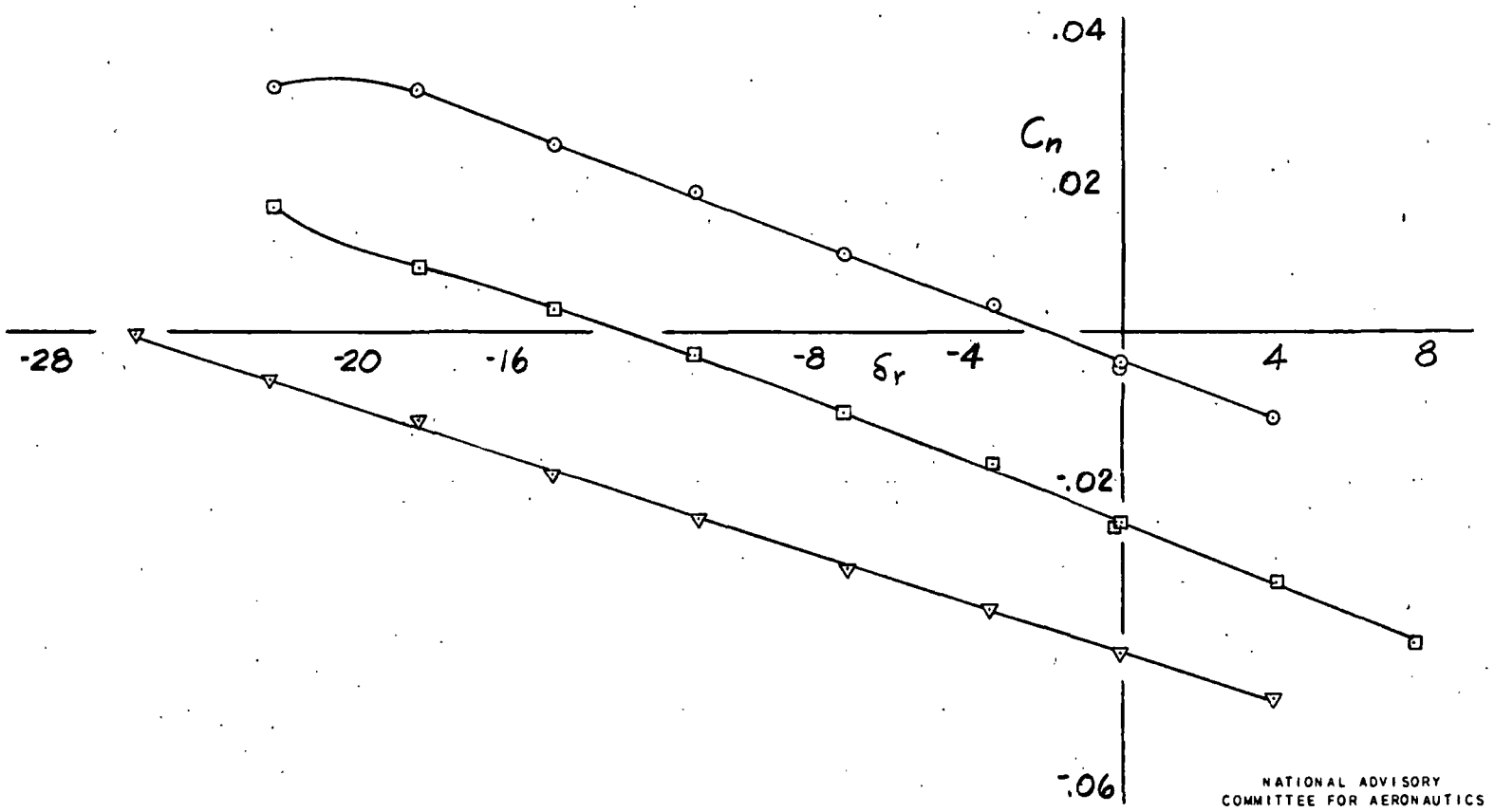

FIGURE 29.- VARIATION OF RUDDER HINGE-MOMENT AND YAWING-MOMENT COEFFICIENTS WITH RUDDER ANGLE FOR THE TEST MODEL ; FLAPS AND GEAR RETRACTED, RUDDER TAB DEFLECTED TO +10°, PROPELLERS REMOVED.

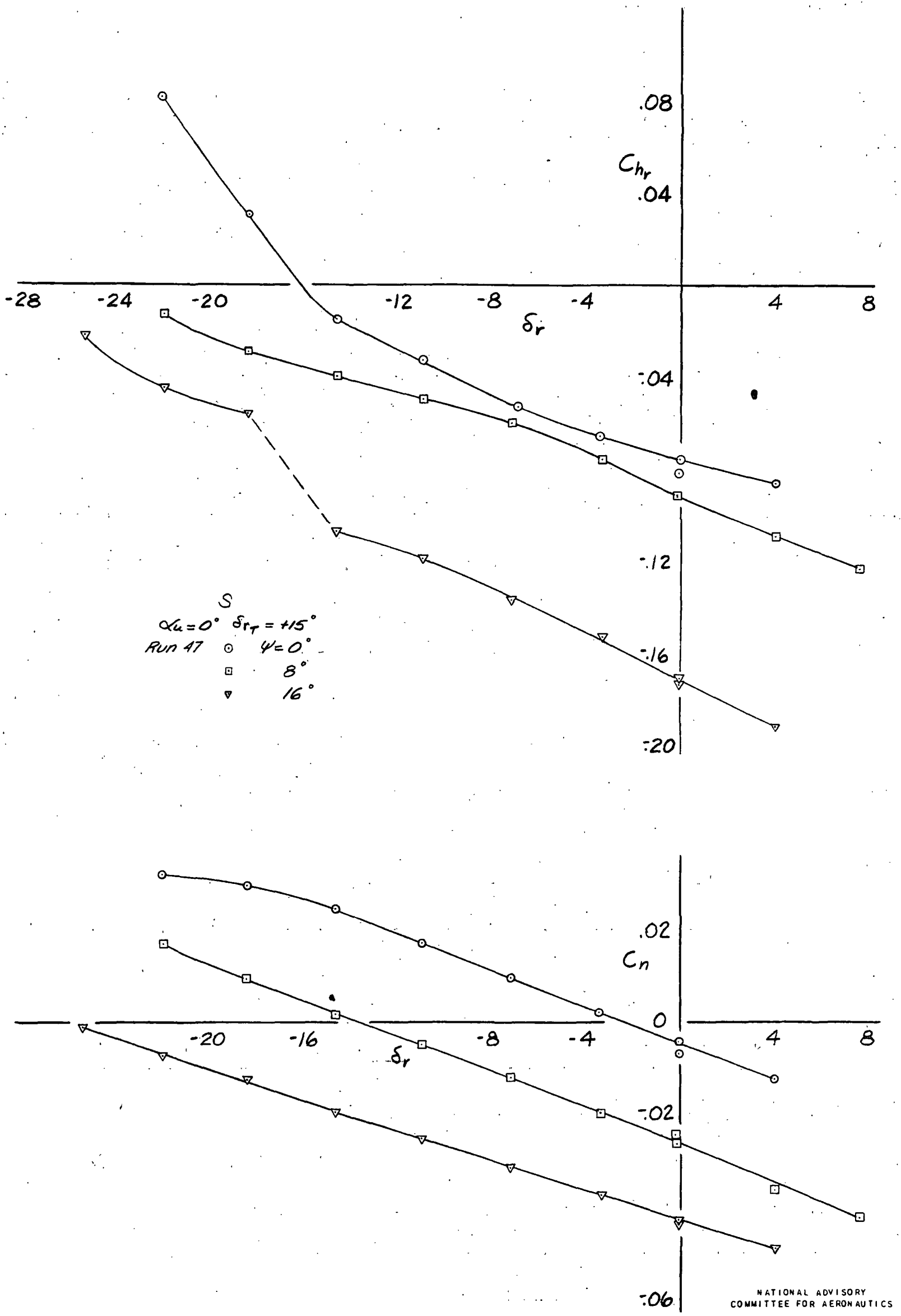

FIGURE 30.- VARIATION OF RUDDER HINGE-MOMENT AND YAWING-MOMENT COEFFICIENTS WITH RUDDER ANGLE FOR THE TEST MODEL; FLAPS AND GEAR RETRACTED, RUDDER TAB DEFLECTED TO +15°, PROPELLERS REMOVED.

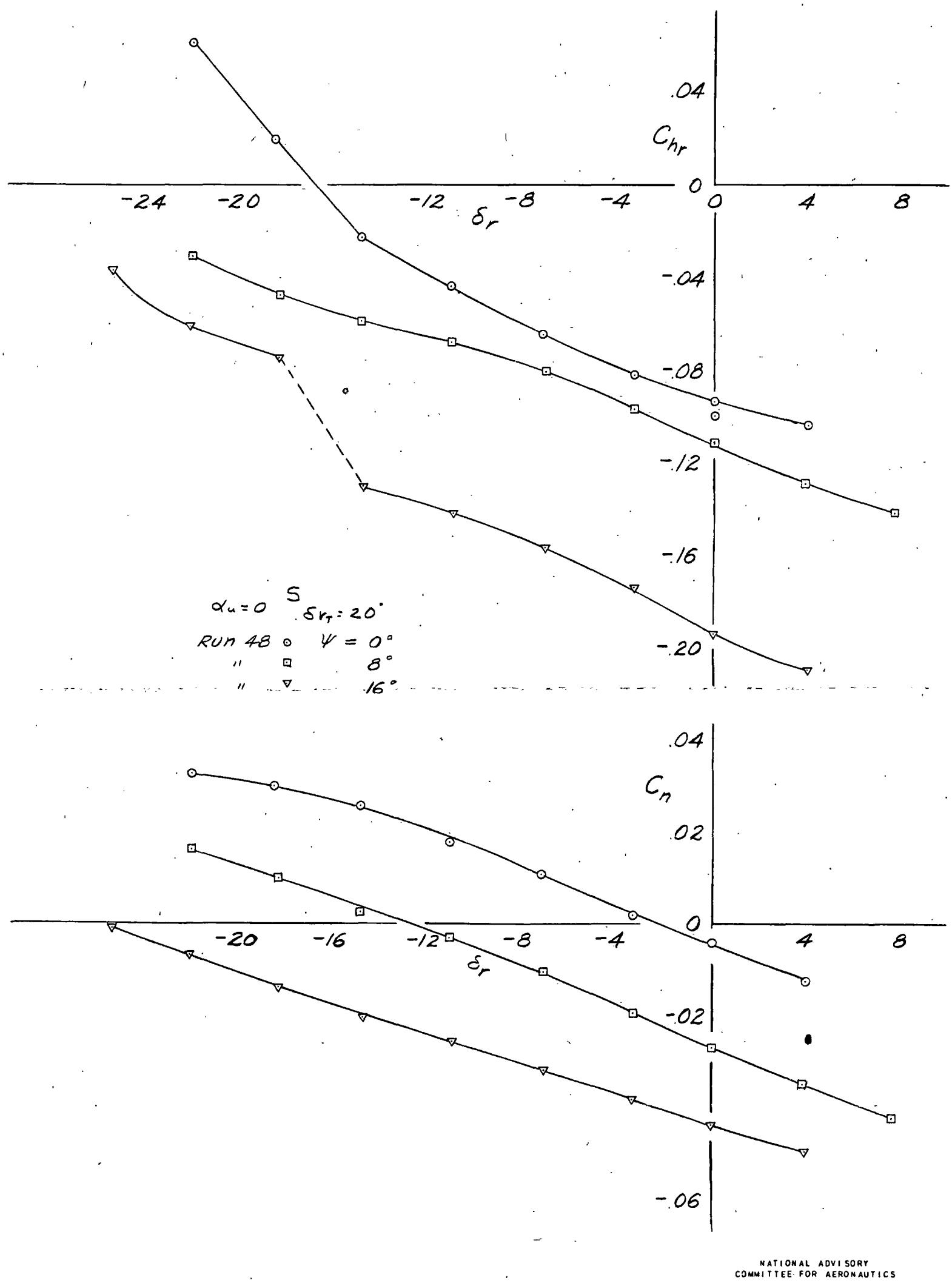

FIGURE 31. - VARIATION OF RUDDER HINGE-MOMENT AND YAWING-MOMENT COEFFICIENTS WITH RUDDER ANGLE FOR THE TEST MODEL; FLAPS AND GEAR RETRACTED; RUDDER TAB DEFLECTED TO +20°; PROPELLERS REMOVED.

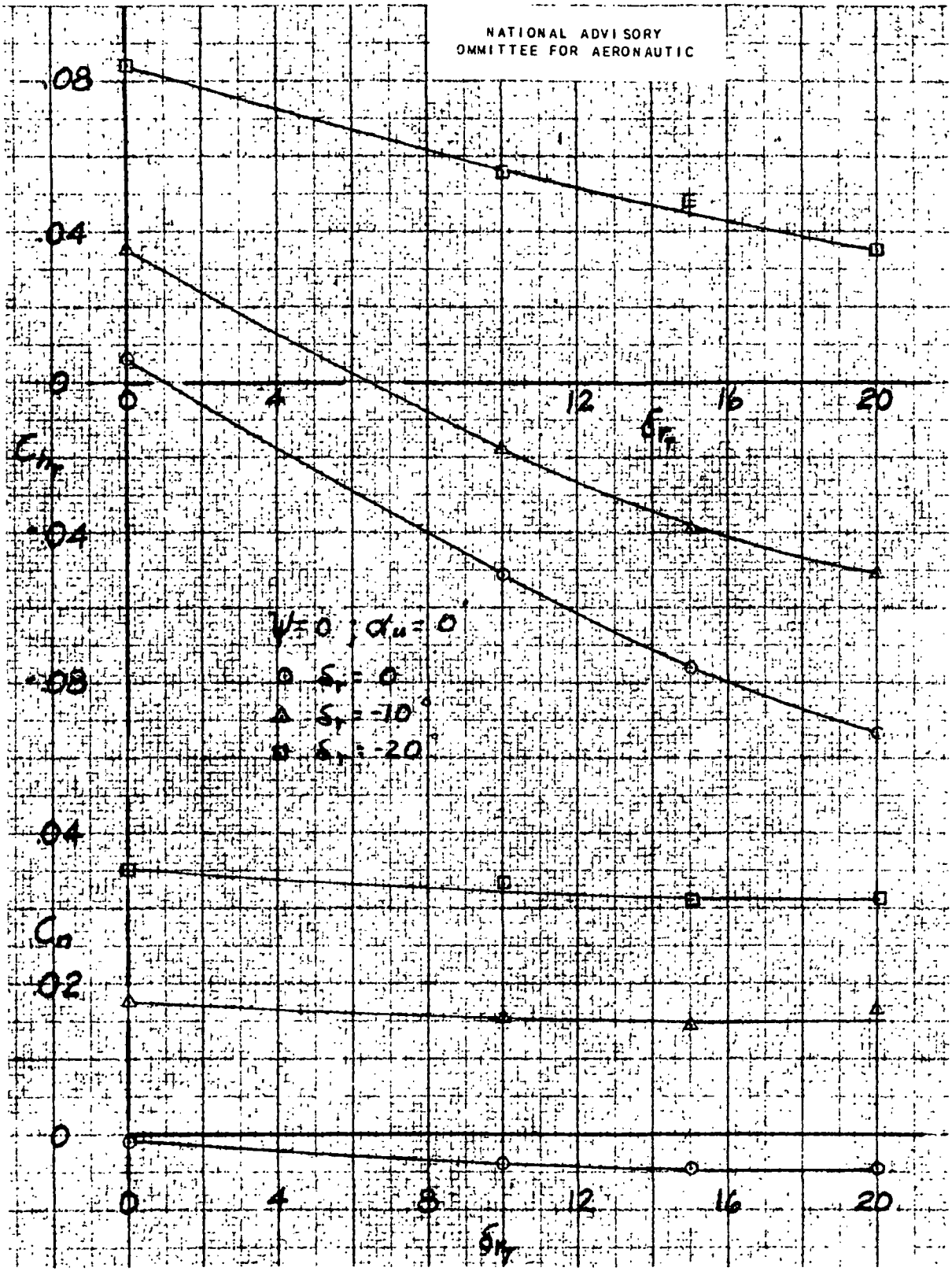

FIGURE 32. - VARIATION OF RUDDER HINGE-MOMENT AND YAWING-MOMENT COEFFICIENTS WITH TAB DEFLECTION FOR VARIOUS RUDDER DEFLECTIONS; $\psi = 0°$, PROPELLERS REMOVED, TEST MODEL.

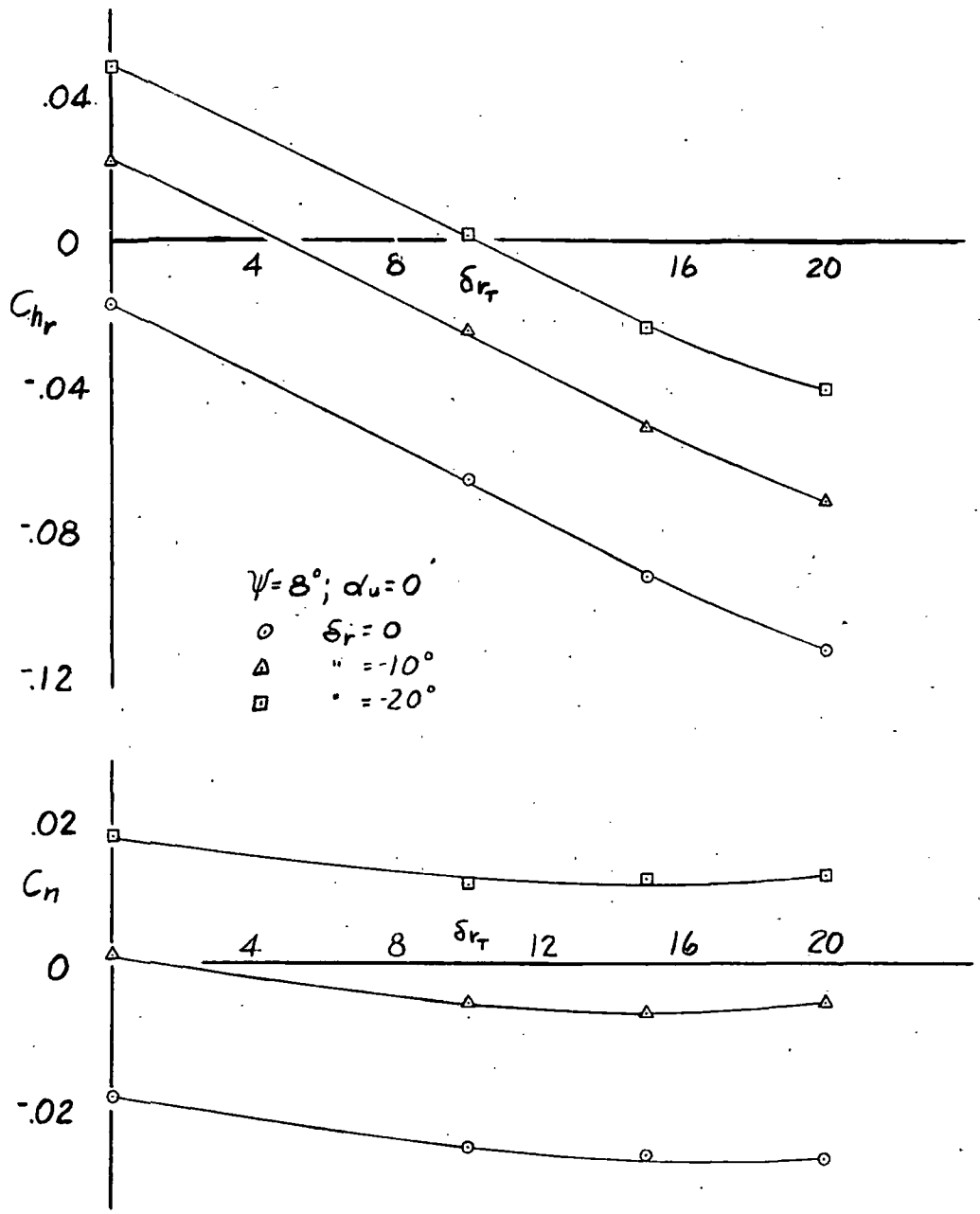

FIGURE 33.- VARIATION OF RUDDER HINGE-MOMENT AND YAWING-MOMENT COEFFICIENTS WITH TAB DEFLECTION FOR VARIOUS RUDDER DEFLECTIONS; $\psi = 8°$, PROPELLERS REMOVED. TEST MODEL.

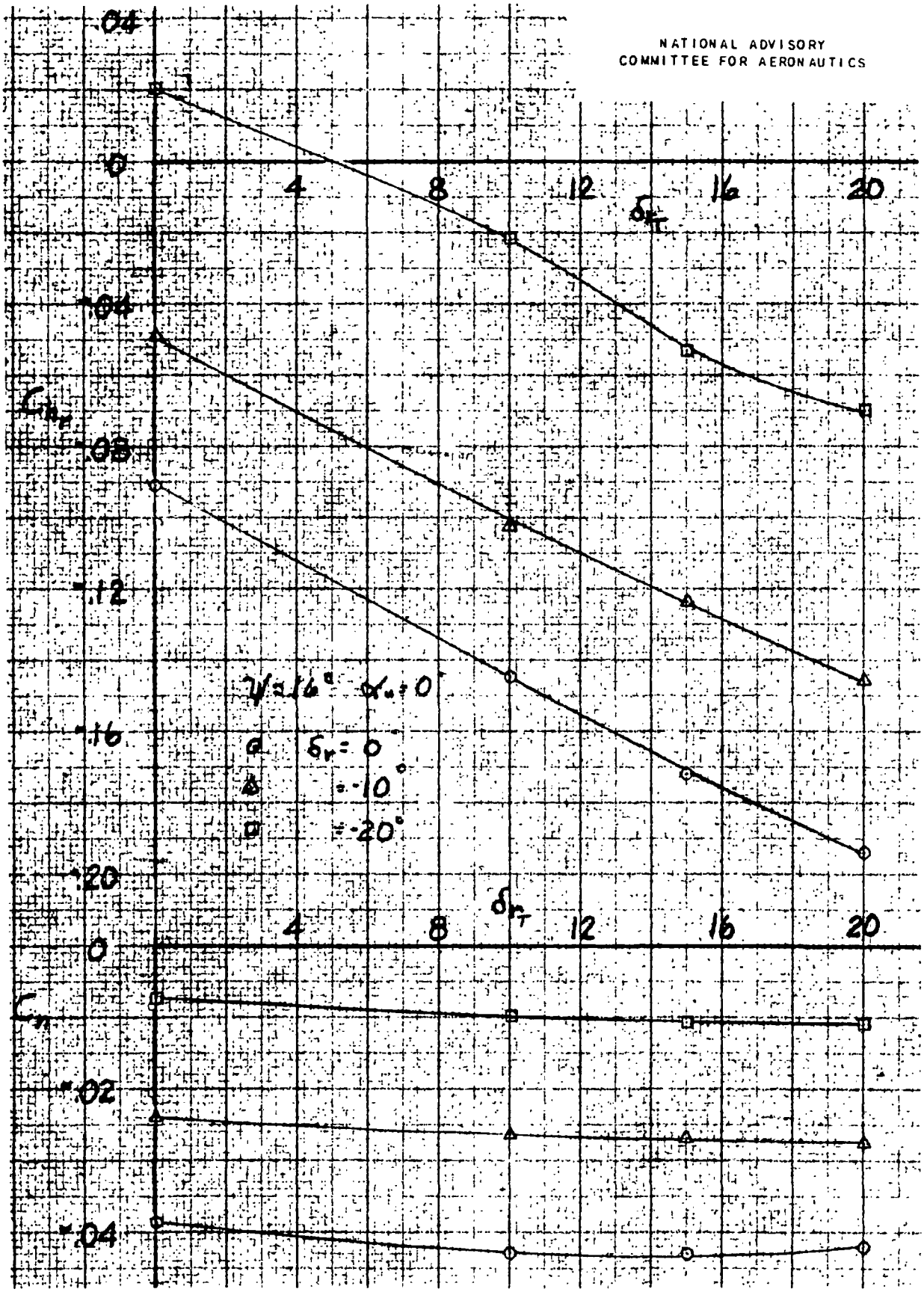

FIGURE 34.- VARIATION OF RUDDER HINGE-MOMENT AND YAWING-MOMENT COEFFICIENTS WITH TAB DEFLECTION FOR VARIOUS RUDDER DEFLECTIONS; $\psi = 16°$, PROPELLERS REMOVED, TEST MODEL.

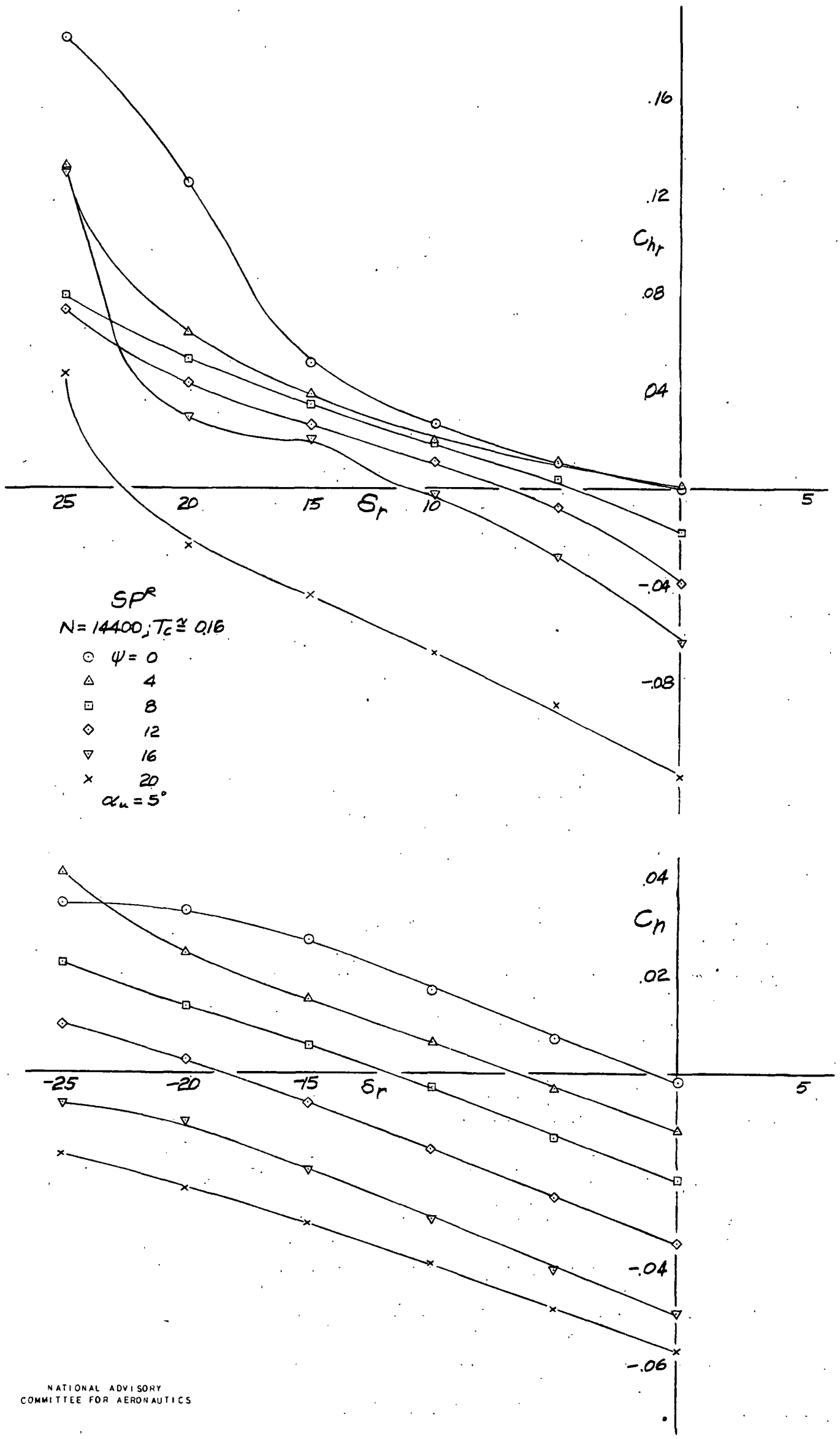

FIGURE 35.- VARIATION OF YAWING-MOMENT AND RUDDER HINGE-MOMENT COEFFICIENTS WITH RUDDER DEFLECTION FOR THE TEST MODEL. RATED POWER ($T_c \cong 0.16$); CLIMBING ATTITUDE.

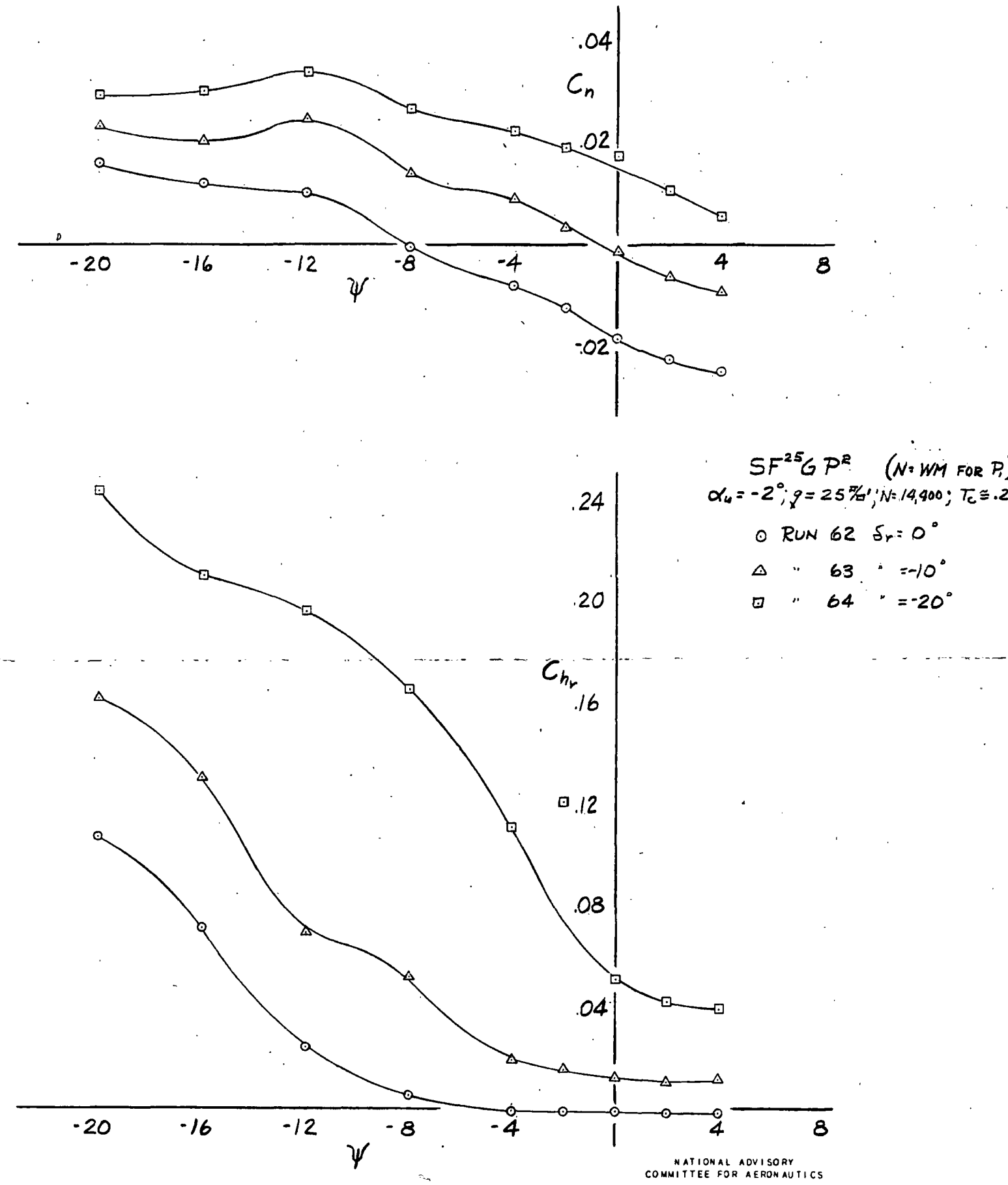

FIGURE 36.- VARIATION OF YAWING-MOMENT AND RUDDER HINGE-MOMENT COEFFICIENTS WITH ANGLE OF YAW FOR THE TEST MODEL. FLAPS DEFLECTED 25°; LANDING GEAR EXTENDED; ASYMMETRIC TAKE-OFF POWER; ATTITUDE FOR 1.2 V_{STALL} ($\alpha_u = -2°$).

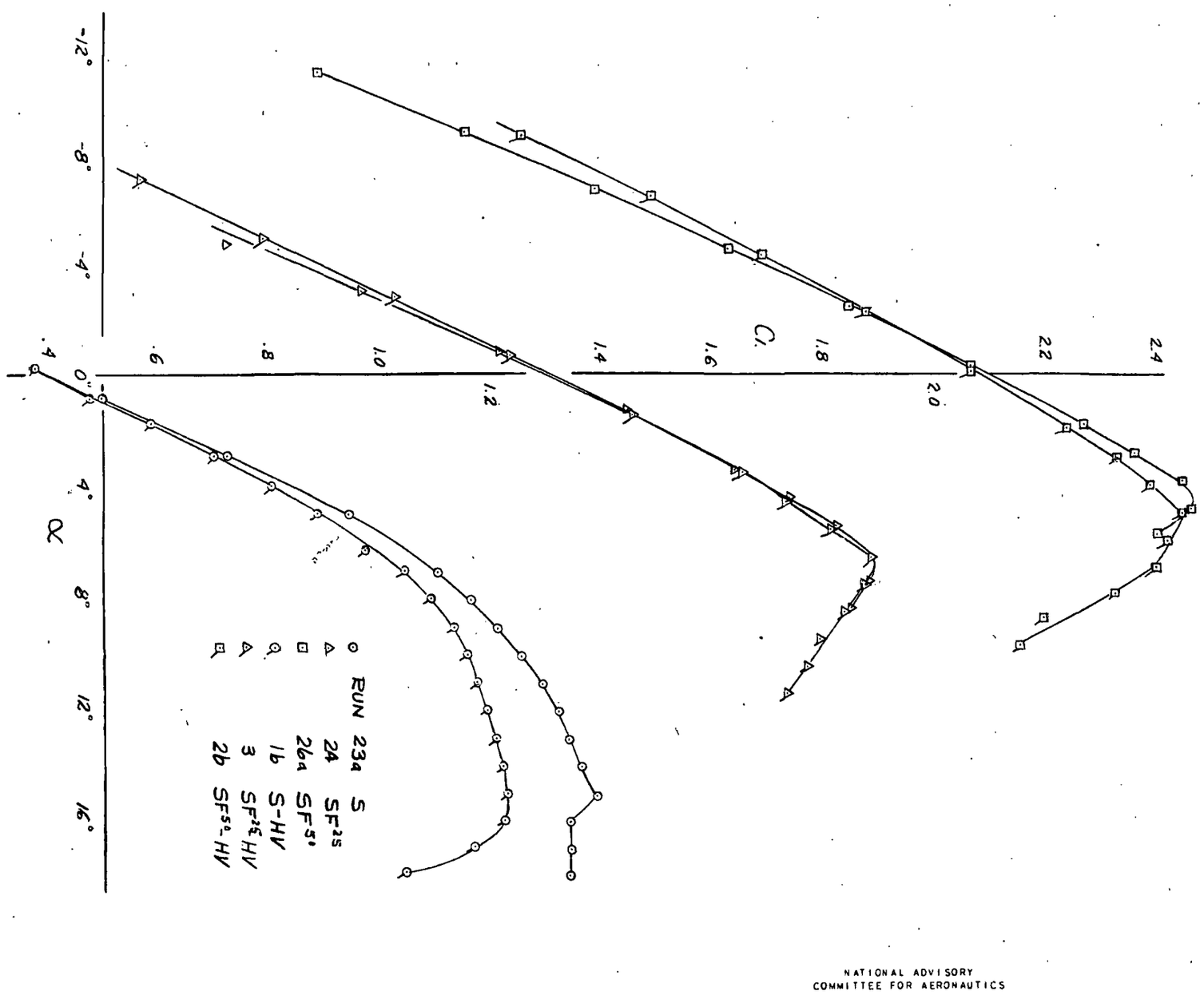

NATIONAL ADVISORY
COMMITTEE FOR AERONAUTICS

FIGURE 37. - THE VARIATION OF LIFT COEFFICIENT WITH ANGLE OF ATTACK FOR THE TEST MODEL WITH FLAPS DEFLECTED; LANDING GEAR RETRACTED; PROPELLERS REMOVED.

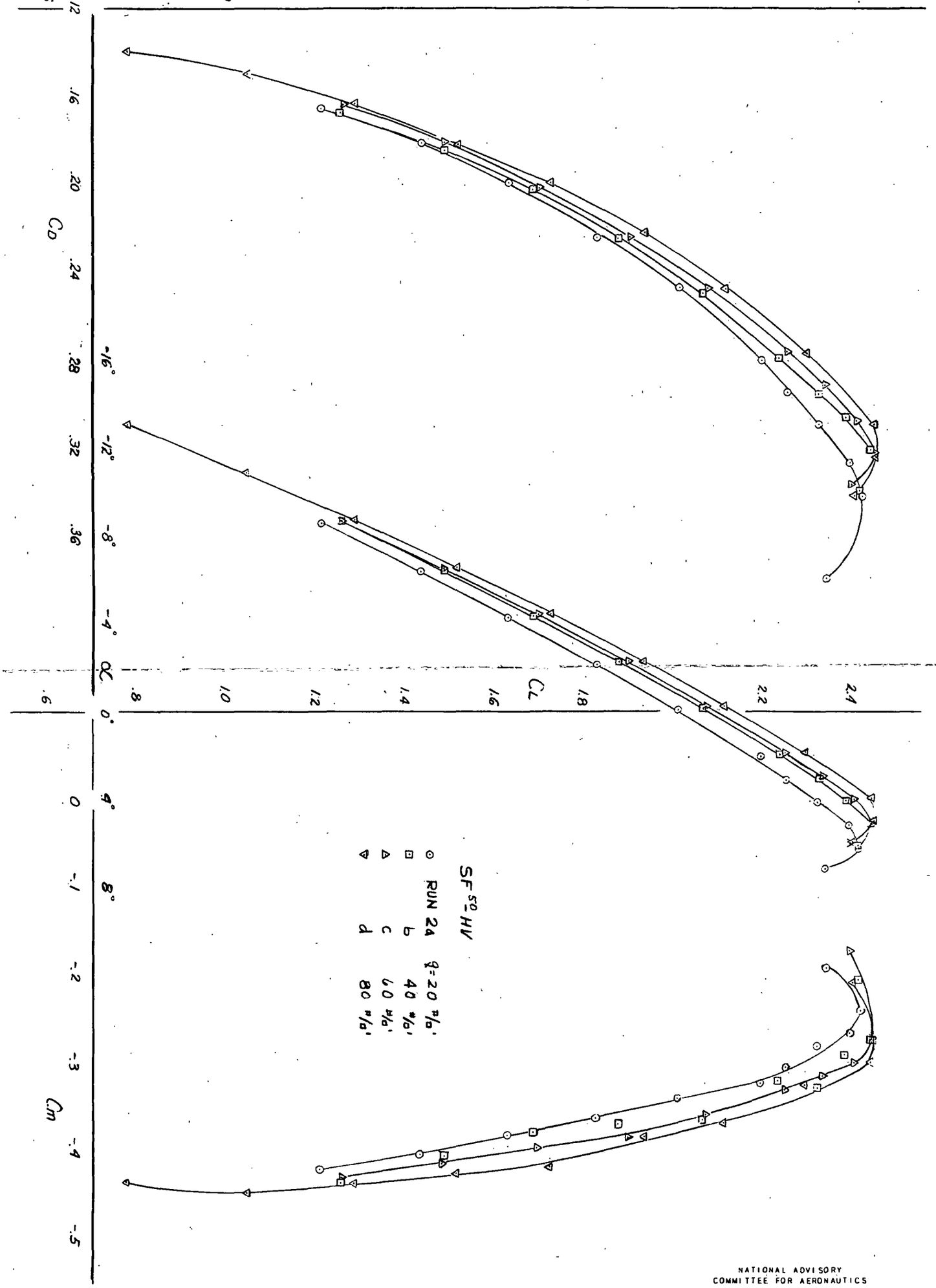

FIGURE 38.- EFFECT OF DYNAMIC PRESSURE ON THE CHARACTERISTICS OF THE TEST MODEL; TAIL REMOVED; FLAPS DEFLECTED 50°.

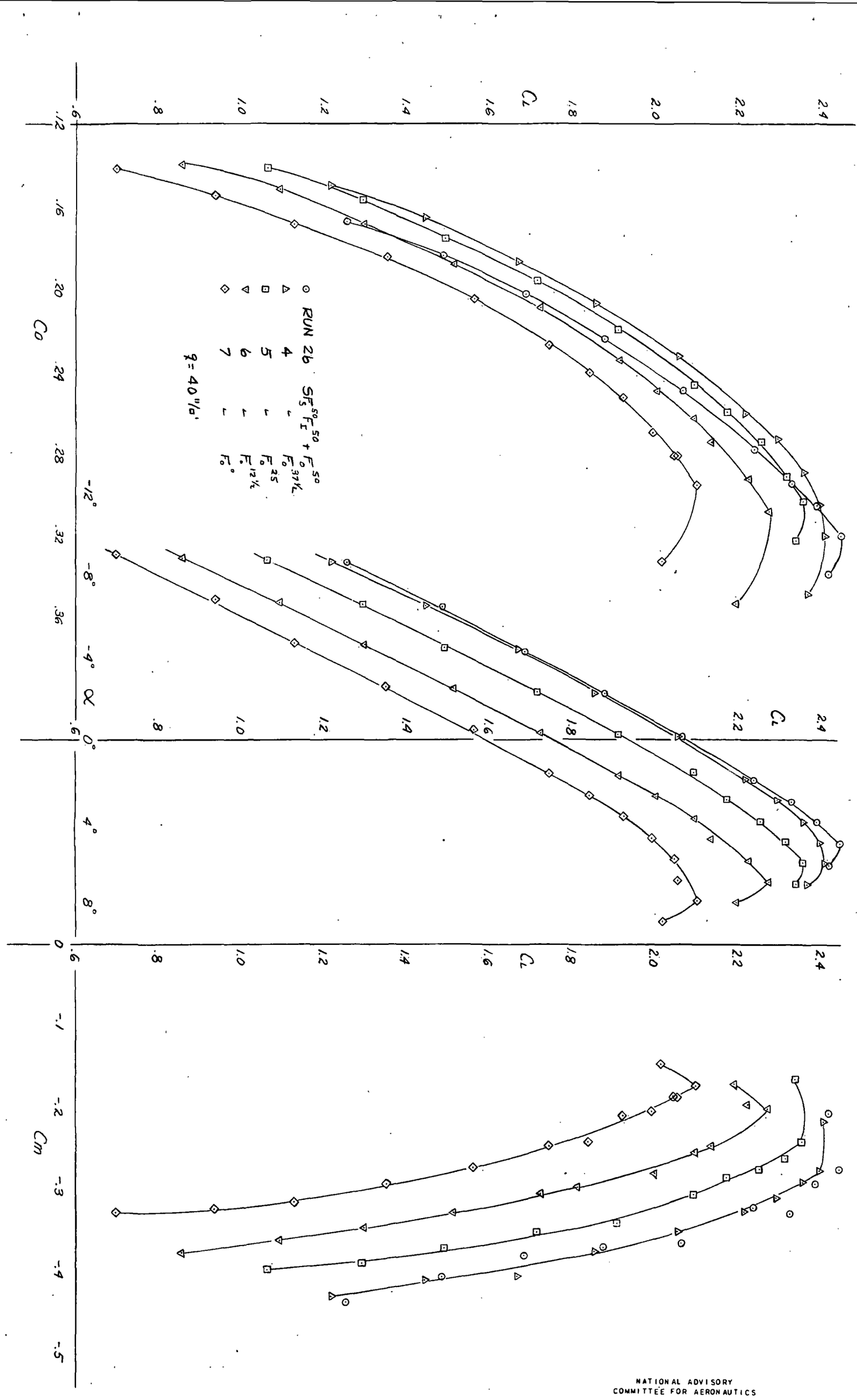

FIGURE 39.— EFFECT OF OUTBOARD FLAP ON THE CHARACTERISTICS OF THE TEST MODEL, TAIL REMOVED.

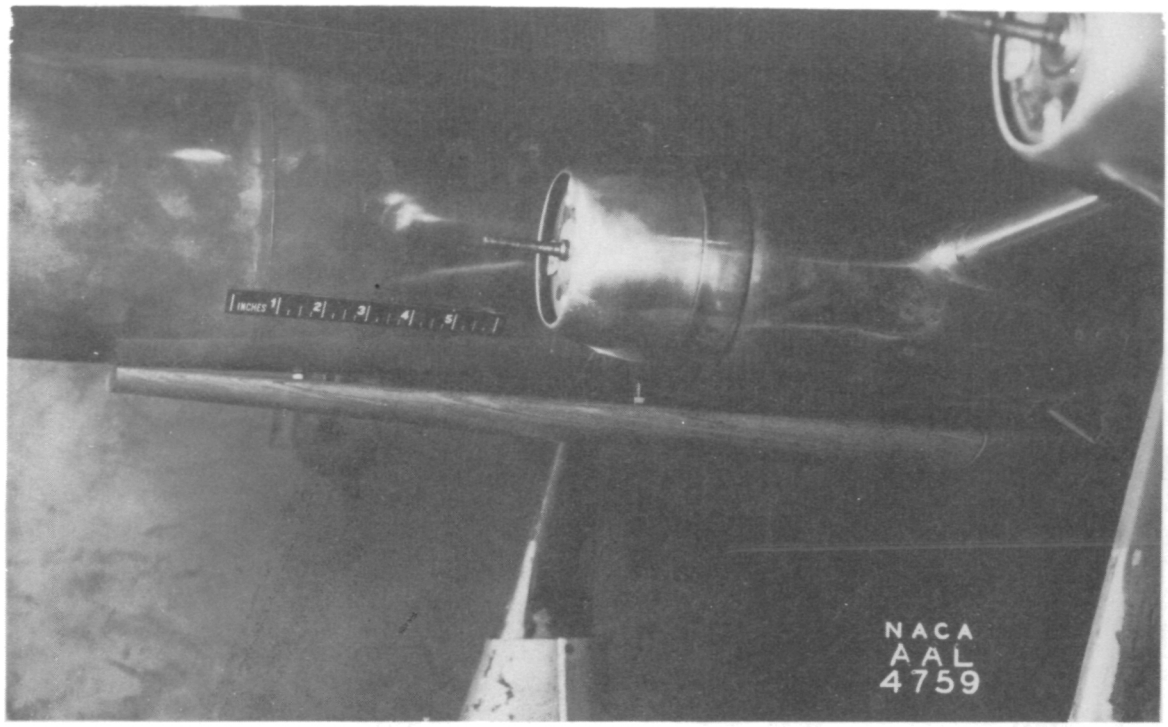

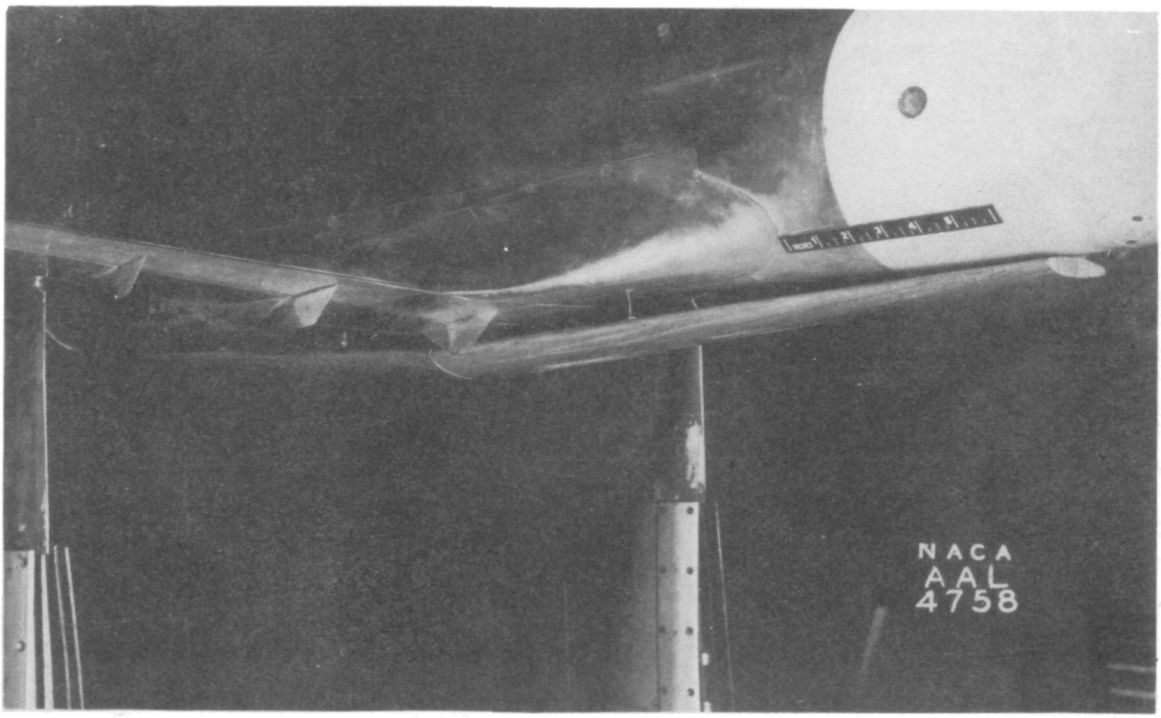

(a) W_1.

Figure 40. - Wing panels mounted under the fuselage of the test model.

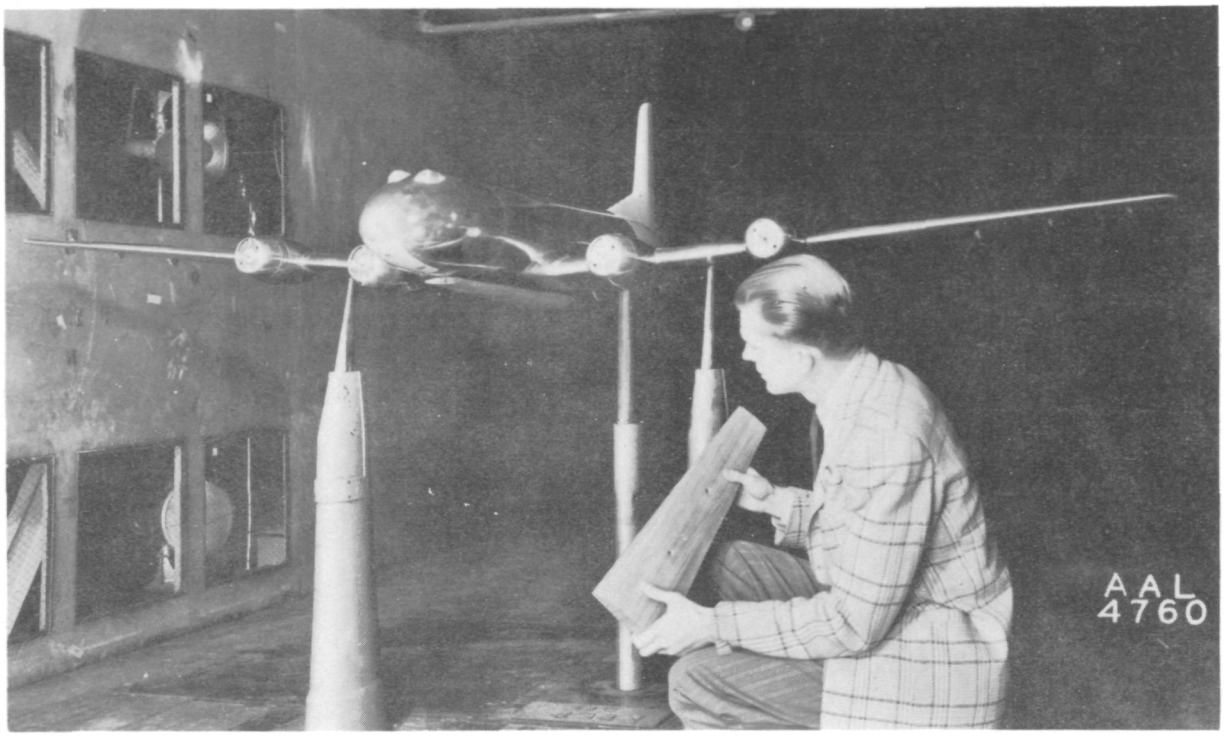

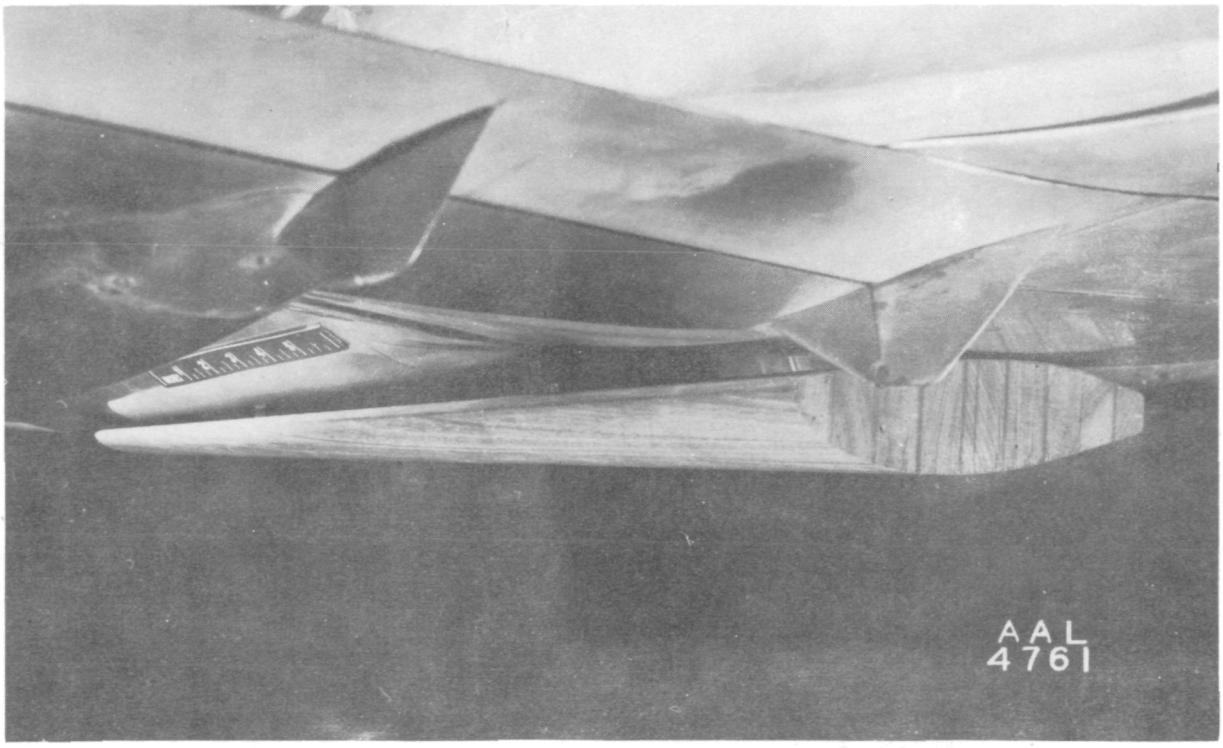

(b) W_2

Figure 40.- Concluded.

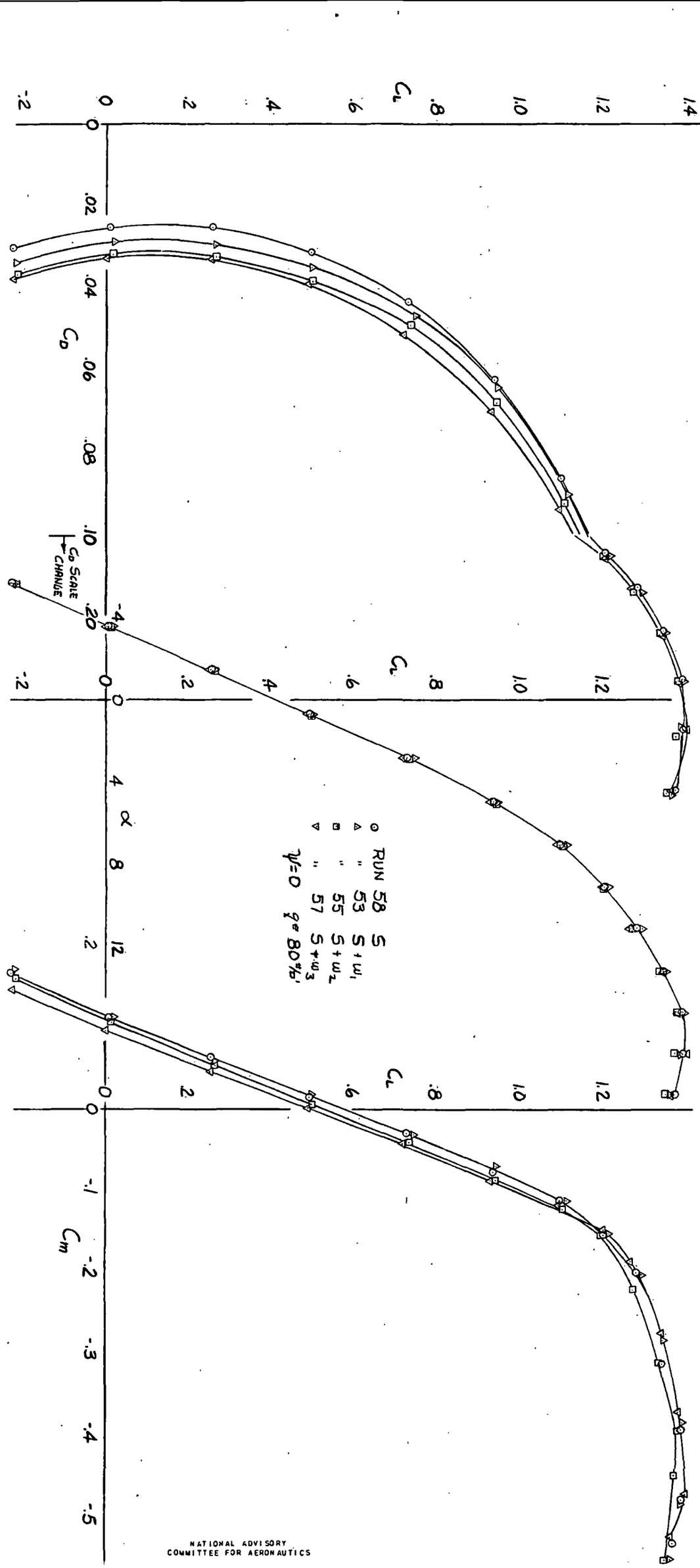

FIGURE 41.- VARIATION OF THE AERODYNAMIC CHARACTERISTICS WITH LIFT COEFFICIENT SHOWING THE EFFECT OF WING PANELS MOUNTED UNDER THE FUSELAGE OF THE TEST MODEL; TAIL ON; PROPELLERS REMOVED.

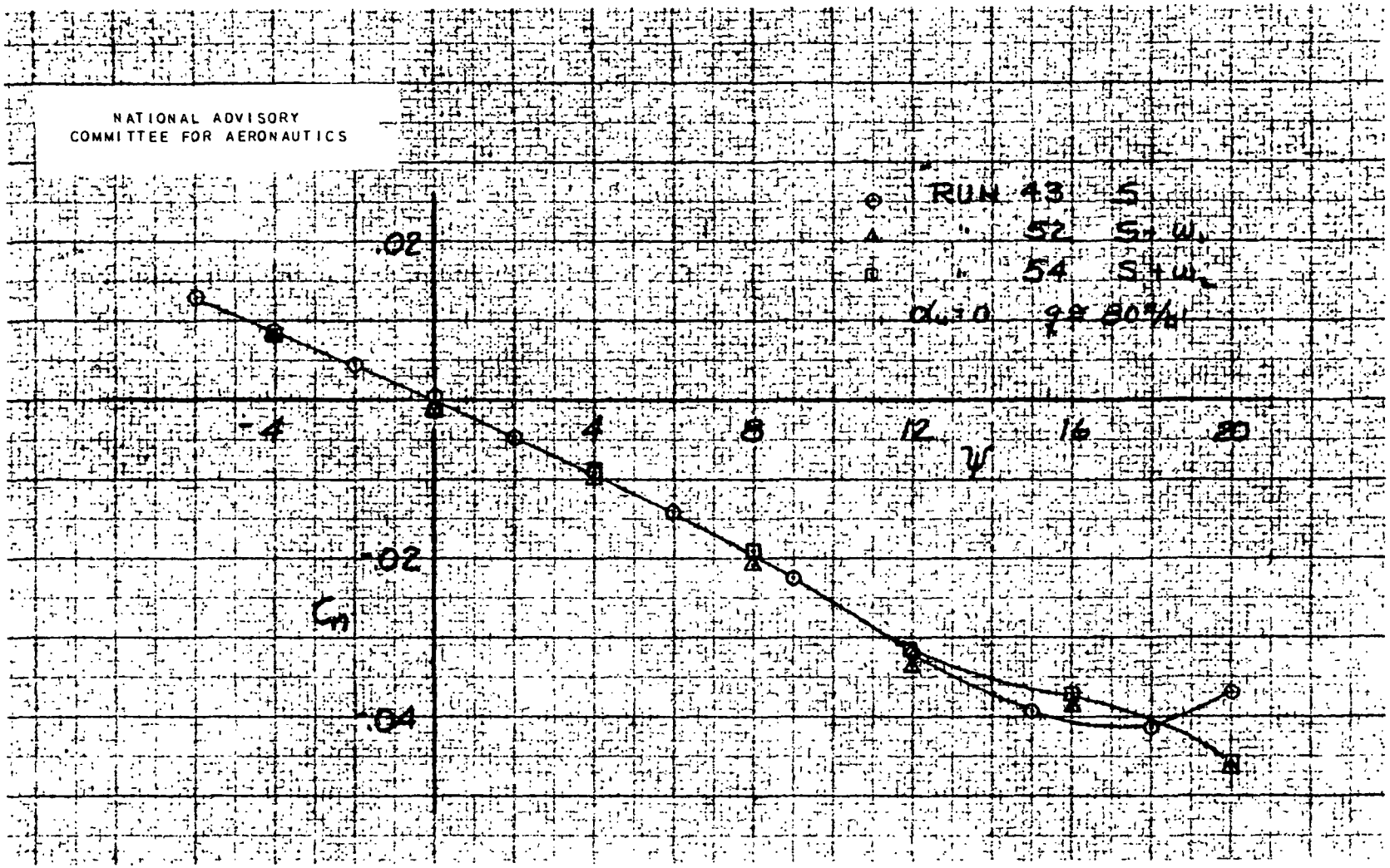

FIGURE 42.- VARIATION OF AERODYNAMIC CHARACTERISTICS WITH ANGLE OF YAW SHOWING THE EFFECT OF WING PANELS MOUNTED UNDER THE FUSELAGE OF THE TEST MODEL; TAIL ON, PROPELLERS REMOVED.

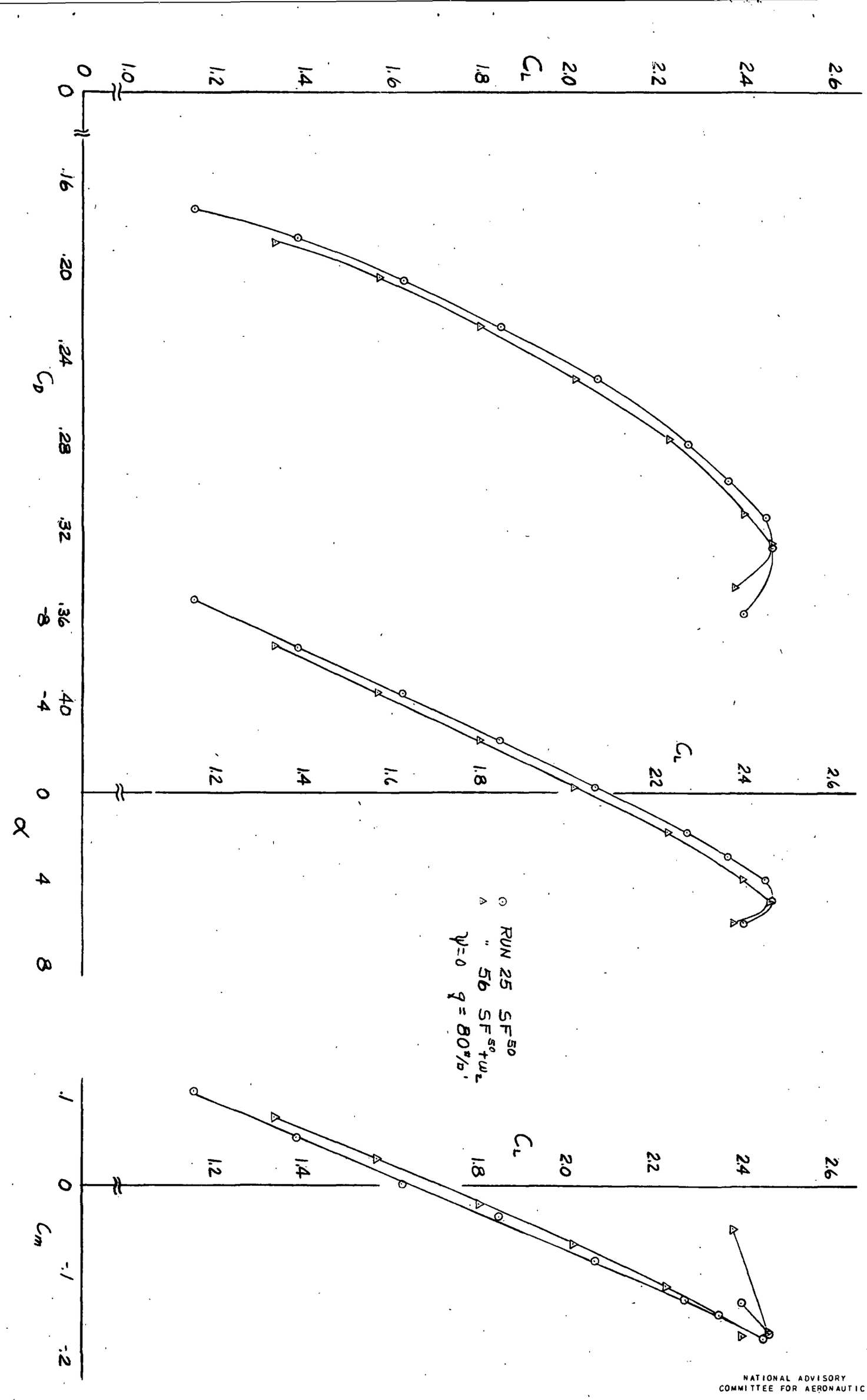

FIGURE 43.- VARIATION OF THE AERODYNAMIC CHARACTERISTICS WITH LIFT COEFFICIENT SHOWING THE EFFECT OF A WING PANEL MOUNTED UNDER THE FUSELAGE OF THE TEST MODEL; TAIL ON; FLAPS DEFLECTED 50°; PROPELLERS REMOVED.

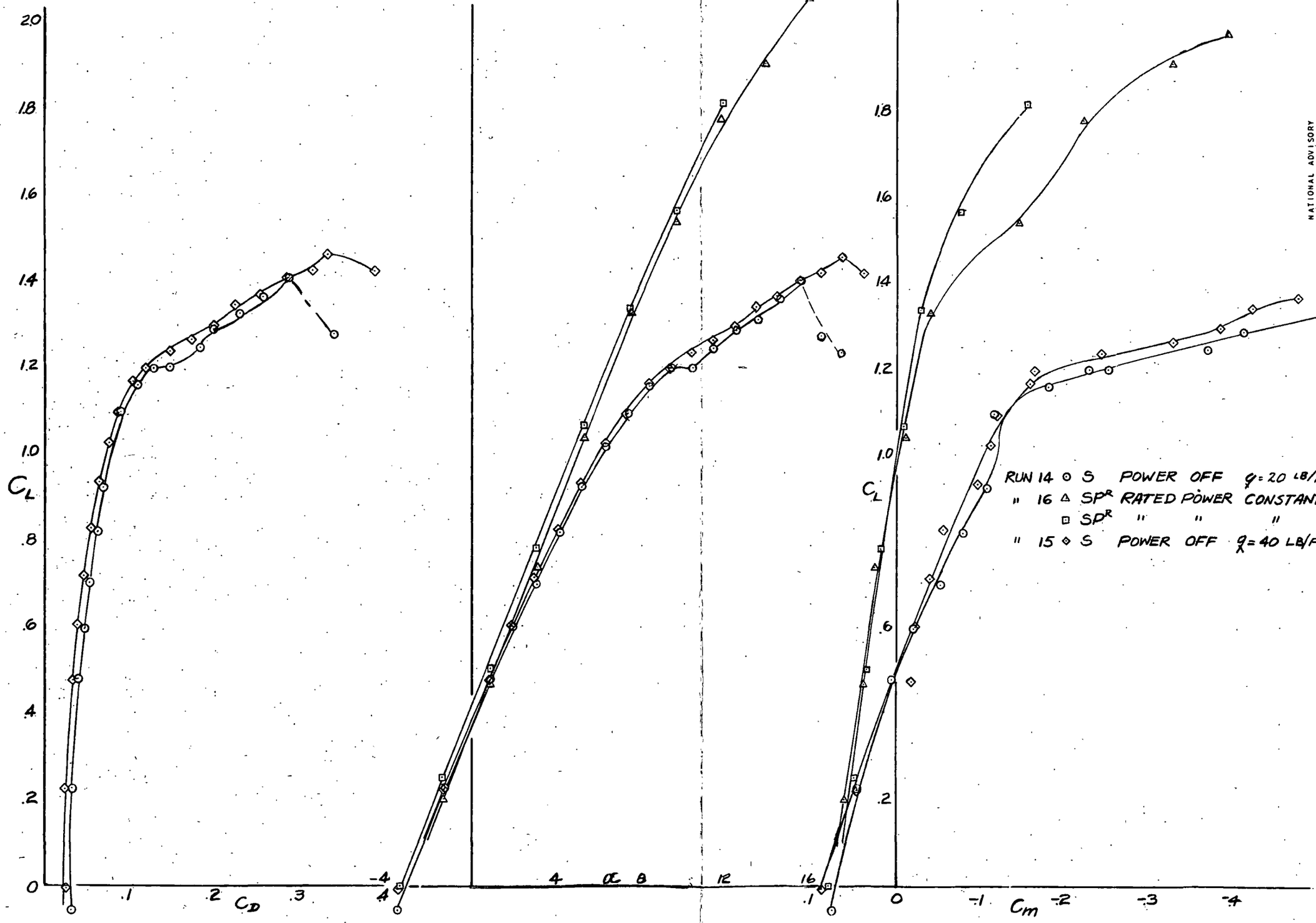

FIGURE 44.- COMPARISON OF METHODS OF POWER OPERATION FOR THE TEST MODEL. FLAPS UNDEFLECTED, TAIL ON.

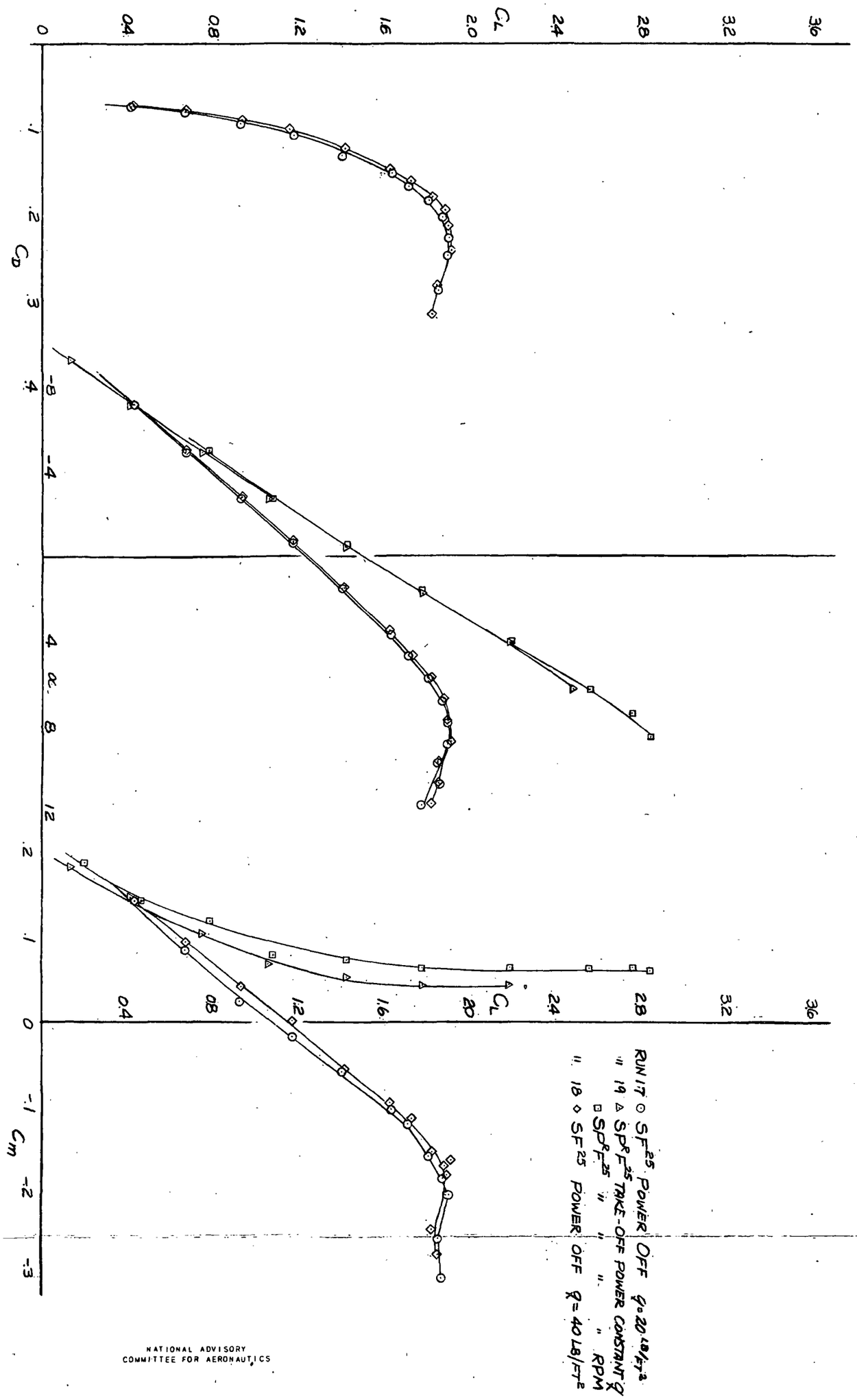

FIGURE 45.- COMPARISON OF METHODS OF POWER OPERATION FOR THE TEST MODEL. FLAPS DEFLECTED 25°, TAIL ON.

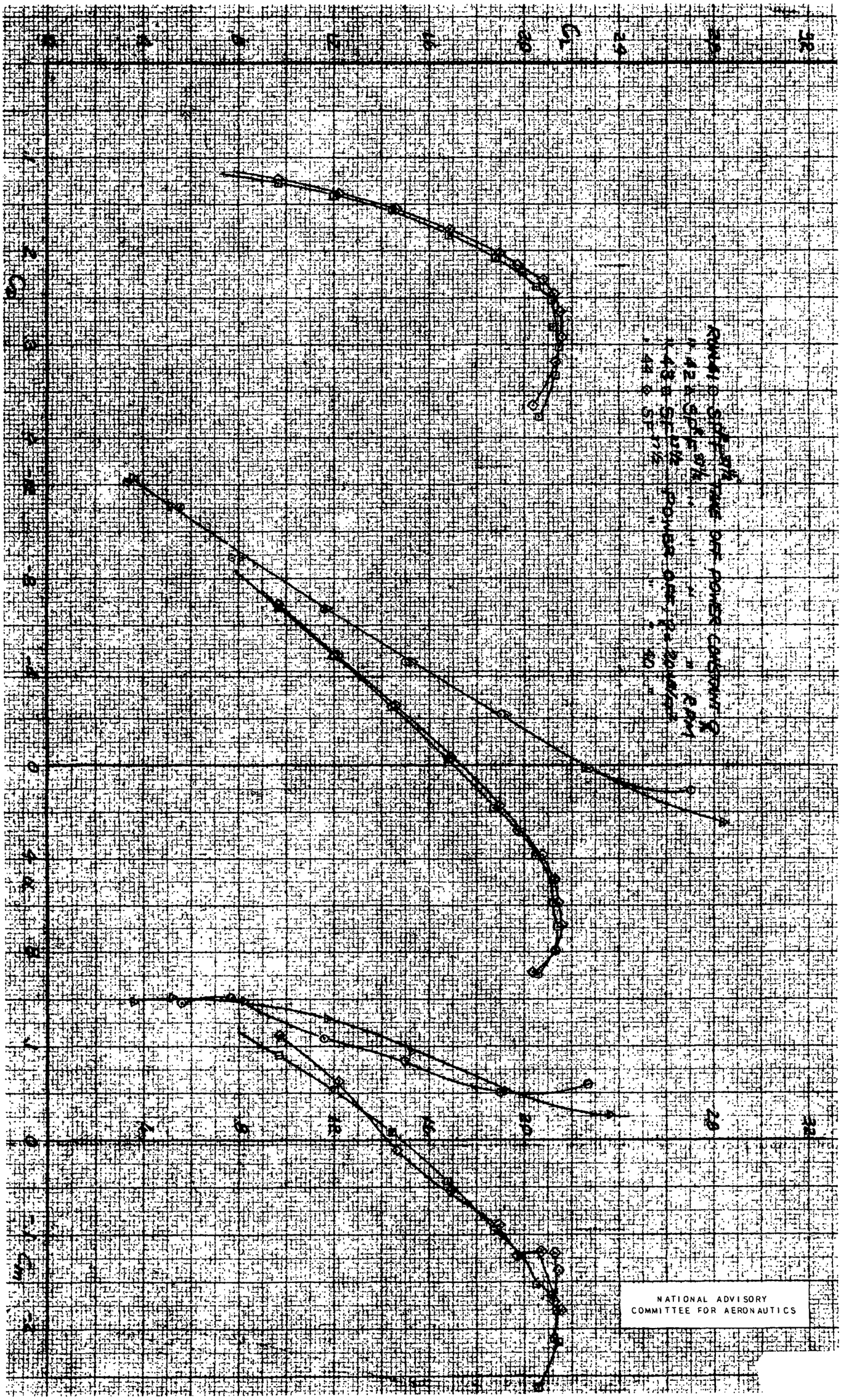

FIGURE 46.- COMPARISON OF METHODS OF POWER OPERATION FOR THE TEST MODEL; FLAPS DEFLECTED 37½°, TAIL ON.

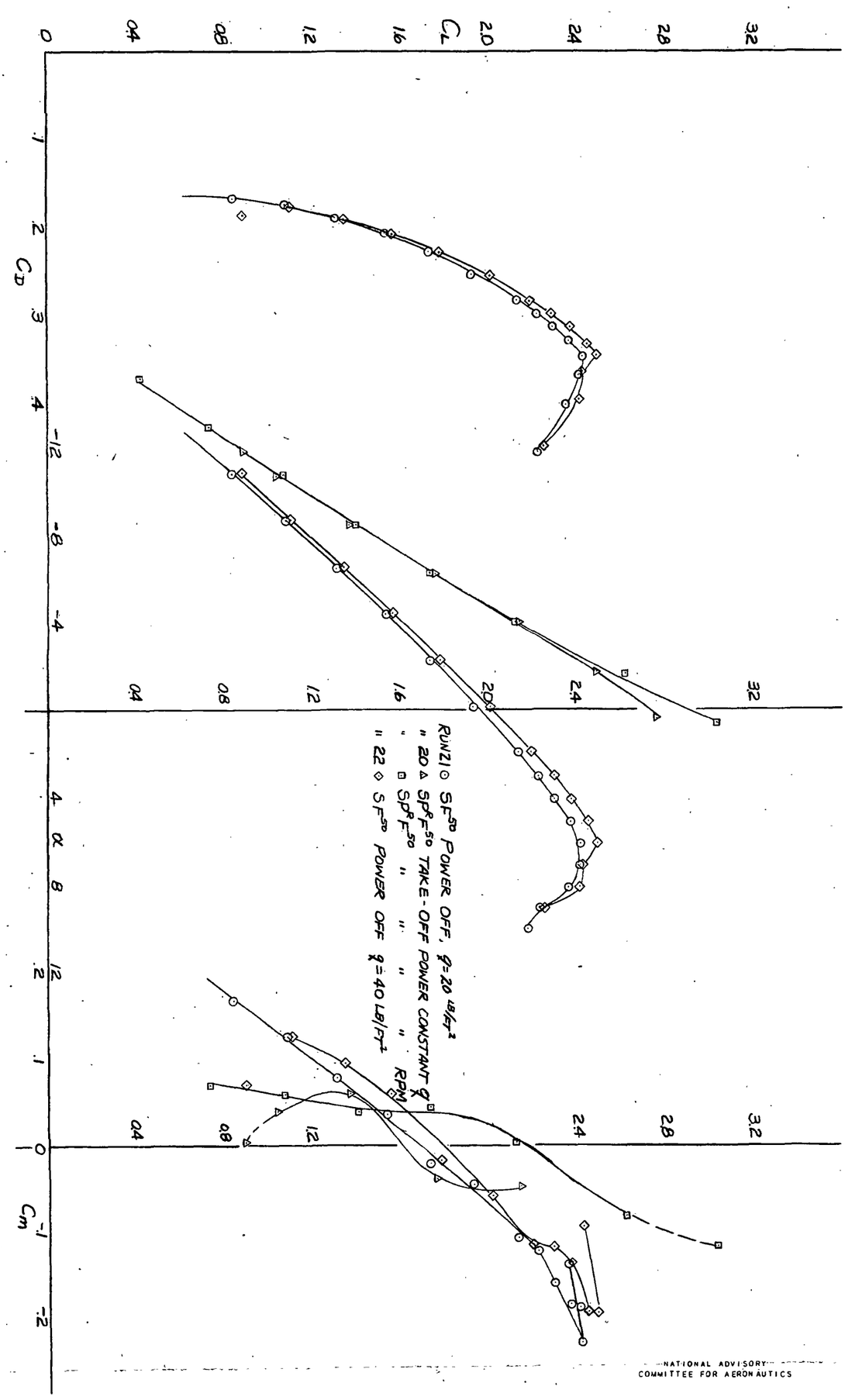

FIGURE 47.— COMPARISON OF METHODS OF POWER OPERATION FOR THE TEST MODEL. FLAPS DEFLECTED 50°, TAIL ON.

FIGURE 48.- VARIATION OF AERODYNAMIC CHARACTERISTICS WITH LIFT COEFFICIENT SHOWING THE EFFECT OF SEVERAL FLAP DEFLECTIONS ON THE TEST MODEL; POWER ON.

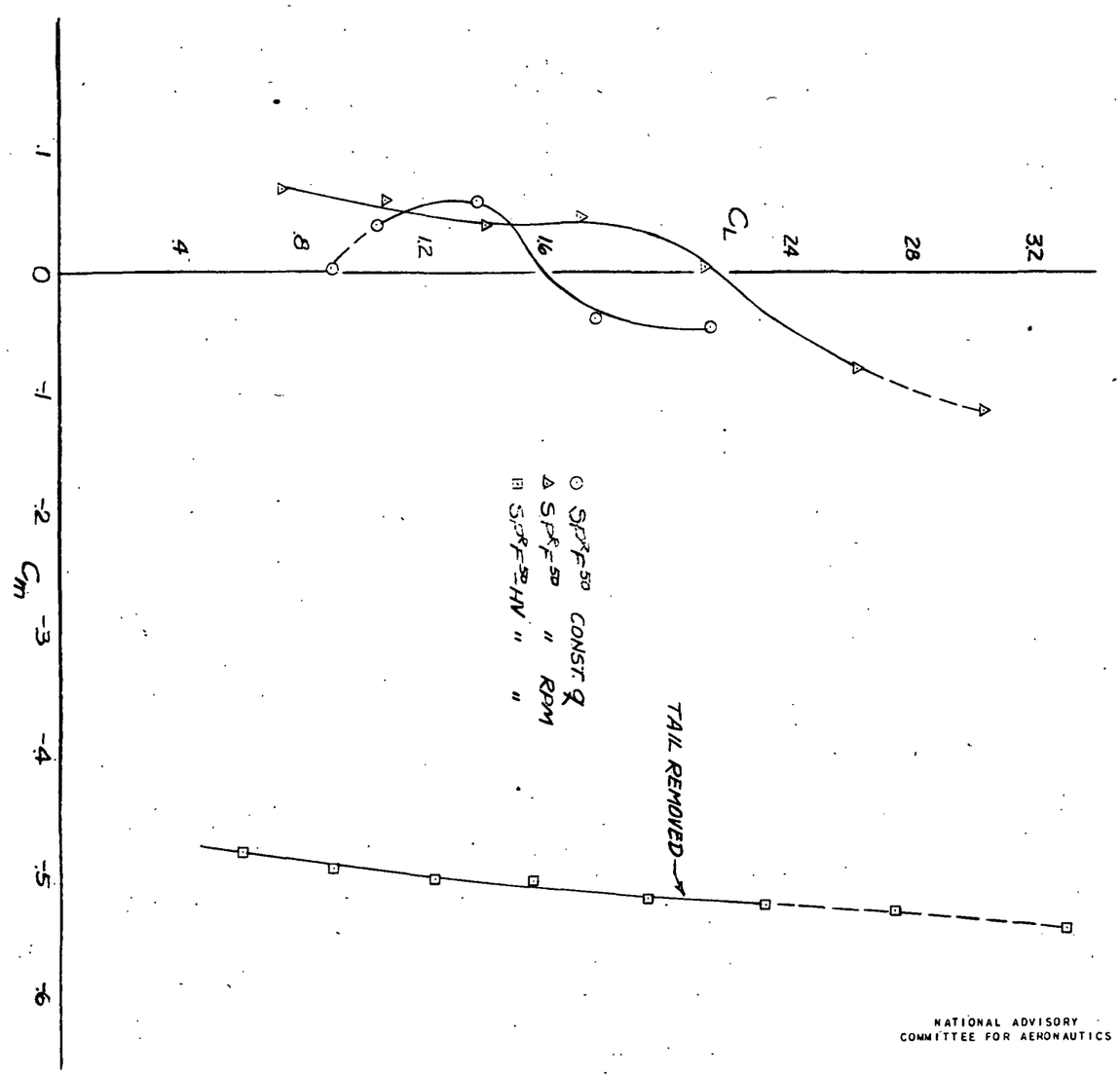

FIGURE 49.— VARIATION OF PITCHING-MOMENT COEFFICIENT WITH LIFT COEFFICIENT FOR THE TEST MODEL WITH TAIL ON AND TAIL REMOVED; FLAPS 50°, TAKE-OFF POWER.

NATIONAL ADVISORY
COMMITTEE FOR AERONAUTICS

○	RUN 24	SF^{25}	
△	25	SF^{50}	
□	19	$SF^{25}P^{R}$	T.O.P.
▽	20	$SF^{50}P^{R}$	50% RP
○	21b	$SF^{25}G$	
△	26b	$SF^{50}G$	
□	21	$SF^{25}GP^{R}$	T.O.P.
▽	22	$SF^{50}GP^{R}$	50% RP

FIGURE 50. - EFFECT OF LANDING GEAR ON THE AERODYNAMIC CHARACTERISTICS OF THE TEST MODEL; TAIL ON, FLAPS DEFLECTED.

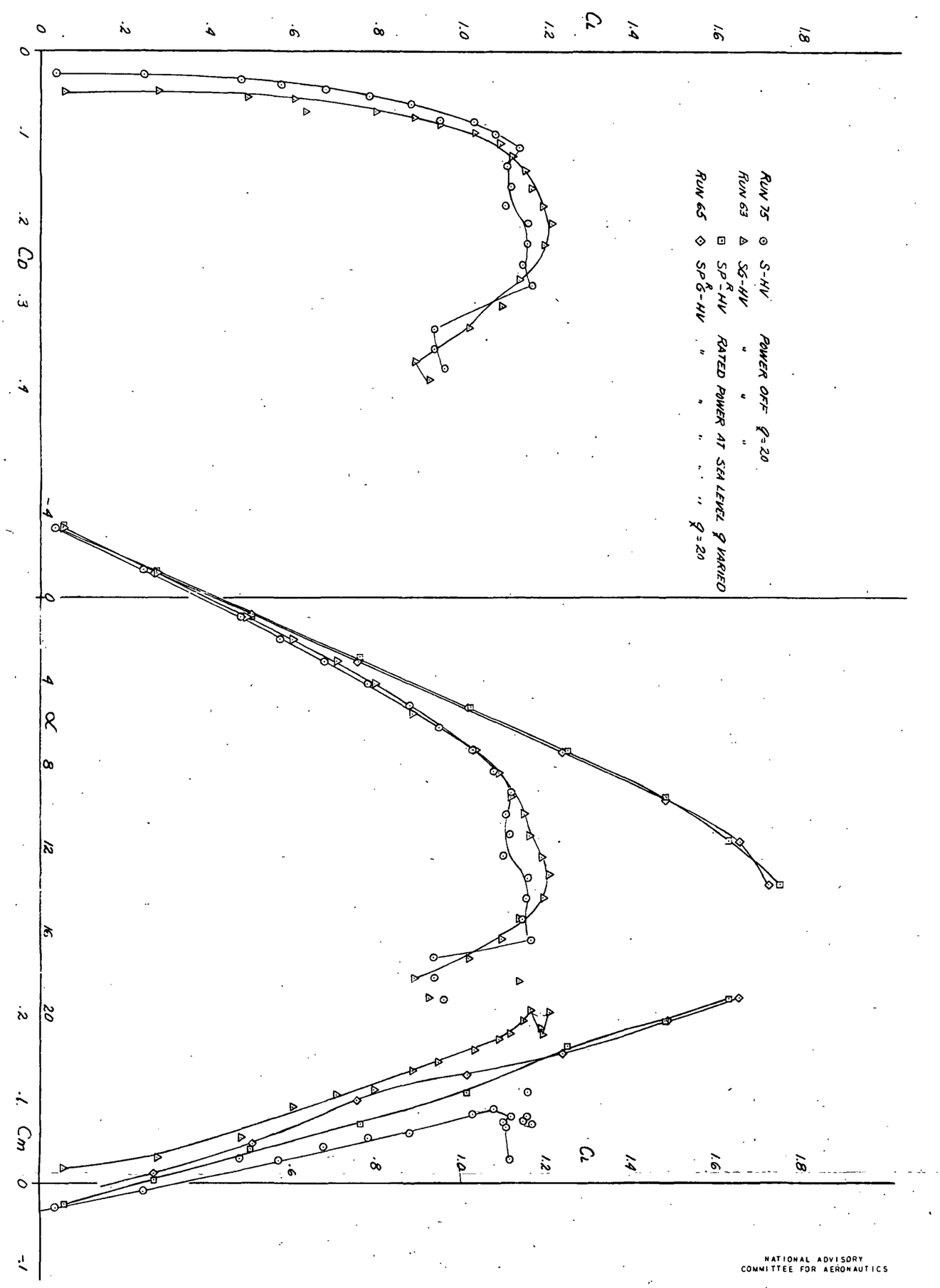

FIGURE 51.— EFFECT OF THE LANDING GEAR ON THE AERODYNAMIC CHARACTERISTICS OF THE TEST MODEL. FLAPS UNDEFLECTED; TAIL REMOVED.

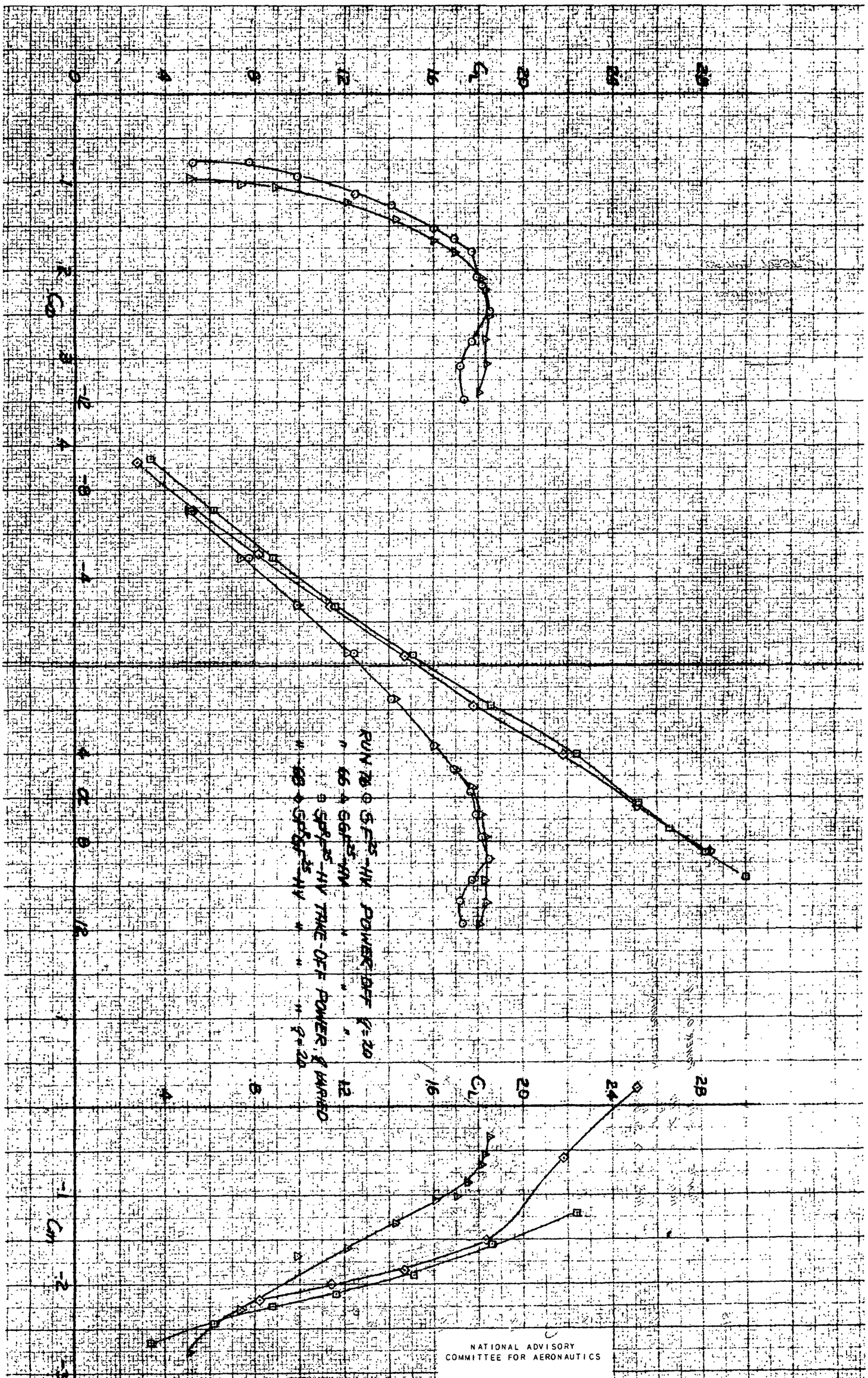

FIGURE 52.- EFFECT OF THE LANDING GEAR ON THE AERODYNAMIC CHARACTERISTICS OF THE TEST MODEL; FLAPS DEFLECTED 25°, TAIL REMOVED.

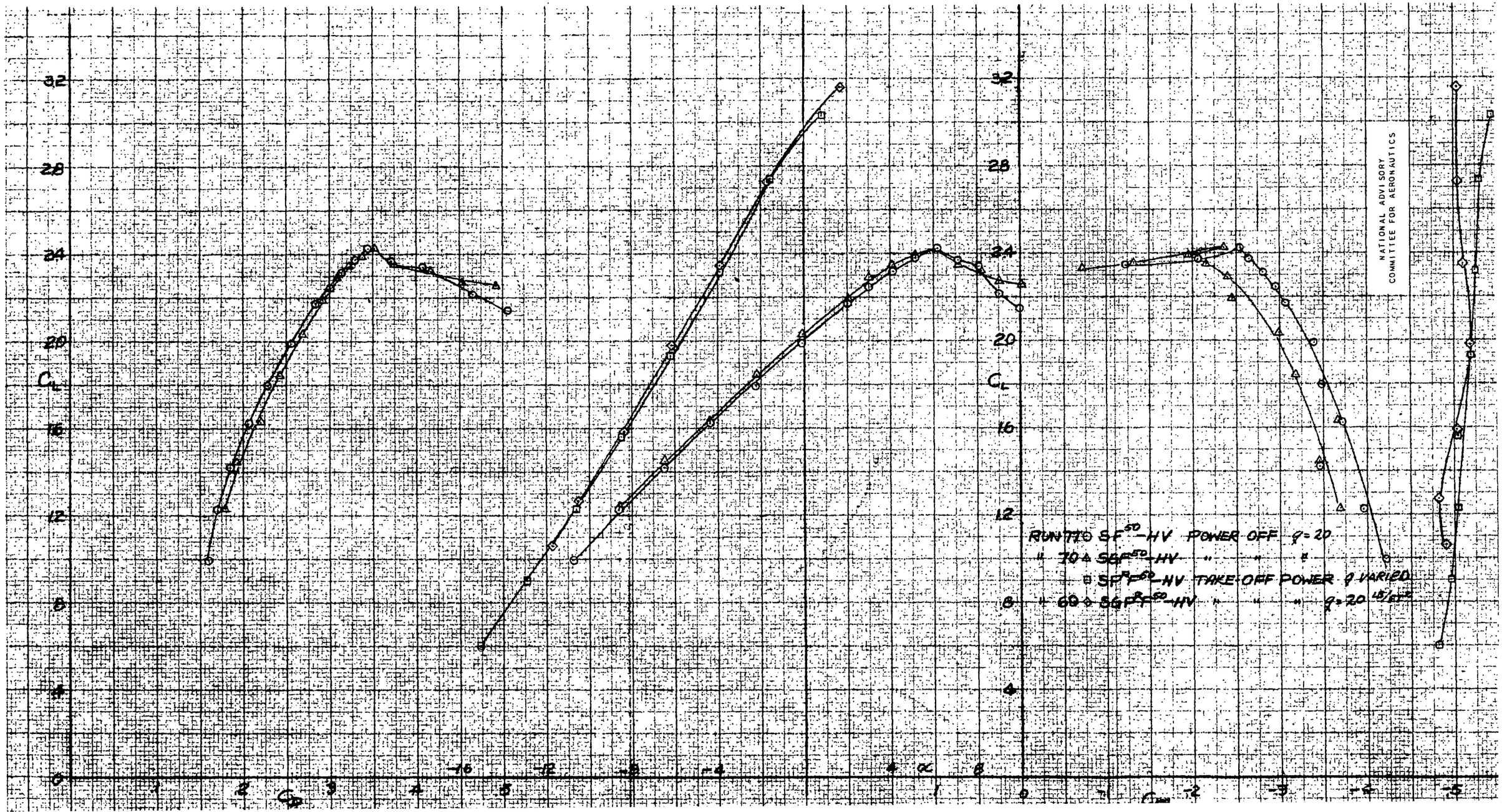

FIGURE 53.- EFFECT OF THE LANDING GEAR ON THE AERODYNAMIC CHARACTERISTICS OF THE TEST MODEL; FLAPS DEFLECTED 50°, TAIL REMOVED.

FIGURE 54.- EFFECT OF THE LANDING GEAR ON THE AERODYNAMIC CHARACTERISTICS OF THE TEST MODEL; FLAPS UNDEFLECTED, TAIL ON.

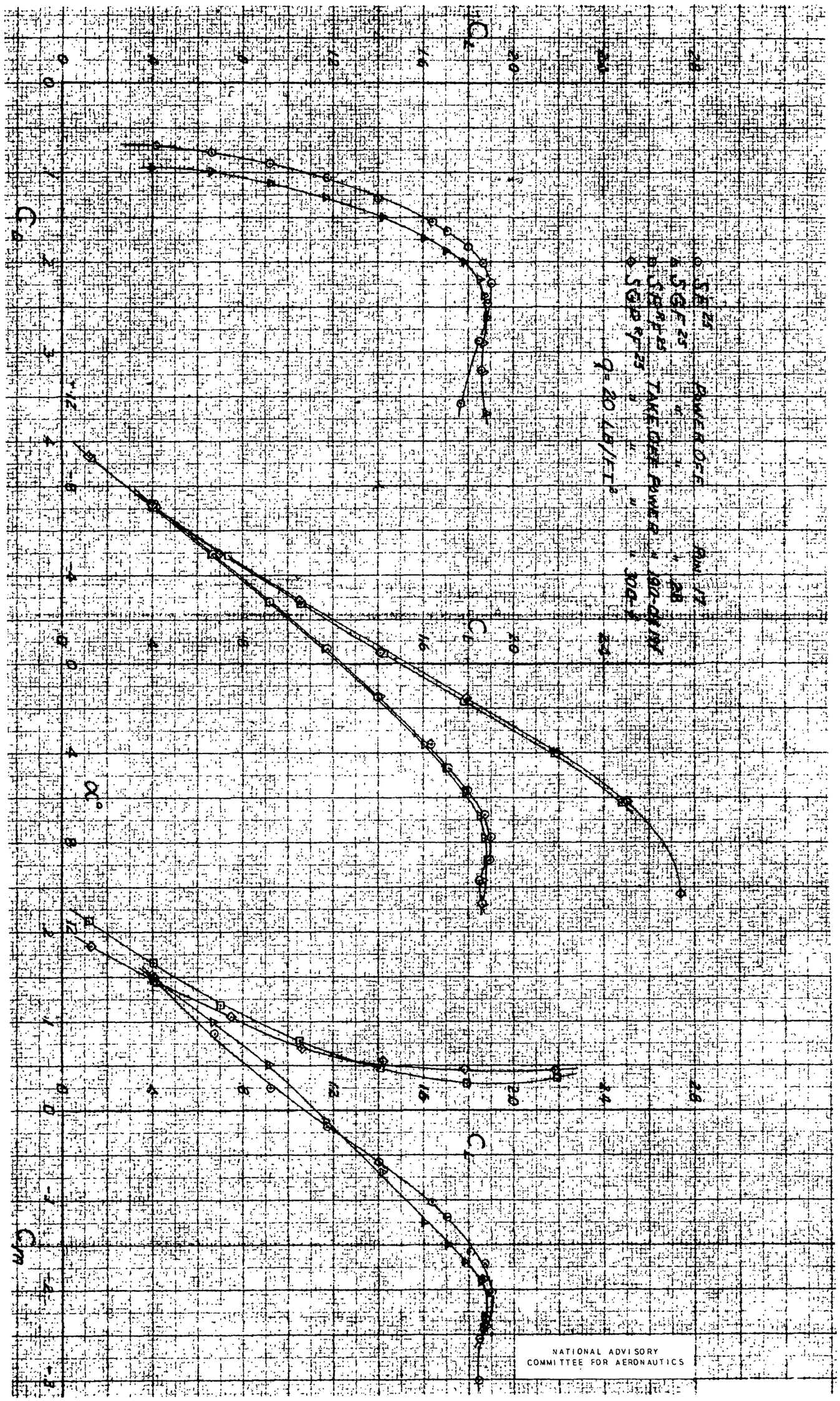

FIGURE 55. - EFFECT OF THE LANDING GEAR ON THE AERODYNAMIC CHARACTERISTICS OF THE TEST MODEL; FLAPS DEFLECTED 25°, TAIL ON.

FIGURE 56.- EFFECT OF THE LANDING GEAR ON THE AERODYNAMIC CHARACTERISTICS OF THE TEST MODEL; FLAPS DEFLECTED 50°, TAIL ON.

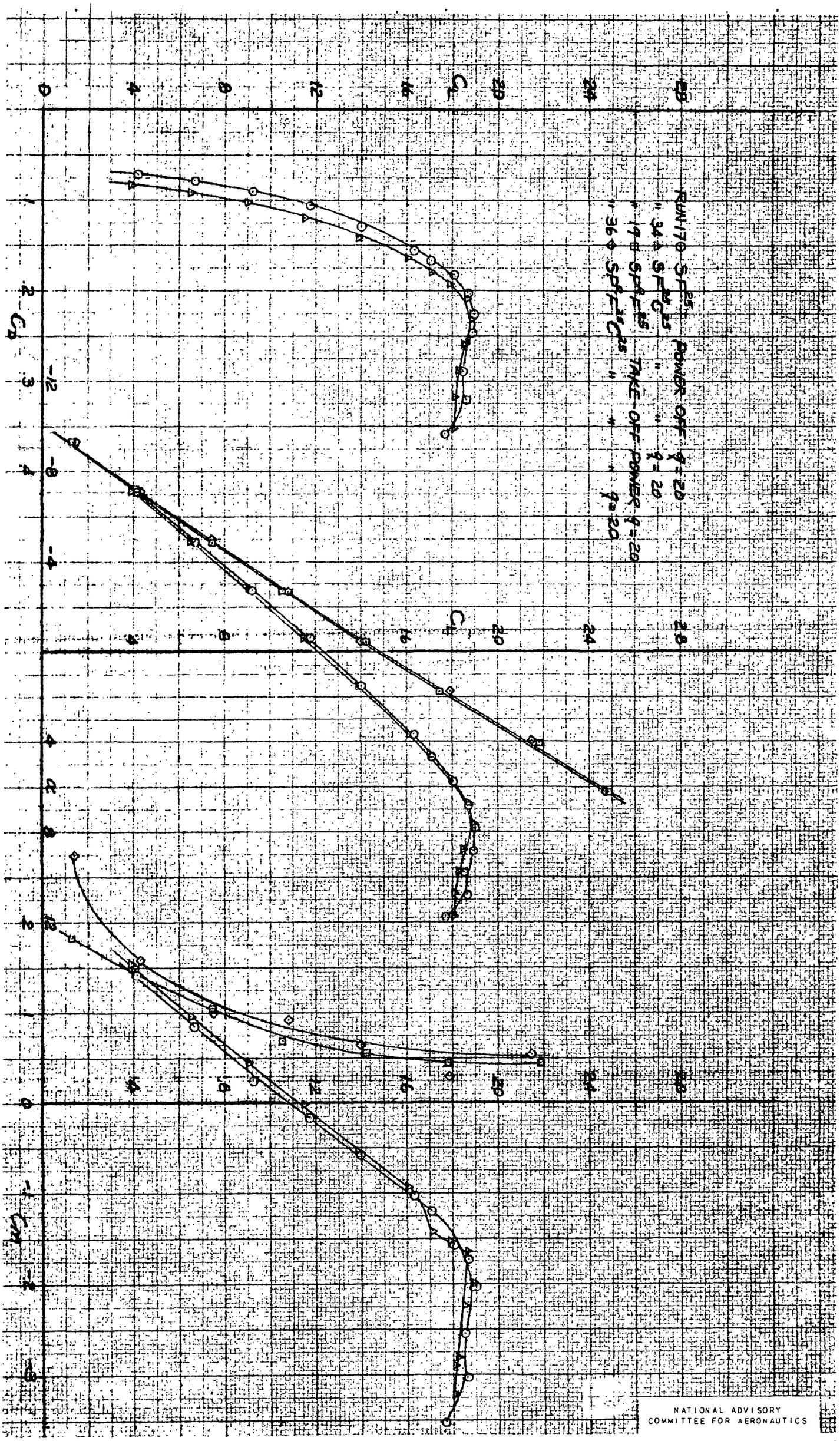

FIGURE 57.- THE EFFECT OF COWL FLAPS OPEN TO 25° ON THE AERODYNAMIC CHARACTERISTICS OF THE TEST MODEL; TAIL ON, FLAPS DEFLECTED 25°.

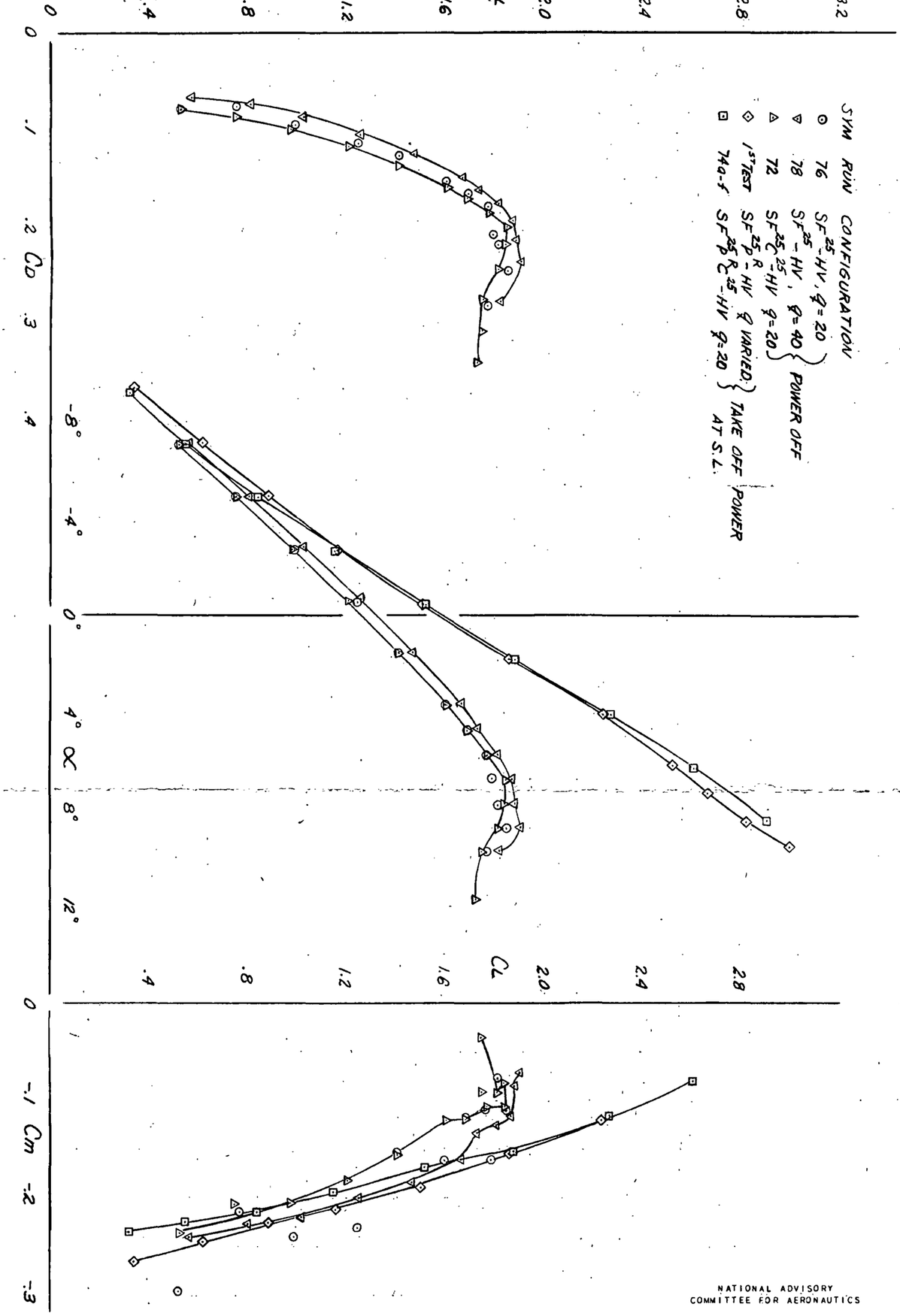

FIGURE 58.— THE EFFECT OF COWL FLAPS OPEN TO 25° ON THE AERODYNAMIC CHARACTERISTICS OF THE TEST MODEL. TAIL REMOVED, FLAPS DEFLECTED 25°.

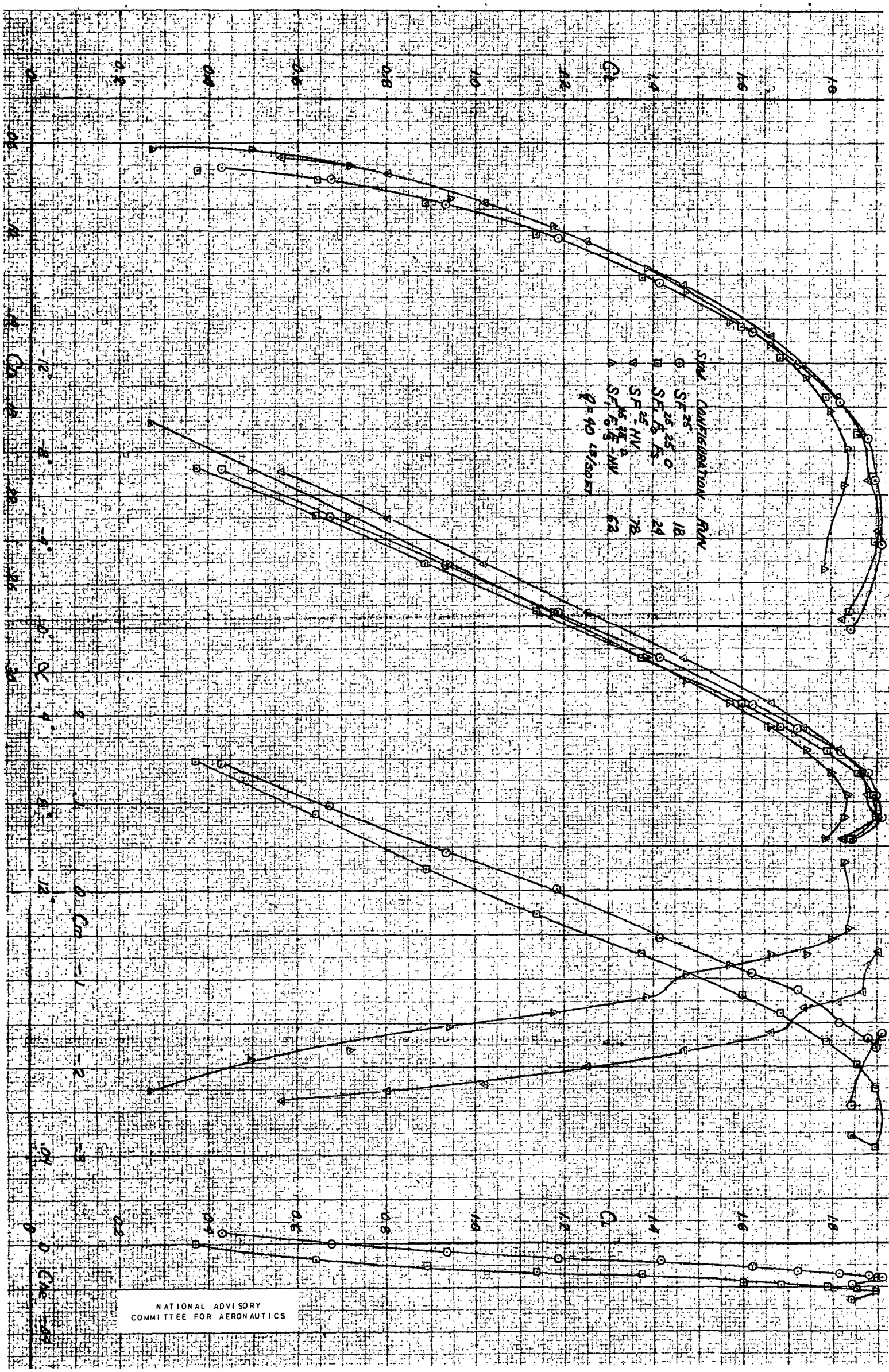

FIGURE 59.- LONGITUDINAL CHARACTERISTICS SHOWING THE EFFECTIVENESS OF THE CENTER-SECTION SPLIT FLAP; WING FLAPS 25°, PROPELLERS REMOVED FOR THE TEST MODEL.

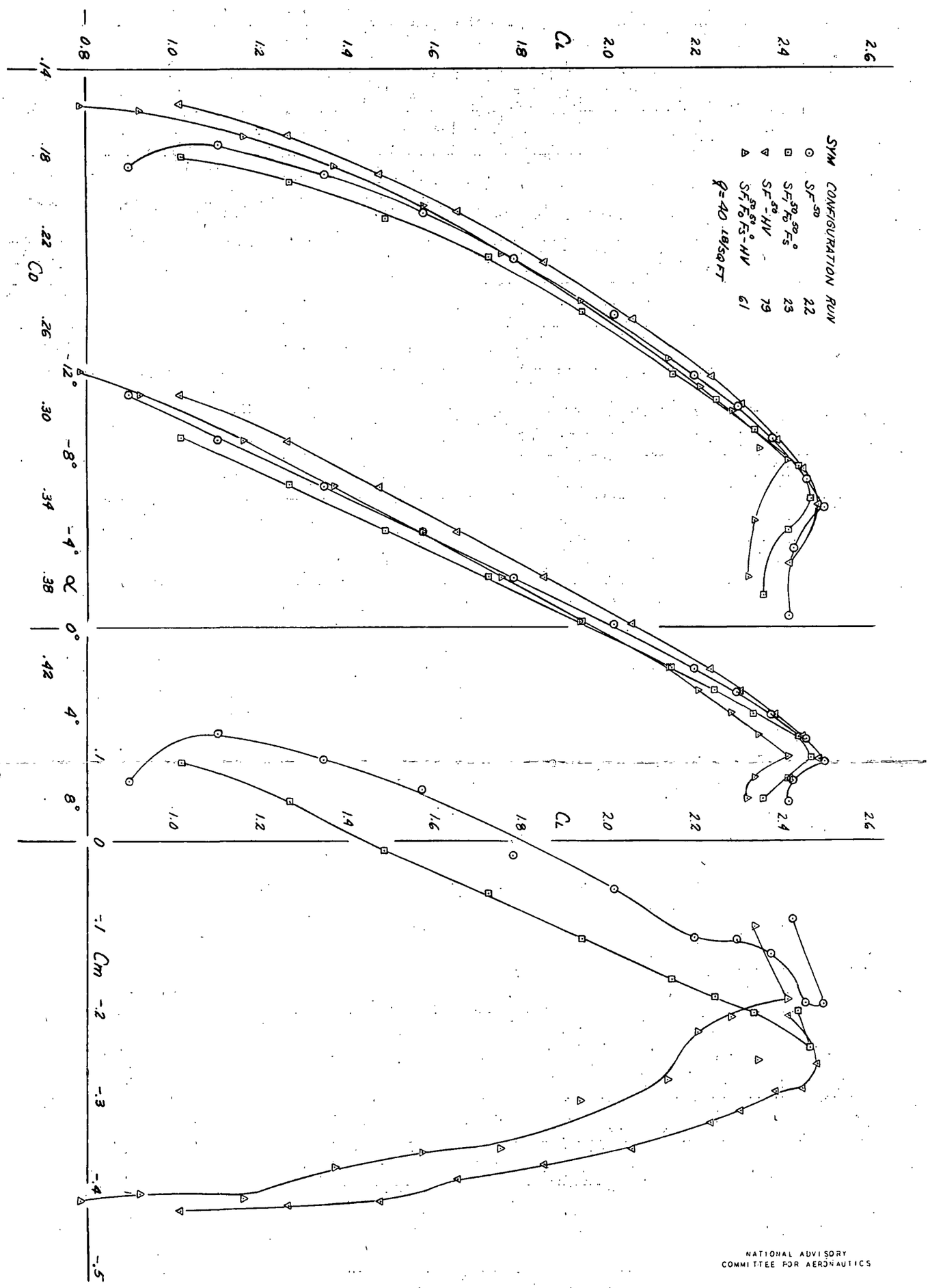

FIGURE 60.- LONGITUDINAL CHARACTERISTICS SHOWING THE EFFECTIVENESS OF THE CENTER-SECTION SPLIT FLAP, WING FLAPS 50°, PROPELLERS REMOVED FOR THE TEST MODEL

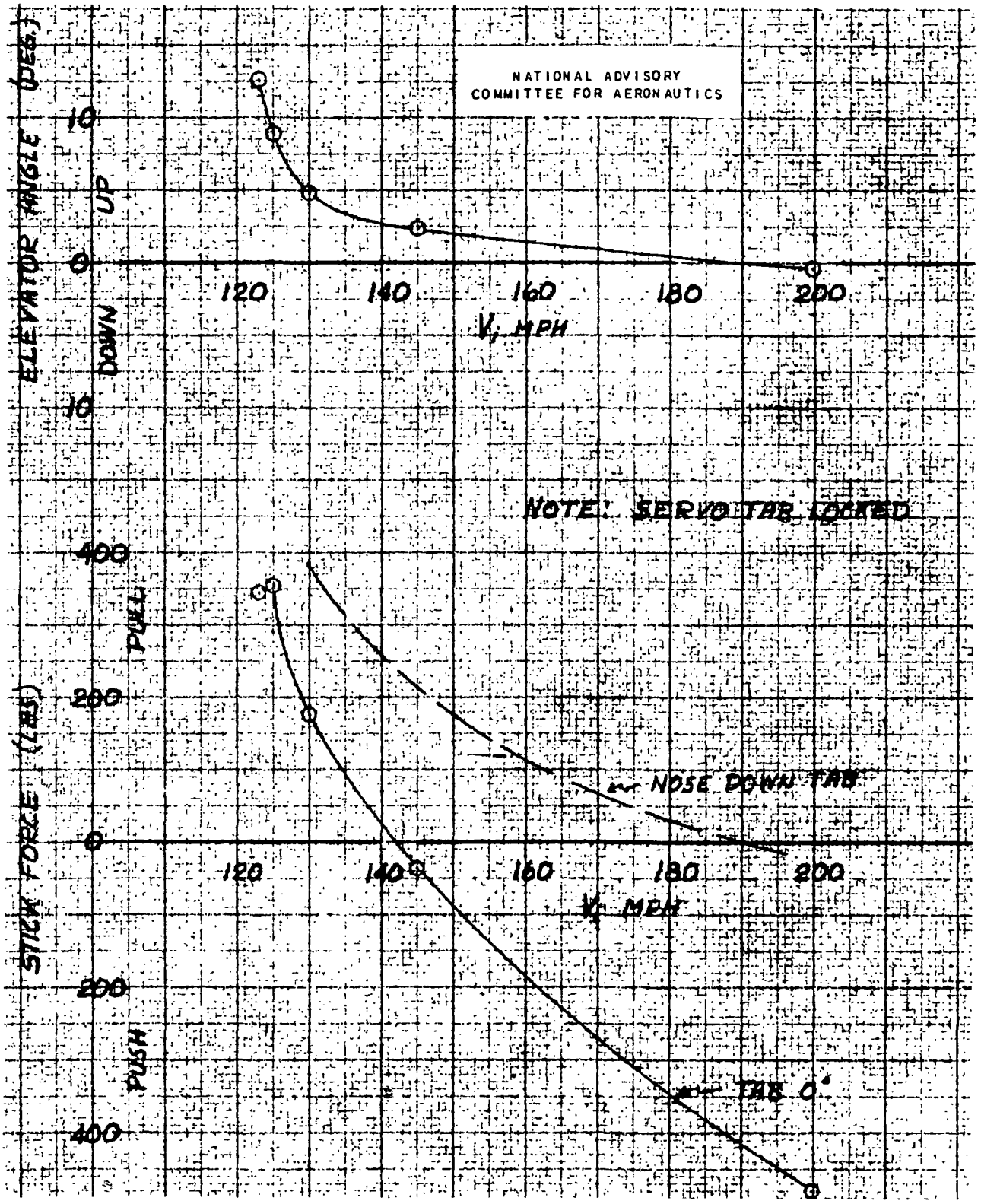

FIGURE 61.- VARIATION OF ELEVATOR ANGLE AND STICK FORCE WITH INDICATED AIR SPEED; GROSS WT. = 125,000 LBS, C.G. @ 25% MAC, PROPELLERS REMOVED. TEST MODEL.

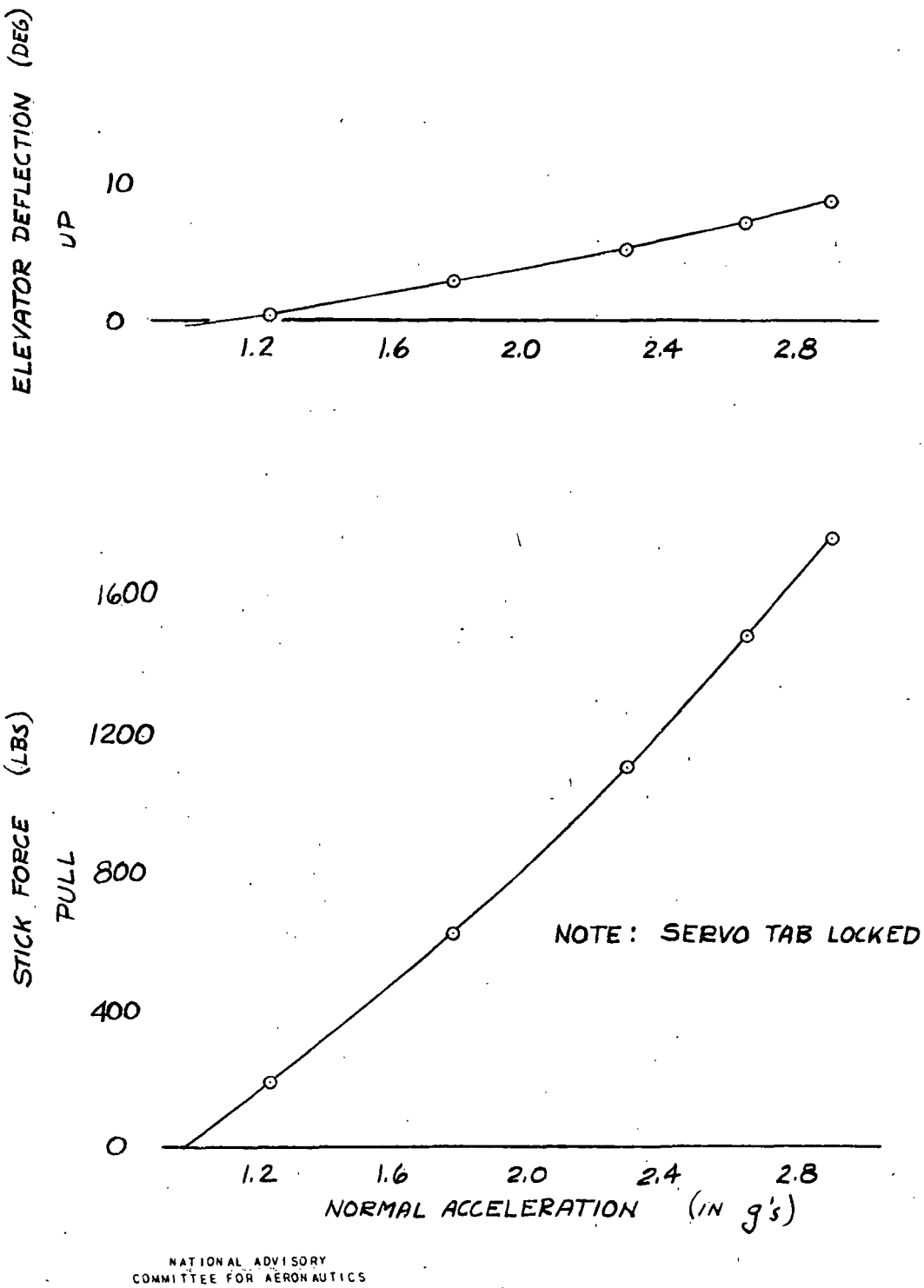

FIGURE 62.- VARIATION OF ELEVATOR ANGLE AND STICK FORCE WITH NORMAL ACCELERATION IN TURNING FLIGHT; GROSS WT: 125,000 LBS; C.G. @ 25 % M.A.C.; PROPELLERS REMOVED. TEST MODEL.

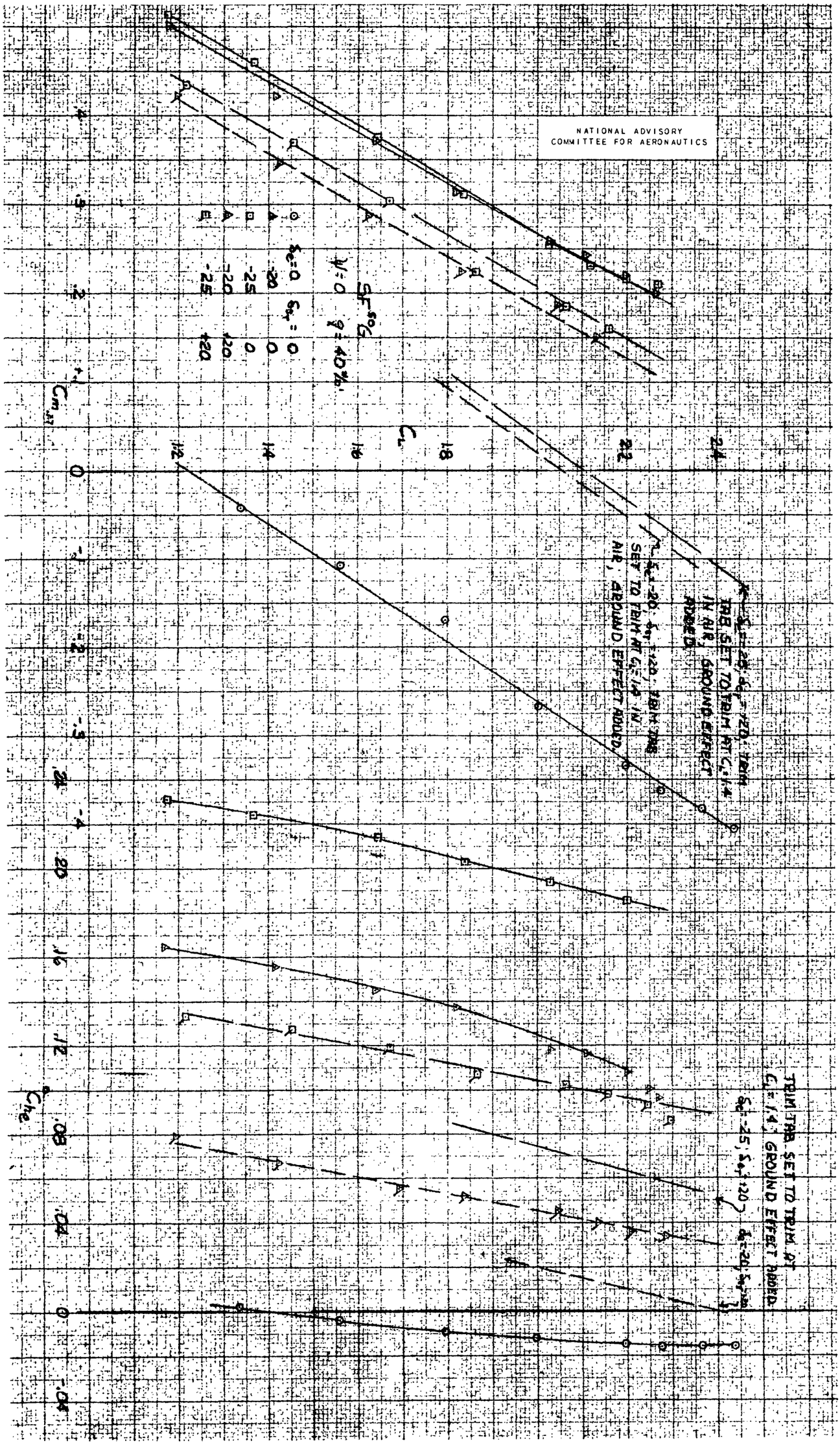

FIGURE 63.- THE VARIATION OF PITCHING-MOMENT AND ELEVATOR HINGE-MOMENT COEFFICIENTS WITH LIFT COEFFICIENT FOR THE TEST MODEL IN THE LANDING CONDITION; FLAPS DEFLECTED 50°, LANDING GEAR EXTENDED, GROSS WT = 125,000 LBS, C.G. @ 17% MAC.

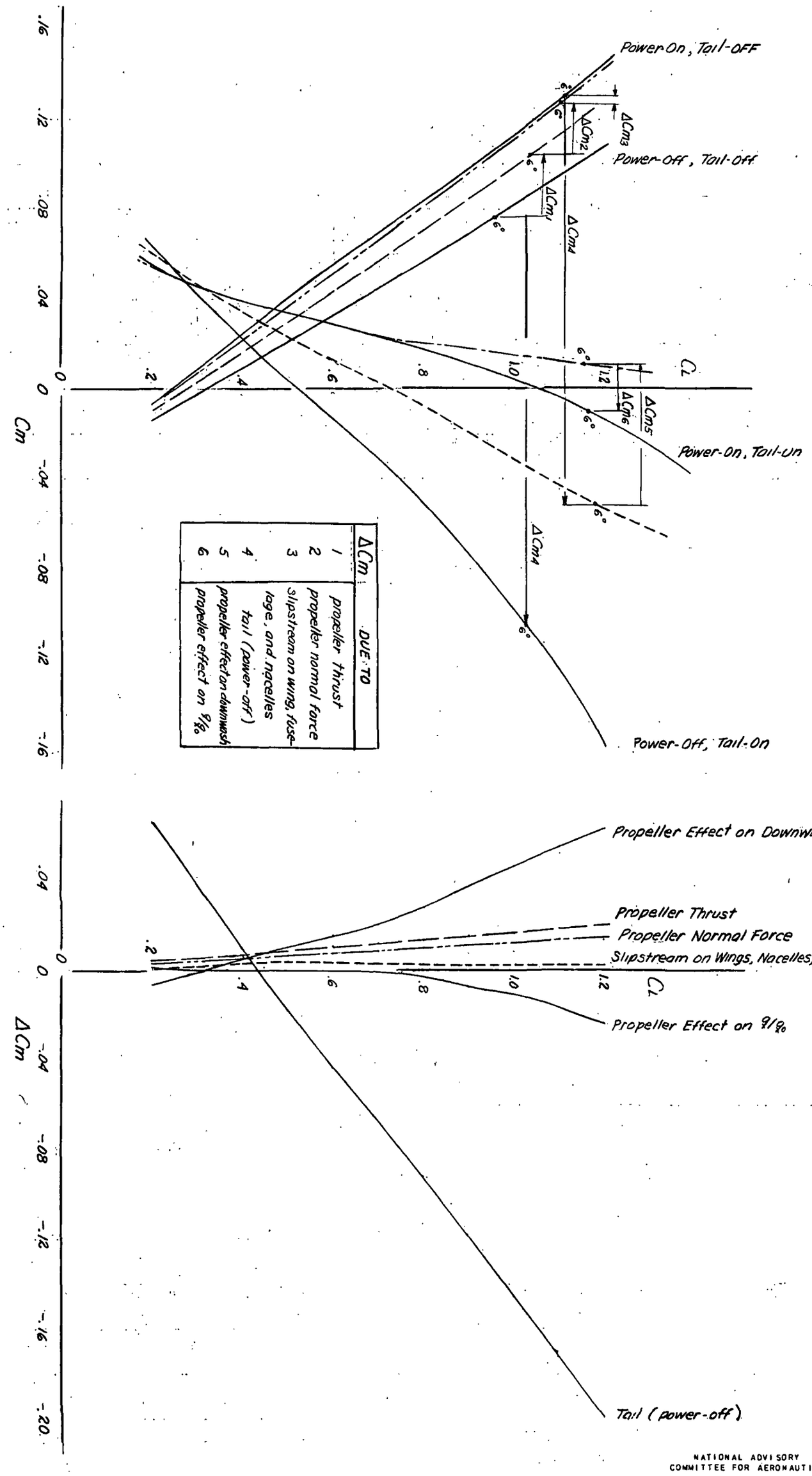

FIGURE 64.— A COMPARISON OF THE COMPONENT POWER EFFECTS UPON THE LONGITUDINAL STABILITY; FLAPS UNDEFLECTED; RATED POWER TEST MODEL

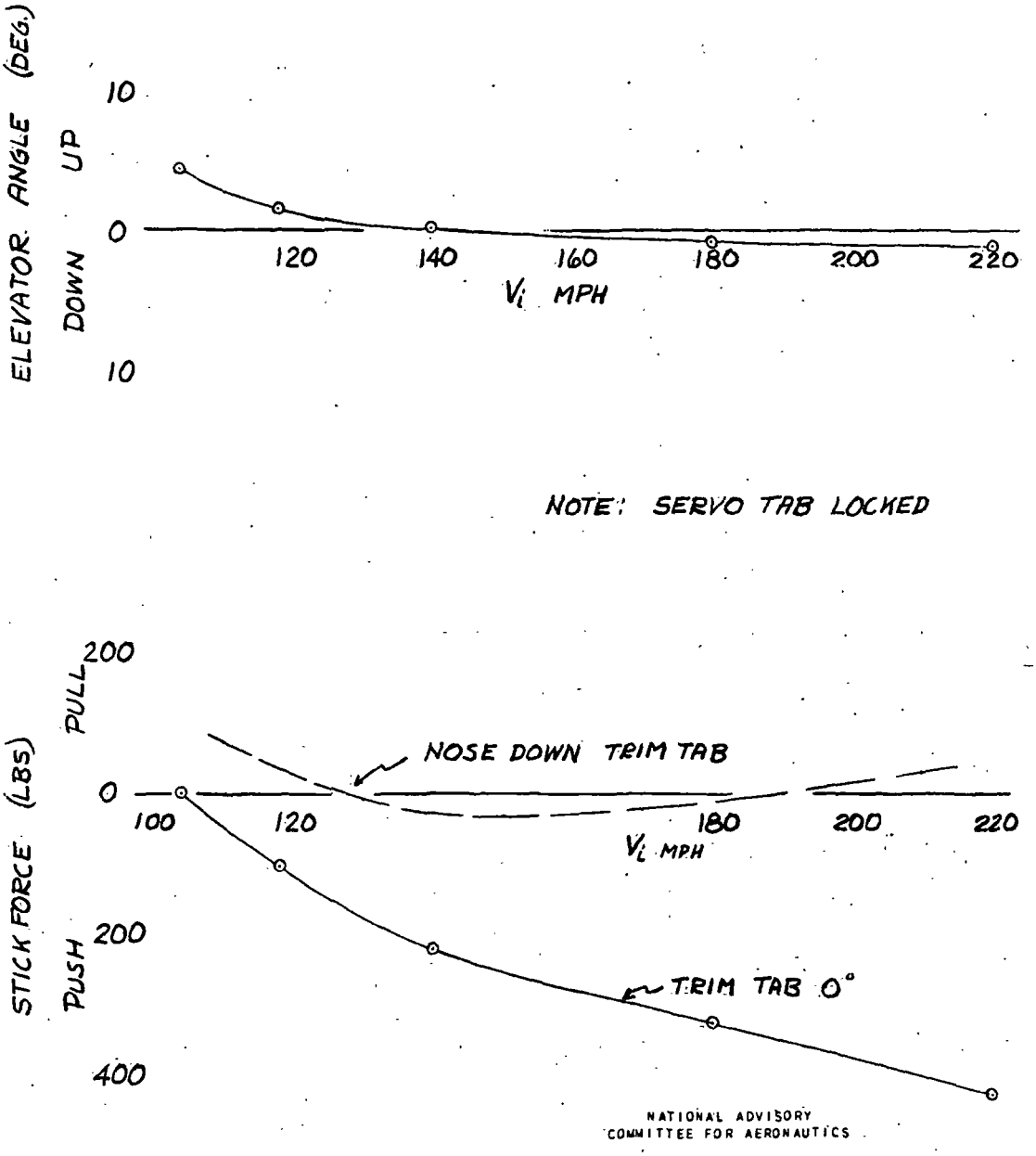

FIGURE 65.- VARIATION OF ELEVATOR ANGLE AND STICK FORCE WITH INDICATED AIRSPEED; GROSS WT. = 125,000 LBS; C.G. @ 25% MAC; RATED POWER @ 5,000 FT. TEST MODEL.

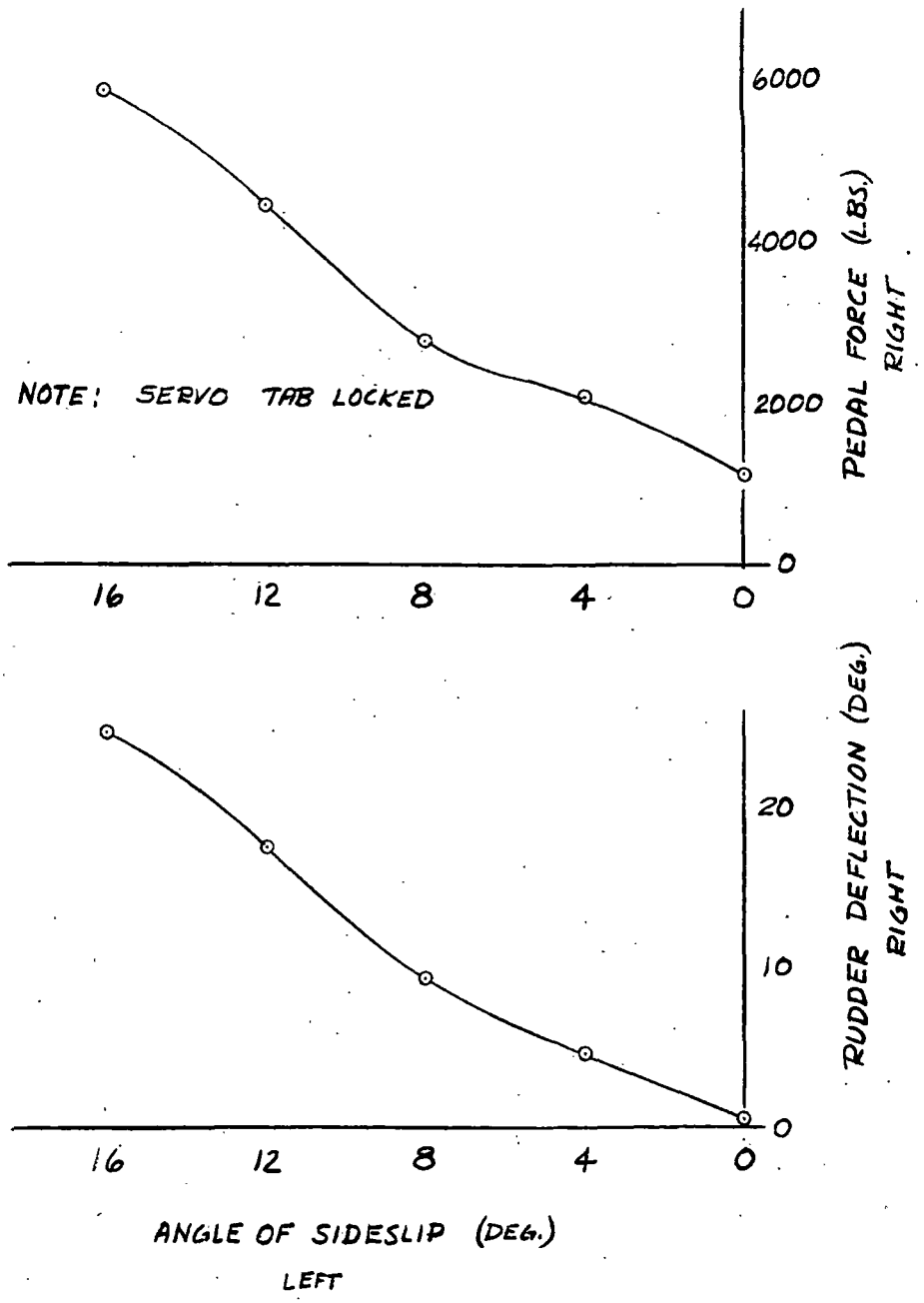

NATIONAL ADVISORY
COMMITTEE FOR AERONAUTICS

FIGURE 66.- VARIATION OF PEDAL FORCE AND RUDDER ANGLE WITH ANGLE OF SIDESLIP; V_i = 200 mph; PROPELLERS REMOVED. TEST MODEL

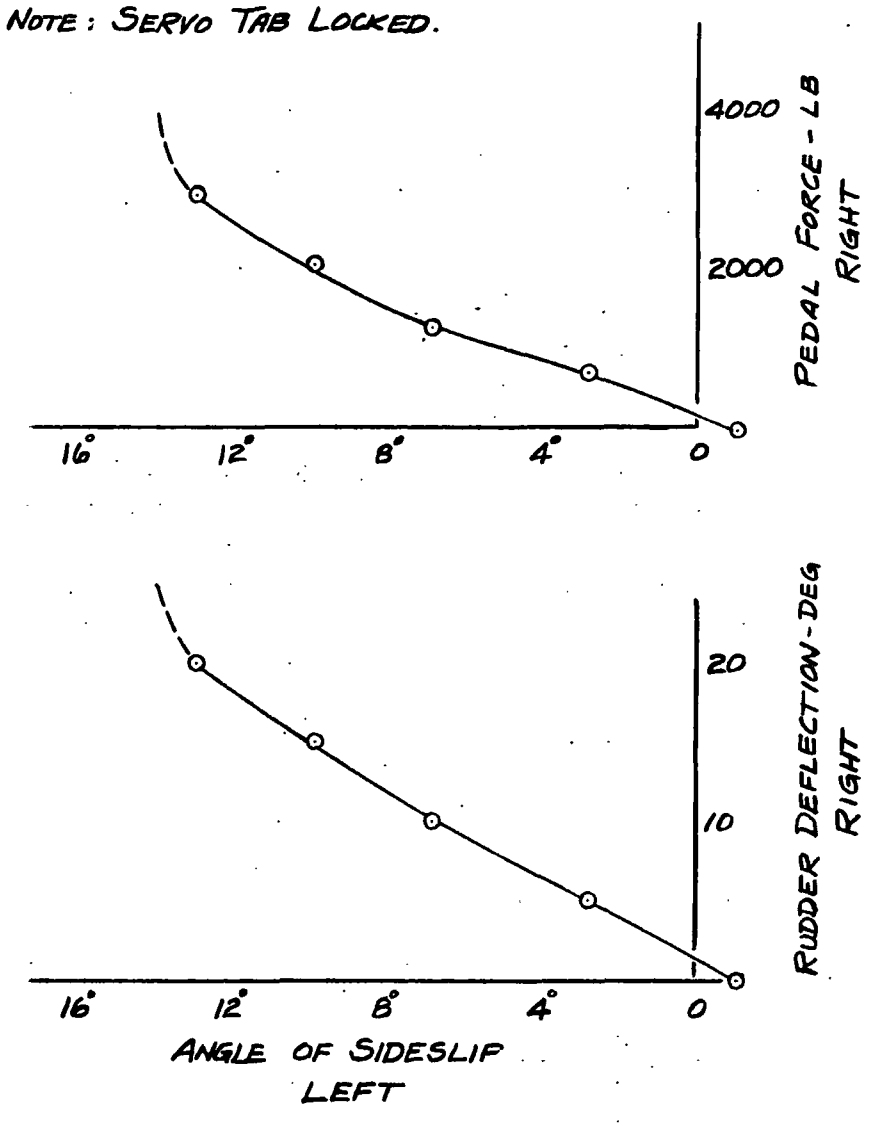

NATIONAL ADVISORY
COMMITTEE FOR AERONAUTICS

FIGURE 67 - VARIATION OF PEDAL FORCE AND RUDDER ANGLE WITH ANGLE OF SIDESLIP FOR THE TEST AIRPLANE; V_i = 140 MPH; RATED POWER AT SEA LEVEL; CLIMB CONDITION.